

P.O.L.

**AN INVESTIGATION OF METEOROLOGICAL EFFECTS ON
CURRENTS IN THE SHELF AND CONTINENTAL SLOPE SEAS
NORTHWEST OF THE U.K.**

**II. RELATIONSHIPS BETWEEN CURRENTS AT DIFFERENT
LOCATIONS AND WITH OTHER VARIABLES**

BY

**J.M. HUTHNANCE, D.L. BLACKMAN, M. DOLMAN,
S. EASTMAN, D.C.C. MACDONALD, C. STAINTHORPE
AND J. WOLF**

**REPORT NO. 6
1989**

**NATURAL ENVIRONMENT
PROUDMAN
OCEANOGRAPHIC
LABORATORY
RESEARCH COUNCIL**

PROUDMAN OCEANOGRAPHIC LABORATORY

**Bidston Observatory
Birkenhead, Merseyside, L43 7RA, UK
Tel: 051 653 8633
Telex: 628591 Ocean B
Fax: 051 653 6269**

Director: Dr. B.S. McCartney

Natural Environment Research Council

PROUDMAN OCEANOGRAPHIC LABORATORY

REPORT No. 6

An investigation of meteorological effects on currents
in the shelf and continental slope seas
northwest of the U.K.

II. Relationships between currents at different locations
and with other variables

J.M. Huthnance, D.L. Blackman, M. Dolman, S. Eastman,
D.C.C. MacDonald, C. Stainthorpe and J. Wolf

1989

DOCUMENT DATA SHEET

AUTHOR J.M. HUTHNANCE, D.L. BLACKMAN, M. DOLMAN, S. EASTMAN, D.C.C. MacDONALD, C. STAINTHORPE & J. WOLF		PUBLICATION DATE 1989
TITLE An investigation of meteorological effects on currents in the shelf and continental slope seas northwest of the U.K. <u>II. Relationships between currents at different locations and with other variables</u>		
REFERENCE Proudman Oceanographic Laboratory Report, No. 6, 115pp.		
ABSTRACT <p>This report concerns data from the continental shelf and slope northwest of the UK in the period 19th August 1982 to 23rd March 1983, notably from the Continental Slope Experiment (CONSLEX). It develops from previous analysis for individual current meter moorings (the subject of an earlier report I) to consider wider groupings of data. These include spatial structure across current meter moorings, and relationships between currents and other variables - temperature, bottom pressure, sea level and meteorological variables.</p> <p>The treatment is principally in terms of three frequency bands (low-, band- and high-pass) covering the ranges: below 1/3 cpd; 1/2 - 5/6 cpd; above 1 cpd (the corresponding filters sum to unity). These bands respectively include: most of the energy; a few spectral peaks; wide-spread rotary near-diurnal oscillations. Correlations, co-spectra and principal component structure are considered for the whole duration of the time series, and for events (slope current reversals, strong current or temperature fluctuations, occurrences of strong near-diurnal oscillations).</p> <p>Currents on the shelf showed extensive coherence <i>inter alia</i> and with meteorological variables, especially at low frequencies, for which there was coherence with alongshelf wind, coastal and shelf-break bottom pressure. These pressure variables were also extensively correlated with north/northeastward phase propagation and coherent with alongshelf wind at low frequencies.</p> <p>Currents over the slope in 500m were principally aligned along the slope but less coherent with each other. In 1000m or more there was still less coherence, and rotary motion suggested eddies in the Faeroe-Shetland Channel.</p> <p>Bottom pressure transferred from ocean to shelf-edge at higher frequencies and from shelf-edge to coast, allowing for correlated winds. Additional coastal variance prevents inference of oceanic bottom pressure therefrom.</p> <p>'Mean' currents were (statistically) stronger to the north/northeast about 3 days after neap tides, by an amount (2cm/s) not clearly related to mean flow strength.</p> <p>This work was supported by the UK Department of Energy. The results may be used in the formulation of Government policy, but at this stage they do not necessarily represent Government policy.</p>		
ISSUING ORGANISATION Proudman Oceanographic Laboratory Bidston Observatory Birkenhead, Merseyside L43 7RA UK Director: Dr B S McCartney		TELEPHONE 051 653 8633 TELEX 628591 OCEAN BG TELEFAX 051 653 6269
KEYWORDS SHELF CURRENTS NORTHWEST EUROPEAN WATERS CONTINENTAL SHELF FAROE-SHETLAND CHANNEL CONTINENTAL SLOPE WYVILLE-THOMSON RIDGE CONSLEX CURRENT METER OBSERVATIONS		CONTRACT PROJECT MLS-83-2 PRICE £29

Copies of this report are available from:
 The Library, Proudman Oceanographic Laboratory.

Contents

	Page
1. Introduction	7
2. Data reduction	7
2.1 Frequency bands	7
2.2 Representative series	7
2.3 Temperature at current meters	8
2.4 Meteorological data	10
3. Analysis for complete series	10
3.1 Cross-correlations and cross-spectra	10
3.2 Bottom temperature	11
3.3 Shelf-break temperature (thermistor chains)	12
3.4 Coastal sub-surface pressure	12
3.5 Bottom pressure	13
3.6 Currents: shelf	14
trends	15
low pass (500m, 1000m, Wyville-Thomson Ridge)	15
band-pass	16
high-pass groupings	16
3.7 Ocean-coast pressure relationship	17
3.8 Momentum balance	19
3.9 Mean flow variation	20
3.10 Heat flux	21
4. Analysis for events	22
4.1 Correlations	23
4.2 Extensive relaxation of slope current	23
4.3 Extensive fluctuations (Faeroe-Shetland Channel)	25
4.4 Pressure event	26
4.5 Individual fluctuations	26
4.6 Diurnal oscillations	27
4.7 Temperature-related events	28
5. Discussion	29
6. Conclusions	33
References	35
Table and figure captions	37
Tables	38
Figures	47

Contents (continued)

	Page
Appendices. Representative Series	54
A. Current moorings and temperature	55
B. Thermistor chains	90
C. Bottom pressure and temperature	93
D. Coastal sea level	110
E. Atmospheric pressure and winds	112

1. INTRODUCTION

Measurements of currents over the continental shelf northwest of the UK took place during winter 1982/3, notably in CONSLEX. These and other nearby contemporary measurements of currents, temperature, bottom pressure, sea level and meteorological variables are detailed in HUTHNANCE et al. (1988; hereafter I) and in other reports cited therein. The context and purpose of the measurements are also described in I, which takes the analysis of currents as far as the treatment of individual moorings.

We here consider wider groupings of data - spatial structure across current moorings and relationships between currents and other variables.

2. DATA REDUCTION

Two sequential aspects to the data reduction were the choice of standardised frequency bands and (within one of these frequency bands) the derivation of a single time series to represent a maximal proportion of the variance in a chosen group of variables (all current components on a mooring, say).

2.1 FREQUENCY BANDS

Three bands were chosen: 'low-pass', 'band-pass' and 'high-pass' (LP, BP and HP). They result from the application of the corresponding filters, illustrated in Figure 1, to the standardised 3-hourly series described in I. Summation of the LP, BP and HP series re-constitutes the original.

As noted in I, most spectral peaks in the current data are near diurnal or slightly higher frequencies (i.e. selected by HP) or at frequencies below $\frac{1}{2}$ cpd (i.e. selected by LP). A few occur at intermediate frequencies 0.6 to 0.8 cpd; the choice of HILOW parameters determining BP (Figure 1) attempts to select these.

2.2 REPRESENTATIVE SERIES

A total of 79 current meters are listed in I, and the data also include 11 bottom pressure and temperature locations, 2 thermistor chains (11 series each), 12 coastal sea level series, and atmospheric pressure and winds from many stations. In seeking correlations between currents at different locations, say,

the number of possibilities for comparing component u_1 at level h_1 with component u_2 at level h_2 becomes too large to comprehend. Given the substantially barotropic nature of the velocity variance at most moorings - or even a representation by one principal component as explored in I - a useful reduction would appear to be a single time series to represent one mooring. (At some locations - D5,E3,E4,F3,G2,G4 - affected by cold bottom waters of the Faeroe-Shetland Channel, separate time series below and above the thermocline are appropriate). A similar reduction also appears useful for each thermistor chain, and for the meteorological data to give just one atmospheric pressure series and two components of wind stress.

The extended form of principal component analysis described in HUTHNANCE (1983) was used. Thus

$$\begin{array}{l} \tilde{y}(t) \\ \text{several series} \end{array} \quad \text{is approximated by} \quad \begin{array}{l} \tilde{x}_1 \varphi(t) + \tilde{x}_2 [\varphi(t + \Delta t) - \varphi(t)] \\ \text{constant } \tilde{x}_1, \tilde{x}_2 \end{array}$$

where t takes discrete values at intervals $\Delta t = 3$ hours and \tilde{x}_1, \tilde{x}_2 and the single time series $\varphi(t)$ minimise the residual variance of the approximation. An iterative procedure is used starting from the principal component for which \tilde{x}_2 is constrained to be zero. (\tilde{x}_2 minimising the residual variance is found, and a revised \tilde{x}_1 , then a revised series $\varphi(t)$ and so forth). Thus $\varphi(t)$ is a better representative time series than the principal component series. The term $\varphi(t + \Delta t) - \varphi(t)$ is an approximation to $d\varphi/dt$ (x constant) and allows some representation of phase differences and of rotating currents by means of \tilde{x}_2 not parallel to \tilde{x}_1 - yet with just one series $\varphi(t)$.

Representative series used 'immediately' are detailed in the Appendices. Further series representing (say) groups of moorings are derived later. For reference, a location map is repeated from I as figure 2, current mooring data are summarised in Table 1 and other data locations in Table 2.

2.3 TEMPERATURE AT CURRENT METERS

All current meter data include temperature series, excepting Oseberg (OS) and Statfjord (ST). These series have been included with east and north components from each current meter on the mooring in forming the $\tilde{y}(t)$ to be approximated/represented. However, a question of units and hence weighting arises. If currents were expressed in m/s, their numerical values would be small, whereas temperature variations expressed in $^{\circ}\text{C}$ would assume large numerical values. Then the approximation by $\varphi(t)$ would be weighted towards a

good representation of the large temperature values to minimise the numerical residual variance. However, we have expressed currents in cm/s and temperatures in °C with the opposite effect; $\varphi(t)$ is weighted towards a good representation of the numerically large values of currents. Then the temperature series are in effect regressed against the currents - $\varphi(t)$ - to determine the corresponding coefficients in \tilde{x}_1, \tilde{x}_2 as part of the approximation procedure.

(In the present case this is deliberate. If equitability were desired in contexts with different units or values, all values should be scaled against the expected data errors. Then data with small relative error would be weighted heavily and approximated more closely).

Typically, temperature variance relative to current variance is a few $(^{\circ}\text{C}/\text{ms}^{-1})^2$ for frequencies at or above 1/25 cycles per day (spectra are shown in I). There is generally a decrease in this value towards higher frequencies (BP and HP) as expected from decreased excursions advecting temperature, for given speeds. The decrease of temperature variance with frequency is more marked for that part correlated with the currents $\varphi(t)$; the HP ratio is typically $0.1 (^{\circ}\text{C}/\text{ms}^{-1})^2$.

Exceptions to the above include large temperature variations at L3, F3, G4 and especially at D5 and G2. At the former three (on Porcupine Bank and in the deeper waters of the Faeroe-Shetland Channel) correlations with currents are generally small, although the 388m temperature at F3 (LP) correlates with increased north-eastward slope currents there $(+6^{\circ}\text{C}/\text{ms}^{-1})$. At higher frequencies at F3, increased temperatures at both 79m and 388m (BP) and at 79m (HP) also correlate with north-eastward currents, albeit less strongly. Although a stronger slope current may be expected to be warmer, the cyclonic polarisation in all frequency bands also correlates the warming with an excursion up the slope. At D5, at 510m depth (LP) and just above the bottom (633m depth, all frequency bands) decreased temperatures correlate with approximately southward flow; approximate coefficients are $(^{\circ}\text{C}/\text{ms}^{-1})$

	LP	BP	HP
510m	8		
633m	12	6	5

and manifest occasional 'overflows' of cold bottom water from the Faeroe-Shetland Channel across the Wyville-Thomson Ridge at its col, D5. At G2, for lower frequencies BP, LP, lowered temperature correlates weakly with roughly alongslope currents (to NE or E - or with offshelf displacement by virtue of the polarisation) but at higher frequencies (HP) the correlation is strong; the

coefficient for bottom temperature is $10^{\circ}\text{C}/\text{ms}^{-1}$ approximately, with raised values lagging offshore displacement.

At L3,L4,PR,MR,B1,C2,C3,D2,E4 and G2 there is no clear trend of temperature/current variance ratio with frequency; at L3,PR,C2,C3,G2 - and F3 - this applies also to that part of the temperature correlated with the current. The correlated temperature/current variance ratio is exceptionally high at D5 and G2 with HP values 20 and 50 $(^{\circ}\text{C}/\text{ms}^{-1})^2$ respectively as already discussed; otherwise D2 has the largest HP value $1.3(^{\circ}\text{C}/\text{ms}^{-1})^2$.

2.4 METEOROLOGICAL DATA

The standardised 3-hourly series described in I include atmospheric pressure from 14 meteorological stations and winds from six. Owing to large atmospheric spatial scales and dynamical balances, these series are highly inter-dependent. Indeed, a preliminary principal component analysis on 11 pressure series (omitting Mull of Galloway, Shannon and Gwennap Head) and 6 pairs of wind component series, all together, indicated only three principal components (roughly: means of pressure and two components of wind) clearly standing out from the noise.

Hence the procedure 2.1, 2.2 above was applied to form representative LP, BP and HP series for just three variables:

atmospheric pressure (AP) using all 14 stations;

wind parallel (WP) to the shelf using one component from all 6 stations;

wind transverse (WT) to the shelf using the orthogonal component from each station. The wind component 'parallel' to the shelf is taken as northwards, for Tiree and Benbecula, and towards N 52.4°E at the other four locations Torshavn, Lerwick, Sule Skerry and Stornoway. The transverse component is then eastwards or towards E 52.4°S respectively.

3. ANALYSIS FOR COMPLETE SERIES

3.1 CROSS CORRELATIONS AND CROSS SPECTRA

Representative series were cross-correlated, and cross-spectra formed, according to data type and sub-groupings as entered in Table 3.

The purpose was to assess the possible spatial extent of relationships between variables, in order to choose groupings within which to seek structural forms. For example, there was widespread significant coherence between low-passed

currents on the shelf (A1,B1,B2,D1,F1,G1,OS and ST). However, in the absence of perfect coherence, the $\frac{1}{2}(8 \times 7) = 28$ individual off-diagonal elements of the cross-spectral matrix are not consistent, e.g.

$$P(A1 \text{ to } B2) \neq P(A1 \text{ to } B1) + P(B1 \text{ to } B2)$$

for pair-wise phase differences P. Indeed, not all pair-wise coherences are significant even though all 8 locations are 'connected' with each other by several 'chains' of significant coherence. Moreover, several other moorings were coherent with one or more of these shelf locations.

Hence further analysis is required to infer consistent structural forms, but the choice of groupings thereto remains subjective (albeit better-informed) after these preliminary analyses. Thus prior ideas and ancillary information will be invoked in the choice as we treat variable types in turn.

3.2 BOTTOM TEMPERATURE

At the deep locations A6,B5,E3,F3 and G4, variations are very small, 0.1°C r.m.s. or less. At the shelf locations B1,C1,D1,F1 and G1, the largest variations result from the seasonal heating/cooling cycle; steady values are followed by a warming (as the seasonal thermocline is mixed down to the bottom) over the approximate periods 27th October - 1st November (B1) 10th October - 30th October (D1) 14th October - 27th October (F1) 10th October - 9th November (G1); cooling follows for the rest of the experiment, but levelling off in March. There is a cooling 'event' on 7-10 October at C1 and D1 which is discussed as part of a wider phenomenon in 4.2. Otherwise, the 1086m depth Rockall Trough location C4 shows the largest fluctuations, 0.3°C rms; typical shelf values are 0.1°C rms (0.2°C rms at F1) - all are principally LP.

Formally, the bottom temperature series (LP) are all significantly coherent with the nearest current mooring, but coherences are generally very low, in particular 0.21 for C4 with C3. The associated phases correspond to a raised C4 temperature after an increased C3 slope current (to the NNE). The shelf bottom temperatures at C1, D1 and F1 have higher coherences with the nearest currents and also are elevated after an increase of those currents to the north or northeast along the shelf edge. The elevation is of the order of $1^\circ\text{C}/\text{ms}^{-1}$ and is confirmed in the representative forms for the current meter moorings (Appendix A). Note that on the mooring C2 (closest to C1) and D1 only the lowest temperature record has this phase relationship.

3.3 SHELF BREAK TEMPERATURE (THERMISTOR CHAINS)

As for bottom temperature at the shelf break, the largest variations result from the seasonal heating/cooling cycle. Steady values (after averaging over a few days) are followed by a warming as the seasonal thermocline is mixed down to the bottom. This can be seen as a succession through the records at individual depths, at both B2 and G1, although the effect of averaging over higher-frequency internal waves is to smooth the apparent temperature dependence on depth and give the impression simply of temporally decreasing stratification, particularly at G1. The warming occurs from 19th October to 31st October at B2 and from the beginning of the record (9th October) to 9th November at G1. These dates closely match those of the nearby bottom warming. Winter cooling then continues until March.

Variations superimposed on this seasonal cycle are about 0.07°C rms. and principally LP and barotropic, at both locations. At B2, many of these variations (especially in January 1983) take the form of cooling 'events' lasting roughly one day and intensified towards the bottom (a characteristic not apparent in the representative mode form, Appendix B). Coherence with the nearby bottom temperature is correspondingly high although the thermistor chain at B2 leads B1 bottom temperature by about $\pi/3$ (LP). As in the case of bottom temperature, coherence with the nearest current mooring is low. At G1 (and to a lesser extent B1) there is some LP coherence with cross-shelf winds (to the north-west) which lead raised temperatures there by rather more than $\pi/2$, but the effect on temperature is only of order $0.01^{\circ}\text{C}/\text{ms}^{-1}$. At higher frequencies there is some correlation with currents but the values of order $0.1^{\circ}\text{C}/\text{ms}^{-1}$ (c.f. Appendix A) are small.

3.4 COASTAL SUB-SURFACE PRESSURE

Widespread significant cross-correlations and coherence in cross-spectra is found between the 12 series extending from Newlyn to Lerwick, especially at low frequencies; for HP the best correlations are with nearby locations. Exceptions are Torshavn, less well correlated for LP, and Stornoway, which has only a short record not well correlated with distant locations. For LP, there is a general phase progression towards the north/northeast (although pairwise values are not fully consistent) and good correlation with longshore winds. At higher frequencies, there is no clear phase progression and less emphatic correlation

with longshelf winds. At all frequencies, there is good correlation between several locations and atmospheric pressure or winds.

Variations range from 7 mb r.m.s. at Torshavn to 25 mb r.m.s. at Aughris Head. Malin Head and all Scottish mainland gauges fell in the range 15 to 18 mb r.m.s. (as did Griminish Point, but its values may be reduced through the gauge being inoperative during the stormiest period). Values at Newlyn, Walls and Lerwick were respectively 10, 12 and 9 mb r.m.s., perhaps indicating less stormy conditions (Newlyn) and decreases away from the mainland towards the shelf edge (Walls and Lerwick). In all cases the LP proportion of variance exceeds 80% except at Millport (73%). (Stornoway is excluded from these comparisons, having only a short record of low variance during a relatively quiet period in February/March 1983.)

In view of the widespread correlations, representative time series $\varphi(t)$ and corresponding structures (\tilde{x}_1, \tilde{x}_2 of 2.2 above) were formed from all the coastal series together, to clarify the relationships suggested by pairwise analyses. Results are illustrated in Appendix D, which shows LP and BP phase progression from Newlyn in the south west to Wick in the north east, for this coherent part of the signal. The large values at Aughris Head are retained, i.e. coherent with elsewhere. On the other hand, Torshavn is essentially independent of the British coastal values, and Walls and Lerwick on Shetland are independent for BP. The representation accounts for 62%, 72%, 44% of all LP, BP, HP variance respectively.

3.5 BOTTOM PRESSURE

These records come from near 200m depth at the shelf edge (B1,C1,D1,F1,G1) and from the deeper waters of the Rockall Trough and Faeroe-Shetland Channel (A6,B5,C4; E3,F3,G4). Variations range from about $2\frac{1}{2}$ mb rms (C1,D1 and A6) to about 6 mb rms (B1,G1,C4 and E3) although a high proportion from the lowest frequencies at C4 suggests a contribution from instrumental drift there. At all locations, the LP frequency band includes 74% or more of the variance. The small variance at C1 and D1 may be partly attributed to termination of their records before winter, but they are 'quieter' than contemporary records at B1, F1 and G1 on the shelf to either side.

Evidence for cross-shelf correlation is generally sporadic and is best for B1, F1 and G1. B1 appears to be roughly in phase with B5; F1, F3, G1 and G4 appear to form a coherent group with E3 and D1 for BP and HP, having overall phase progression to the northeast (see representative mode figure in Appendix C) and

comparable amplitudes on and off the shelf. C1, C4 and D1 are similar at higher frequencies (D1 lags slightly). Cross-shelf pressure relationships are discussed further in 3.7.

Along-shelf correlations between B1, C1, D1, F1 and G1 are generally good and confirmed in the derivation of representative series and forms. The figure in Appendix C shows a northeastward progression of phase, representing a few hours lag from B1 to G1. Amplitudes increase overall in this direction at lower frequencies, although C1 and D1 have smaller correlated signals in accord with their lesser variance. For LP (only) there is also good correlation with along-shelf wind, particularly for F1 and G1 at the lowest frequencies with a pressure increase $0(1 \text{ mb})/\text{ms}^{-1}$ for wind to the northeast, and lagging the wind by about 1 day.

The deep Rockall Trough records A6 and B5 are well correlated, with just a slight lag and larger amplitude at B5. The deep Faeroe-Shetland Channel records E3, F3 and G4 are also well correlated but show changes from low (LP) to high (HP) frequencies: a phase progression to the southwest and reduced amplitude at F3 are both reversed. At the lowest frequencies 84% of the variance is in a mode with opposite signs in the Rockall Trough and Faeroe-Shetland Channel (and larger amplitude in the latter). There is no clear correlation between this mode or generally between deep pressure and the meteorological series.

3.6 CURRENTS

Shelf moorings are discussed first. Then we consider the measurements from current meter moorings as separated into frequency bands, commencing with the lowest frequencies or 'trends', i.e. the varying means and trends of 25-day blocks (the first step in spectral analyses - see I). Initial pairwise comparisons concentrate on cross-shelf 'sections' of moorings, and on moorings in approximately the same water depth along the continental shelf or slope.

Shelf moorings showed extensive coherence involving A1,B1,B2,C2,D1,D2,F1,G1, OS,ST at all frequencies (although statistics are lacking for OS and ST 'trends') and correlations with meteorological series, especially LP alongshelf winds. Accordingly (figure 3a) the mode form shows the phase at all these moorings to be within about $\pi/4$ for the LP along-shelf flow, and one representative series accounts for 68% variance. Spatial variations of phase are more rapid with increasing frequency. Statfjord and especially Oseberg dominate the BP signal on account of their reduced-frequency 'near-diurnal'

oscillations noted in I. For HP the oscillations just above diurnal frequency at G1 predominate as discussed in I and GORDON et al. (1987). There is a second area of such oscillations over the Hebrides Shelf (figure 3a); in between, the shelf near the Wyville-Thomson Ridge is less able to support HP frequencies (GORDON et al. 1987). Only about 50% or less of the variance is accounted for by one BP or HP series as coherence does not extend along the whole array.

The representative series (figure 3a) for these shelf currents is strongly correlated with the representative series for coastal pressure (coefficient 0.83), alongshelf winds (0.79) and bottom pressure on the shelf (0.64) for LP. BP and HP correlations are 0.42 or less. Principal component mode forms between these variables suggest magnitudes of about 1cm/s, 2mb, 1m/s and 0.4mb respectively to correspond, positive pressures accompanying flow and winds to the north/northeast. Coastal pressure increases relative to currents with increasing frequency.

Trends were apparently coherent between several of the deeper Faeroe-Shetland Channel moorings, although statistics are poor with only a few 25-day blocks. Principal-component structure was found for a 'bottom water' grouping E4B, F3B2, G4B3 (with E4T) and for an 'upper-water' grouping B4,C2,F3T2,G2B,G4T1 (extending back to the Rockall Trough). The most energetic bottom waters at such low frequencies are at F3; that part at E4 and G4 which is correlated is of opposite sign although E4T has the same sign. All are principally aligned along the Faeroe-Shetland Channel. Again, F3 shows the most energetic upper waters at such low frequencies; however, all the group show currents in the same sense and aligned principally along the slope.

Low pass (LP) time series along the slope in approximately 500m water, 1000m water depth and along the Wyville-Thomson Ridge showed some coherence, and consistent structures were sought by forming representative series and forms for these groupings (figure 3b).

Less consistency is shown along the slope than along the shelf with a similar range and number of moorings, variance accounted for by one representative series being 52% (500m), 54% (1000m). However, the coherent form for the 500m moorings except L2 (which has only a short record) shows currents aligned principally along the local slope and in phase. (D5B1 at the col of Wyville-Thomson Ridge shows flow across the Ridge). The 1000m series are dominated by the greater energy in the Faeroe-Shetland Channel, and at F3 in particular. A rotary (eddy) character is evident there, with a large phase difference between E3 and F3. B4, C3 and F3B2 currents are aligned with the

slope. One representative series accounts for 64% of the variance of the four (only) Wyville-Thomson Ridge series; D1, D2 and D5 bottom are in phase for east/northeastward flow, and magnitudes are similar (figure 3b). However, the varying direction of local topography is clear in the distinctive alignments of D1, D2 and D5B1 (across the Ridge). D5T1 appears less constrained, having a more rotary character (but the figure still shows the portion coherent with the other series).

The deeper moorings at A5, MR and FR do not show consistent coherence with other locations.

No consistent coherences were found between the 500m, 1000m or Wyville-Thomson current series, and representative series for bottom or coastal pressure.

Band pass (BP) coherences are generally lower, with widespread significance only between shelf moorings as discussed above. A few other series (G4B3, D5T1, E4B) showed significant pair-wise coherence with some of the shelf series, but only for G4B3 is there significant coherence (0.4 with 9h delay) with the series representing all shelf moorings.

The top meters at F3 and G4 were coherent and approximately in phase for currents to the north-west/south-east, but amplitudes were greater at F3 (as for LP).

High pass (HP) coherences are higher again in local groups, e.g. A1,B1,B2,D1 and F1,G1,ST,OS within the shelf moorings but also B1,B2,B3,B4 and G1,G2B,G2T2 across the shelf. Amplitudes are greatest at the shelf-break locations B2 and G1 in accord with HP shelf-wave forms (GORDON et al. 1987). All currents are polarised clockwise (Appendix A) and B1,B2 and G2 show a lag at depth relative to near-surface. Otherwise, B1 to B4 are close in phase and lag A1, but D1 is widely separated in phase as are all the Faeroe-Shetland Channel locations. No consistent relationship was found between any of these groups and meteorological variables; much of the energy is in diurnal oscillation 'events' which are probably initiated by impulsive forcing rather than maintaining coherence - see 4.6 below. The section-B currents appear to correlate with and lag (2h) the bottom pressure at B5, and the F1,G1,ST,OS currents have a similar relationship with representative series for shelf-edge bottom pressures.

3.7 OCEAN-COAST PRESSURE RELATIONSHIP

There is increasing interest in using sea level measurements as a monitor of ocean circulation, the build-up of the GLOSS network (PUGH, 1987) being notable as an adjunct of the World Ocean Circulation Experiment. The question of how coastal values relate to oceanic values beyond the continental shelf has been considered theoretically by HUTHNANCE (1987) in relation to the along-shelf scale of the phenomena involved; features of scale greater than the decay distance of a shelf wave would be expected to transfer. CONSLEX included six deep-water bottom pressure records, five from the shelf edge and seven from adjacent coastal locations, affording a unique opportunity to examine the transfer in practice.

The analysis was carried out for each frequency band (LP, BP, HP). An individual mean was subtracted from all series, then all deep pressure series (say) at any one time were fitted by a mean, a linear trend and a sinusoid in along-shelf distance to extract components of different length scale. 'Along-shelf' distance was defined as distance S of 58°N or (if N of 58°N) as projected distance along N 52.4°E from 58°N 9°W. Disappointingly, even the unusually large number of locations along the shelf proved insufficient to define a sinusoid reliably; no meaningful results were obtained for the shorter length scales so-represented; we refer only to the mean and trend henceforth. Even the trend was only defined reliably for LP. Thus a time series was formed for variations in deep sea pressure averaged along the shelf, and likewise for the trend along the shelf (and similarly for shelf edge pressure and coastal pressure, in each of the three frequency bands).

Various regression analyses were carried out between these series, and statistical confidence assessed for variance reduction (with the F test) and regression coefficients (t test). In these tests, degrees of freedom were taken as

$$n/\int R d\tau; \quad R(\tau) = \frac{n \sum \varphi(t) \varphi(t+\tau)}{(n-\tau) \sum \varphi^2(t)}$$

where n is the series length and φ the residual 'noise' after regression. The division of n by an integral time allows for correlation between successive members of the time series.

Mean deep pressure determined less than 20% of mean coastal pressure variance, but this sufficed for 95% confidence and an HP regression coefficient near 1

(table 4). Including also wind in the regression, more coastal variance was accounted for (70% in one case) but then for LP and BP only the wind regression coefficient was significantly non-zero. Evidently deep pressure makes only a small contribution to coastal values, whose variance greatly exceeds deep pressure variance. Accordingly, in the converse regression coefficients are necessarily much less than 1. Significance was generally not found for wind as a determinant of deep pressure or between trends in deep and coastal pressure.

To improve the assessment of ocean-coast pressure relationships, the intermediate shelf edge pressure series were introduced.

Mean shelf-edge pressure determined 55% of coastal pressure (LP, with a regression coefficient near 2) increasing to a determination of 85% with wind included as a determining factor (the regression coefficient on pressure then decreasing to near 1). Evidently coastal mean pressure (LP) is well 'explained' by mean shelf edge pressure and winds which are themselves correlated. For BP and HP, shelf-edge pressure is a significant contributor to coastal pressure with a regression coefficient near 1, but wind only contributes for BP (for HP, scales of the natural continental shelf wave motion in the sea are perhaps too short to match the wind field - GORDON et al. 1987). In the converse regression coefficients were less but significantly non-zero, and wind only improved the accounting for shelf-edge pressure for LP (to a total 62%). Between shelf-edge and coastal pressures, correlations were lower for BP than for LP or HP to either side, suggesting lack of one consistent relationship in this intermediate band.

Mean deep pressure only determined 6% of shelf-edge pressure, but adding wind increased the variance accounted for to 35% (the only significant case for LP). By contrast, for BP and HP mean deep pressure contributed over 56% of shelf-edge pressure with regression coefficients near 1 but no further contribution from the wind.

Trends in deep and shelf-edge pressure were significantly correlated (32% BP; 48% HP) despite being unreliably determined themselves. Regression coefficients were less than for mean values and may indicate a reduction of cross-slope transfer with reduced length scale, as suggested theoretically, or merely the degrading effect of more noise on regression coefficients.

In summary, trends only related between the deep ocean and the shelf edge (BP & HP). Winds only contributed to shelf edge (LP) and coastal (LP & BP) pressure signals. Deep signals are less than shelf edge signals which are less than coastal signals, but regression coefficients are near 1 for the appearance of

the shelf-edge signal in the coastal record (all frequency bands), for the deep signal at the shelf edge (BP & HP) and overall (HP). In the reverse sense (coast to ocean) however, with a reduction of variance, regression coefficients are necessarily smaller.

3.8 MOMENTUM BALANCE

Ocean - shelfedge - coast pressure differences contribute to the on-offshore (x) momentum balance

$$\frac{\partial u}{\partial t} - fv = -g \zeta_x + \frac{\tau^x}{\rho h}$$

or

$$\rho \Delta x_1 fv = \Delta p - \tau^x \Delta x_2 / h \quad (1)$$

after multiplying by ρ , integrating over a breadth Δx of shelf across which the pressure difference is Δp and neglecting $\partial u / \partial t$ for small cross-shelf currents at low frequencies. Here Δx_1 is a local shelf width used with the alongshelf current observed locally as a time series in CONSLEX, but $\Delta x_2 / h$ is an alongshelf average to multiply the single time series

$$\tau^x = .0012 \rho a W WT \quad (2)$$

for wind stress across the shelf (LARGE et al. 1981). Table 5 gives parameter values used in (1) and (2).

For the alongshelf mean of (1), both across the shelf (coast - shelf edge pressure difference) and across the slope (shelf edge - deep pressure difference) correlations with the geostrophic term fv in (1) are good at low frequencies (LP), 67% of variance being accounted for. Regression coefficients are near 1 across the slope, but suggest that the measured along-shelf currents do not extend across the full shelf width Δx_1 given in table 5. For BP and HP, by contrast, the variance accounted for is very small and insignificant, probably through violation of the geostrophic approximations (small $\partial u / \partial t$) leading to (1). However, wind stress τ^x does explain some HP (only) variance: 20% across the shelf and 8% across the slope. In the latter case, the regression coefficient for the wind stress term in (1) suggests an effective depth less than the 500m assumed.

Along-shelf trends in (1) showed (barely) significant correlations between the term fv and pressure difference only across the slope for LP, accounting for only 12% variance and with an inconsistent coefficient.

Along-shelf momentum terms are generally weaker than the geostrophic terms in (1) and must be evaluated from individual records or the alongshelf trend in

pressure. In particular, pressure gradients were less along the shelf than across. For these reasons, no consistent balance has been found, although typically the geostrophic terms were dominant when evaluated between adjacent locations. (Exceptions were F3 top and bottom and G2 in the Faeroe-Shetland Channel, where alongshelf acceleration exceeded alongshelf pressure gradient; the Coriolis term was largest, nevertheless.) In such an evaluation, $fu = 0(10^{-6} \text{ ms}^{-2})$ corresponds to a surface slope $0(10^{-7})$ or $\Delta p = 1 \text{ mb}/100 \text{ km}$ which is down to the noise level of the pressure records. At higher frequencies where cross-shelf flow is less constrained, shorter flow scales impair the representativeness of the records over the distance between moorings.

Regression against acceleration terms (in addition) was less successful than between geostrophic terms (described above). Bottom friction - neglected in (1) - was found to be weaker than the terms retained, of which wind stress was weakest in total (LP+BP+HP).

The cross shelf balance is considered again in 4.3 for extensive fluctuations of the slope current.

3.9 MEAN FLOW VARIATION

In addition to 'event'-type fluctuations in the slope current, an investigation was carried out to determine whether there was any consistent variation over the spring-neap tidal cycle, as suggested by some earlier observations (BOOTH et al. 1983). Possible causes of such a fluctuation might be rectification of tidal currents to form a slope current (expected to be small; HUTHNANCE, 1984) and greater friction reducing the slope current at spring tides. For this analysis, the 3-hourly data described in I was used, without the reduction to representative series described in section 2 above.

The MSf spring-neap period ~ 14.7653 days was taken as 14.75 days = 118x3h with error ≤ 0.2 days over the CONSLEX duration. Tide tables for elevations in the area show an average 'age' of 1.5 days, and the times of new and full moon over the duration of CONSLEX average to day 231.5 (1982) plus the appropriate number of MSf periods. Thus, to sufficient approximation, spring tides occur at 14.75 day intervals from 2.0 days after the start (day 231.0) of the CONSLEX time series.

Fourier coefficients at 14.75 day period were found from the maximal set of complete 14.75 day blocks of good data for each current series (E and N component at each meter). Up to 24 coefficients were also found similarly at

other periods 14.75 days \pm 3n hours ranging to 1 more and 1 less cycle in the good data. The coefficients for the half of these periods furthest from 14.75 days were taken to indicate the non-tidal 'noise' level. For 91 of 154 series, the 14.75 day 'signal' exceeded this noise; by chance, this would happen on average for only 57 of the 154, suggesting that there is a significant tidal signal in the series taken together. The phases of these 91 spring-neap cycles had standard deviations (determined by the noise level) averaging ± 1.8 days.

The phases themselves are distributed as shown in table 6, with a clustering around 9 and especially 12 days through the 14.75 day cycle beginning on day 231, and no series 180° out of phase at 5 days. Thus there is a clear bias towards stronger currents to the N and E about 3 days after neaps and minimum tidal friction.

Amplitude values of the 14.75 cycle averaged 2.5cm/s and were compared with the mean current component; a significantly non-zero regression coefficient was found only when the comparison set was reduced from all moorings to those on the slope: L2,L3,PR,B3,B4,C2,C3,D2,E2,E3,F3 and G2. Even then, the coefficient 0.07 ± 0.04 is much smaller than most spring-neap effects, and indicates a lack of proportionality between the magnitude of the cycle and the mean current.

A direct tidal forcing can be discounted, the MSf potential being less than 10% of the Mf potential, whose consequences are not evident in the nearby Fourier coefficients calculated.

Thus current fluctuations with a spring-neap period are apparent above 'noise', especially in the slope current. However, the fluctuations are smaller, less dependent on mean current and lagged in comparison with an immediate effect of spring-neap variations in friction. This is consistent with the current system as a whole following the slope current in response to variations in weak friction ('weak' relative to inertia). Even less friction around neaps allows a small but cumulative increase in currents - hence the further phase lag of 3 days $< \pi/2$ in the spring-neap cycle.

3.10 HEAT FLUX

BOOTH (1985) has calculated heat fluxes from $3\frac{1}{2}$ years' records of temperature and current near 57°N 9°W at the Hebrides shelf edge, as contributed by fluctuations u', T' within his 25-hr averaging period (for $u \rightarrow \bar{u}$ defining $u' = u - \bar{u}$). He found small onshore fluxes on average at both 35m and 105m in 134m of water (approximate depths). However, the upper level had a pronounced

summer peak onshore, up to 110kWm^{-2} in June and August, and an offshore peak up to 40kWm^{-2} in September/October. These values include tidal contributions which probably dominate within the 25-hr averaging.

The 3-hourly CONSLEX data as derived in I and used here excludes tidal contributions but allows an assessment of longer-period contributions to heat fluxes. Two calculations were carried out after initially removing record-length means from the current u and temperature series T at each current meter. Firstly, 30-day periods were taken commencing with 1982 day 235, day 250,, day 415; means \bar{u} , \bar{T} were formed over each 30-day period; the heat flux contributions $\rho C_p \bar{u} \bar{T}$ and $\rho C_p (\bar{u} - \bar{u})(\bar{T} - \bar{T})$ averaged over the 30 days were calculated. Typically, these two contributions were comparable but varied in apparently random fashion from one period to another. Secondly, average heat fluxes for the whole record were formed as combined contributions from the lowest frequencies (varying means and trends of 25-day blocks) and frequencies $n/25$ cycles per day (from spectral analysis of the 25-day blocks as in I). It was clear that contributions from low frequencies (corresponding to LP) dominate.

Figure 4 shows largest fluxes along the slope in the Faeroe-Shetland Channel and across the Wyville-Thomson Ridge. The apparently consistent southward average over the Hebrides Shelf and slope must be viewed with caution having regard to the fluctuating lowest-frequency contributions thereto. On-offshelf values of order 10^4 kW/m are comparable with the peak higher frequency contributions found by BOOTH (1985) and are potentially significant in the shelf heat budget. However, along-shelf values are an order of magnitude larger and the actual on-offshelf flux depends critically on the topographic guidance of the slope current along depth contours.

4. ANALYSIS FOR EVENTS

Table 7 lists short periods during CONSLEX when some records are distinctive. These include all events for currents listed in the table of I, and others where the temperature or pressure records have strong signals.

Events are short (only four of 28 exceed 25 days - just) so that cross correlations of the time series are appropriate in seeking structure (rather than spectral analysis using 25 day blocks of data hitherto).

4.1 CORRELATIONS

Variables manifesting or possibly implicated in each event are listed in table 7. Cross-correlations were carried out between these variables (including also the three meteorological series in all cases) for the duration of the events, for LP, BP and HP. As discussed in 3.1 above, the pairwise relationships are not consistent in the absence of perfect correlation; they assist a subjective choice of variables within which to seek structural forms (generalised principal components) through the derivation of representative series (2.2 above). Both correlations and subsequent structures are discussed according to event type (as given in table 7).

4.2 EXTENSIVE RELAXATION OF SLOPE CURRENT

On two occasions during CONSLEX, the normally persistent north/northeast current along the slope stopped. An extensive fall in coastal sea level was also apparent. Pairwise correlations are generally better for LP than BP - an improvement again for HP represents relatively little of the event's variance. Most of the listed current moorings (table 7) correlate with each other at LP; the same holds for the bottom pressures and for the coastal pressures. There are also correlations between different variable types, including along-shelf winds. A notable feature of event 4 was the cooling at the shelf break (recorded on the bottom pressure rig at C1) following northerly winds (DICKSON et al. 1986). Event 25 was remarkable for the fall in sea level at Lerwick; at 37cms the difference between successive monthly means (January and February 1983) was the largest ever recorded there. (A similar fall was recorded at the site of the Conoco Hutton field tension leg platform near $61^{\circ}\text{N } 1\frac{1}{2}^{\circ}\text{E}$, and on mainland gauges from Heysham in the Irish Sea northwards and around to Wick).

The extensive nature of these events is confirmed by the large proportion of LP variance over the whole domain accounted for by one representative series for each variable type.

Event	4	25
days	277-291	393-410
bottom pressure		
stations (Table 7)	11	8
% representation	73	73
coastal sub-surface pressure		
stations (Table 7)	10	11
% representation	93	90
currents		
moorings (Table 7)	6	17
% representation	89	60
overall		
series (Table 7)	10	8
% representation	86	86

(For currents, the representative series for each mooring form the starting point. Then the various series, one for each data type, form the basis for the overall representation.)

Coastal pressures include series from Newlyn to Lerwick (and Torshavn, but small and out of phase in both cases). Amplitudes are greatest on the Malin-Hebrides Shelf, and phase propagation is rapid towards the north/north-east (less clear in event 25). Bottom-pressure variations are largest at B1 and G1, together with the Faeroe-Shetland Channel (event 4) or the Rockall Trough (event 25). Phase propagation is rapid (event 4) but event 25 shows some N-S and ocean-shelf delay. Currents are largest at B1, C2 and additionally D1 (event 4), C3 and especially F3 (event 25). Phases show progression from A to B to C & D in both cases, with near simultaneity along the Faeroe-Shetland Channel for event 25.

For both events, changes of alongslope current correlate well with changes of pressure difference across the current at individual sections. Principal components were calculated for the examples

Event	4	25
days	281-290	393-410
pressure difference	G1 - G4	F1 - F3
alsongslope current	G2, 299m	F3, 388m
variance in principal component	88%	86.5%
inferred stream width	22km	20km
inferred transport change	4.9Sv	7.5Sv

(For comparison, the mean transport along the slope in the Faeroe-Shetland Channel has been estimated as 7 ± 4 Sv; GOULD et al. 1985; $1\text{ Sv} = 10^6 \text{ m}^3/\text{s}$). The stream width is inferred via geostrophy from the principal component's relative coefficients for pressure difference and current, and the transport change assuming a depth 500m for the flow.

The overall 86% representation for both events 4 and 25 is rather flattering, because most variance (in the units used) is contained in the series synthesising currents, coastal pressure and atmospheric pressure; bottom pressures are smaller as are the winds (appropriately on account of less certain measurement). Nevertheless, both events show reduced north/north-eastward currents in phase with lowered coastal pressures and alongshelf winds in the same sense. The lesser bottom pressures show a lag (except for the Faeroe-Shetland Channel in event 25); atmospheric pressures lead (consistent with the eastward tracking of weather systems).

4.3 EXTENSIVE FLUCTUATIONS (FAEROE-SHETLAND CHANNEL)

F1, the deeper current moorings in the Faeroe-Shetland Channel, and to some extent I2, show particularly large LP fluctuations in currents during days 410-440. These currents had extensive pair-wise correlations and some correlation with contemporary bottom pressure and temperature along the Channel and West Shetland Shelf. Temperature records near the thermocline (between upper Atlantic water and deep cold Norwegian Sea water) also fluctuated widely; they are partially included in the moorings' representative modes (2.2/3 above). In contrast with the extensive fluctuations of upper-slope currents (4.2 above) coastal pressures are less correlated with each other or the currents. The representative series only accounts for 59% of the coastal pressures, and in any case is dominated by AU,GR,UL and WI. The five bottom pressure series are better represented (85%); the usual lead of F1 over G1 appears to contrast with a reversed progression to the south-west in the Faeroe-Shetland Channel. An attempt at overall representation, however, does not satisfactorily relate any of the other variables to the currents (themselves poorly accounted for - 53% - in a representative series dominated by the deep moorings FG,G4,I2 and upper levels at E3,E4 and G2).

4.4 PRESSURE EVENT

A dip in bottom pressure was apparent at the operating shelf gauges B1 and especially F1 and G1 around days 330-333, as well as at several coastal gauges, most markedly Wick. Cross-correlations and representative series show similar behaviour for LP at all bottom pressure gauges on the shelf and to a lesser extent off-shelf, and at all coastal gauges with north/northeastward phase propagation. Most variance was LP although some correlation occurred for BP and HP also. An overall representation (combining representative series for bottom pressure, coastal pressure and meteorological variables) showed that all were closely related, atmospheric pressure leading coastal and offshore pressure in turn (with magnitude decreasing in the same order).

4.5 INDIVIDUAL FLUCTUATIONS

On several occasions a signal or slope current reversal at one or a few moorings is strong enough to attract individual attention. A priori these events' correlations are limited in spatial extent; being primarily LP in character their temporal statistics are also poor; inferences from individual cases of good correlation with meteorological series (say) should be treated with caution.

For events 1, 13 and 23 the fluctuations are not apparently correlated with nearby bottom pressure records, perhaps owing to their limited horizontal extent or confinement to depths not affecting the bottom pressure. In these cases correlations with meteorological data (only) were sought, and occurred for LP. Southward currents at B4 in event 1 followed a decrease of atmospheric pressure with a phase lag $0(60^\circ)$ and no strong correlation with winds. During event 13, currents throughout depth at G2, and the alongshelf wind, are extremely well represented (97% overall) by a single time series, in relation to which the wind to the southwest is found to lead the current to southwest by about 90° . During event 23, the three meteorological series and the current at C3 are all closely related to one representative series showing a reversed and then northward slope current lagging alongshore winds in the same sense, and offshore winds, by about $\pi/3$; positive atmospheric pressure was in advance of these winds by $\pi/2$ approximately.

For the other events there were pairwise correlations between some bottom pressure records; deep Rockall Trough records (event 11) or deep (15,20) or all

Faeroe-Shetland Channel records (7,26) were grouped to form representative series; another was formed from all contemporary coastal series in each case, their generally good LP correlation applying equally to event periods.

The Rockall Trough event 11 is primarily a reversal of current at C2, which dominates the related fluctuation at C3. Contemporary fluctuations in bottom pressure at B1 and C4 were much larger than at the other Rockall Trough sites, but dissimilar and smaller than coastal variations which in turn were less than those of atmospheric pressure. None follow the C2 fluctuation very closely.

Fluctuations at moorings in the E line in the Faeroe-Shetland Channel (events 15 and 20) are accompanied by a similar ranking of pressure variations, but the coastal values increase to the south-west and Newlyn and the Malin Shelf have a phase lead. The currents at E2 and E3 (top two meters) do not appear to be closely related to these variations in event 15 (nor to currents elsewhere) but for event 20 a single representative series substantially describes the upper currents at E3 and E4, bottom pressures in the Faeroe-Shetland Channel, coastal pressures and the longshore wind. While the currents rotated cyclonically from south-eastward via northward to south-westward, adjacent coastal pressures were high-low-high in sequence and the longshore wind component was to the north/north-east with a shorter reversed interlude.

A reversal at F1 and F3 (event 7; especially F3 bottom two meters) is less well matched with contemporary coastal pressures and the longshore wind, and the bottom pressures (dominated by F1 and G1) are even less well matched. A north-westward flow at Statfjord (event 26) is accompanied by a corresponding variation in bottom pressure, coastal and atmospheric pressures and winds (LP). In this case the bottom pressure variation is very similar at all positions E3, F1, F3, G1 and G4. The much lower BP variance ($\sim .04$ LP) is less well related between bottom pressure locations and between variable types; currents and coastal pressure have greater variance relative to other variable types.

4.6 DIURNAL OSCILLATIONS

Motion at near-diurnal frequencies was noted in I as a consistent spectral peak in shelf and upper-level current records, and has been interpreted for earlier data in GORDON et al. (1987) as a shelf-wave response to impulsive wind forcing. The table 7 events (chosen subjectively for large amplitude) show occurrences local to one or two of the CONSLEX cross-shelf sections, at HP frequencies (events 5,12,14,16,18,22) and/or BP for events including the OS

mooring (14,22,24,28). (As discussed in GORDON et al. (1987) these oscillations are related to the maximum shelf-wave frequency, which is less at OS; the depth contrast on which the waves propagate is only between the shelf and the Norwegian Trench at OS rather than between the shelf and the Faeroe-Shetland Channel or Rockall Trough).

Excepting event 12 at I2 distant from any bottom pressure records, it was found that the corresponding BP or HP bottom pressure was correlated pair-wise on the respective side (S or NE) of the Wyville-Thomson Ridge. A representative series was formed accordingly (from all bottom pressure records for event 5 with more extensive correlation). Coastal pressure records were grouped similarly to form representative series for UL,MI,PO,MA,AU south of the Wyville-Thomson Ridge (events 16,18 and also 24 for which they were well correlated) and LE,WA,WI northeast of the Wyville-Thomson Ridge (events 14,22,24 and also 16 & 18 for which they were well correlated). TO,LE and WA were grouped for event 28, and all except Newlyn for event 5. Thus it was found that bottom pressure records on the respective side of the Wyville-Thomson Ridge were well accounted for (68-91%) by just one representative series during such events. Shelf-edge and deep records were comparable and all in phase, or showed just small delays to the north/north-east (events 5,24) or in deep water (event 16). Coastal pressures were similarly accounted for (69-94% for UL,MI,PO,MA,AU; 76-94% for LE,WA,WI). A temporal sequence WI,LE,WA was apparent (events 14,16,18,22,24) with largest variances at WI. Overall current-pressure relationships were weak, however. There were hints of a closer relationship with the winds, although they do not sustain an oscillation like the currents. Most of these diurnal oscillation events follow strong, rapidly-varying winds at one or more nearby recording stations (e.g. Sule Skerry) consistent (in general terms) with GORDON et al. (1987). In events 16,22 and 28 initially, rapid variations of wind were recorded not in time but in space, leaving open the possibility of a local impulse between stations. In all cases except event 18, strong changes of LP current also occurred, suggesting that this might also be a forcing mechanism (yet to be explored theoretically) for HP oscillations.

4.7 TEMPERATURE-RELATED EVENTS

As indicated in table 7 these are strong signals identified in temperature records (and often current records too) from a single mooring. Owing to their localised nature and the general lack of correlation with local pressure records

(or even current records in many cases) comparison was made only between any adjacent thermistor chain and bottom temperature series, the mooring representative series and the meteorological series.

Fluctuating increases of upper-level temperature correlated with relaxations of the northward slope current occurred at B3 during event 2. Surprisingly, these fluctuations are coherent with changes in atmospheric pressure, more than with winds; such coherence is probably coincidental for the short duration of the event, which is local to B3 in contrast with the large spatial scale of the atmospheric pressure variation.

Events 3 and 9 both comprise southward flows of cold water near or over the Wyville-Thomson Ridge at I2 and D5 respectively. However, these events are not well related to contemporary meteorological variables, which have different relationships inter alia for the two events.

Events 6 and 21 comprised marked changes of temperature at F3 (a warm period, especially at 388m, following eastward flow) and G4 (a cold period at the top meter, 195m depth). Neither was manifested in deeper measurements of temperature on the mooring or the adjacent bottom pressure rig. The event 6 temperature variation at F3 had a similar relationship with the current as for the whole record, and could plausibly have been forced by a contemporary alongshelf wind to the north-east. However, the G4 event 21 was not in the usual relationship with currents; the mean north-eastward flow, relaxed initially, was gradually restored through the period; correlation with meteorological variables was poor and a temporary influx of colder water from the north-west side of the Faeroe-Shetland Channel seems likely.

Events 8, 17 and 19 on the West Shetland shelf edge show in the bottom temperature and G1 thermistor chain records - where relevant - at G1, F1 and G1 respectively, and only at these single locations. Although they may be influenced by the dominant meteorological forcing on the shelf, such localisation suggests that 'eddy' structure in the temperature field, apparent at 0(10km) in satellite images of sea surface temperature, also plays a role. This is reinforced by a departure from usual temperature-current relationships in these events.

5. DISCUSSION

CONSLEX was carried out from August 1982 to March 1983, primarily during the winter season with little stratification down to about 500m depth, expecting to

observe simpler barotropic motions with greater energy from meteorological forcing. Indeed, temperature variations were generally small, typically 0.1°C rms except for the seasonal cycle, and we have continued the philosophy by constructing representative series controlled by the currents (and not the temperature variations) on each mooring. Larger variations occur at greater depth in permanent thermoclines, notably at L3 and in the Faeroe-Shetland Channel. Nevertheless, any conclusions apply principally to the winter season because seasonal stratification broke down two months into the experiment (and soon after the later deployment of Faeroe-Shetland Channel moorings).

The breakdown of seasonal stratification was itself noteworthy for taking longer at G1 than at B2, where the lower layer warming (as recorded by the thermistor chain) was quite rapid. Stratification intensity and form, wind and wave activity and sources of interior mixing all play a role; the latter perhaps forms the more likely distinction between the two sites; internal waves were prominent as high-frequency temperature fluctuations during the period of lower layer warming.

Currents on the shelf and slope were found in I to be largely barotropic, enabling one principal component to represent a large proportion of each mooring's variance. The representative series used here account for a yet larger proportion of variance (necessarily, by definition) but Appendix A shows principally barotropic forms. Exceptions where upper and lower series have been constructed (guided by I) are in the Faeroe-Shetland Channel, the division being according to the depth of the cold bottom water from the Norwegian Sea. By using only the representative series, we have neglected motion which is incoherent in principle and baroclinic in practice.

Sea level was found to be the oceanographic variable with most spatial coherence in CONSLEX, as in several earlier sets of observations on continental shelves (see e.g. ALLEN, 1980). However, this statement applies only to the 'mainland' coasts of Great Britain and Eire. Torshavn on the Faeroes was little correlated and had much less variance. Newlyn (to the south, and independent of forcing around Scotland) Walls and Lerwick (towards the shelf edge on Shetland) also had less variance than most ports.

Widespread coherence extended to other LP variables on the shelf; bottom pressure, currents and alongshelf winds. The coherence decreased with increasing frequency, and markedly over the slope and in deeper waters. Although the observations were not sufficiently detailed to resolve several mode forms, and indeed wind forcing prevailed, this character is suggestive of a

response dominated by first mode continental shelf waves. At low frequencies these have currents predominantly of one sign along the shelf and are mostly confined there, balanced geostrophically by an across-shelf slope to an extreme elevation at the coast, and form a natural response following winds of large scale relative to the shelf width (GORDON et al. 1987). Higher frequencies correspond to shorter scales along the shelf and eventually to reduced speeds and expected distances of propagation and correlation, as well as shorter-scale, meteorological forcing. Other modes with relatively stronger currents in deeper slope waters are slower and hence decay and decorrelate in a shorter distance along the slope. This is in accord with the observation of reduced along-shelf coherence at higher frequencies and in deeper water.

Over the slope, however, the along-slope alignment of the mean and varying current (already remarked in I) shows the expected topographic control of low-frequency flow. A near geostrophic balance for cross-shelf momentum is also supported by direct evaluation of the Coriolis and pressure terms, for LP, and indirectly by the decorrelation of these terms with increasing frequency for which assumptions implying geostrophy are violated (section 3.8).

Bottom pressure and coastal sea level records were not closely tied by such a geostrophic balance. Indeed, the direct regression of coastal on oceanic pressure was most significant for HP. There appear to be two overall breaks in the ocean-coast relationship. Slope currents (and alongshelf currents too) may be generated by adjacent eddies, changes in shelf geometry and perhaps other short-scale factors, introducing geostrophic differences between oceanic and shelf pressures. Additional motion on the shelf (coastal currents, eddies thereon, meteorological forcing of reduced scale at fronts, say, or combined with complex coastal geometry) is found to give coastal pressure (CP) large additional variance not correlated with offshore bottom pressure (OP). An effect of the latter is that, even if OP transfers fully to the coastal signal CP, i.e.

$$CP = OP + N$$

the additional 'noise' N prevents the reverse inference: writing

$$OP = a CP + N'$$

we have

$$\text{varOP} = a^2(\text{varCP} = \text{varOP} + \text{varN}) + \text{varN'}$$

and hence

$$a^2 = (\text{varOP} - \text{varN'})/(\text{varOP} + \text{varN}).$$

Thus the additional coastal variance N severely weakens coastal measurements as

a monitor of oceanic variations. There are theoretical reasons for expecting better results through reduced N around islands with small total extent (including shelves; HUTHNANCE, 1987).

We have scarcely tested theory (HUTHNANCE, 1987) regarding ocean-coast transfer in relation to alongshore scale. Surprisingly, even the along-shelf extent of CONSLEX, with pressure recorders in seven sections and a comparable array of coastal gauges, proved insufficient to define alongshelf scales in the data, only a mean and a trend (marginal) being deducible. This disappointment results to some extent from limitations of the array, but also from rather weak oceanic pressure signals in this area, and effects of wide and variable shelf geometry, so that all records are 'noisy'. The issue is significant because sea-level is a relatively easily monitored integrated measure of ocean circulation and is now a popular candidate as a continuing indicator thereof. However, it seems unlikely that a more extensive array than CONSLEX will be deployed (to address this question alone). At least in areas with strong oceanic signals, satellite altimetry with coastal levels offers promise for the better spatial coverage required for a proper test.

The fortnightly variation in flow to the north east, with a statistically significant maximum to the north east typically 3 days after neap tides, suggests a tidal friction control on the 'general circulation'; comparison with other directly-forced tidal frequencies discounts direct tidal forcing, and there is no clear correlation of fortnightly amplitude with strength of mean flow. Because the phenomenon has been found on a statistical basis throughout the array, a similar analysis of other long time series of currents would be appropriate to determine the extent of this fortnightly variation. A basin-wide scale is an open possibility. The timing is consistent with a slope current response to weak friction varying over the spring-neap tidal cycle, with a lag of less than $\pi/2$. Surface slopes involved in accelerating the variation are quite small, i.e. feasible but hardly detectable: σ/ρ is $O(0.5 \times 10^{-5} \text{ s}^{-1} \times 0.02 \text{ ms}^{-1} / 10 \text{ ms}^{-2})$ or $10^{-8} = 1 \text{ cm} / 10^3 \text{ km}$: about 0.1 x slope current driving.

Other large variations of the slope current occurred, notably when it relaxed extensively in events 4 and 25 around days 280 and 400 respectively. These two events accorded with the LP data overall in the alongshore coherence and relationship of shelf currents, coastal sea level, shelf edge bottom pressure and alongshelf wind.

Events otherwise lack a coherent picture. A majority as described in sections 4.5 and 4.7 appear to be local in character and suggest the presence of 'eddies'

as seen in satellite IR images of sea surface temperature (in the rare absence of cloud). Eddies may propagate from elsewhere (e.g. the polar front or the Norwegian Coastal Current) or result from instability of the slope current. Time scales are just a few days so that their stochastic nature implies a need for regular monitoring of a more detailed nature than in CONSLEX, if such events are to be predicted deterministically.

The heat flux estimates included contributions at long periods (> 25 days) comparable with all other sub-tidal components. Even the five months typical of CONSLEX records thus gives poor statistics, and several years as at one Hebrides shelf-edge location (BOOTH, 1985) are required for any estimate of a seasonal variation. The spatial variability in the estimates also suggests the need for a comparison between closer moorings to establish the spatial scales of variability and hence for deployments required to determine a budget. The longshelf dominance also implies a need for accurate flow direction in estimates. However, the values do imply significance for the shelf-sea heat balance.

The eddies referred to above are more prominent and of larger scale in the Faeroe-Shetland Channel, where the stratification, between North Atlantic water above and cold Norwegian Sea water below, is reflected in a two-layer character of the observed flow.

For these reasons, plus a lack of information on adjacent oceanic flow generally, and perhaps other causes too, barotropic modelling (GORDON et al. 1987) was less successful in describing currents over the deeper slope than on the shelf. Larger scale shelf phenomena and especially the associated coastal elevations are well described; this can include impulsively forced near-diurnal oscillations if the meteorological context is known with sufficient detail.

Owing to the prevalence of forcing and the complex geometry (albeit the simplest shelf sector around Britain) it has not been considered feasible to pursue an analysis in terms of coastal trapped waves as so successfully demonstrated for the Australian Coastal Experiment (e.g. CHURCH et al. 1986).

6. CONCLUSIONS

Deep temperature fluctuations in the bottom of the Rockall Trough or Faeroe-Shetland Channel are small.

Shelf temperature fluctuations were $0(0.1^{\circ}\text{C rms})$ and mostly LP, superimposed on the seasonal cycle. Bottom temperatures at C3 and on the shelf increased by

$0(1^{\circ}\text{C}/\text{ms}^{-1})$ with the 'slope current' to the north/northeast.

Coastal pressures are extensively correlated (especially for LP which is dominant) and also correlate with atmospheric pressure and winds. Phase propagates north/northeastwards for LP and BP.

Shelf-break bottom pressure is also extensively correlated with north/northeastward phase propagation, and coherent with alongshelf wind, for LP.

There is evidence in deep bottom pressures of a Rockall Trough - Faeroe Shetland Channel 'see-saw' oscillation at very low frequencies.

Deep pressure transferred fully to the shelf break only for BP and HP (in alongshore mean; alongshore trend transferred in part). Shelf break pressure transferred fully to the coast in alongshore mean (only) provided that correlated winds were allowed for. The importance of wind (principally a contribution to coastal pressure) in these relationships decreased with increasing frequency. Owing to extra variance in the coastal record, regression coefficients are reduced for the reverse inference (deep pressure from coastal values).

Currents on the shelf show extensive coherence inter alia and with meteorological variables, especially LP alongshelf wind; such coherence decreases in extent as frequency increases. There is LP coherence between shelf currents, shelf break bottom pressure, coastal pressure and alongshelf wind.

Currents over the slope in 500m are principally aligned along the slope but are less coherent inter alia than shelf currents.

Currents in 1000m or more are more energetic and rotary in the Faeroe-Shetland Channel (although F3B2 is aligned along the slope for LP).

HP currents (or equivalently BP at OS and ST) have greatest amplitudes near the shelf break: the other notable locations are B2 and G1. They are polarised clockwise.

A momentum balance was successfully observed only for LP, with near-geostrophy between variations of along-slope flow and cross-slope pressure difference. This is significant in showing that the lack of ocean-shelf LP pressure transfer is associated with geostrophic flow along the slope.

Currents are (statistically) stronger to the north/northeast about 3 days after neap tides and presumably minimum tidal friction. The amplitude of variation, about 2cm/s , is not clearly related to the mean flow strength.

The heat flux contribution from long periods > 25 days is comparable with all other sub-tidal components.

REFERENCES

- ALLEN, J.S. 1980 Models of wind-driven currents on the continental shelf.
Annual Review of Fluid Mechanics, 12, 389-433.
- BOOTH, D.A. 1985 Heat flux across the Scottish shelf edge.
Ocean Modelling, 64, 14-15. (Unpublished manuscript.)
- BOOTH, D.A. & ELLETT, D.J. 1983 The Scottish continental slope current.
Continental Shelf Research, 2, 127-146.
- CARTWRIGHT, D.E. 1983 On the smoothing of climatological time series, with
application to sea level at Newlyn.
Geophysical Journal of the Royal Astronomical Society, 75, 639-658.
- CHURCH, J.A., WHITE, N.J., CLARKE, A.J., FREELAND, H.J. & SMITH, R.L. 1986
Coastal-trapped waves on the East Australian continental shelf.
Part II: model verification.
Journal of Physical Oceanography, 16, 1945-1957.
- DICKSON, R.R. & McCAYE, I.N. 1986 Nepheloid layers on the continental slope
west of Porcupine Bank.
Deep-Sea Research, 33A, 791-818.
- GORDON, R.B., FLATHER, R.A., WOLF, J., KANTHA, L.H. & HERRING, H.J. 1987
Modeling the current response of continental shelf waters to winter
storms: comparisons with data.
pp 503-512 in, 19th Annual OTC conference, Houston, Texas.
- GORDON, R.L. & HUTHNANCE, J.M. 1987 Storm-driven continental shelf waves over
the Scottish continental shelf.
Continental Shelf Research, 7, 1015-1048.
- GOULD, W.J., LOYNES, J. & BACKHAUS, J. 1985 Seasonality in slope current
transports N.W. of Scotland.
International Council for the Exploration of the Sea, C.M. 1985/C:7,
Hydrography Committee, 7 pp. & figs. (Unpublished manuscript.)
- HUTHNANCE, J.M. 1983 Sub-tidal motion on the Scottish continental shelf,
August-September 1971.
Continental Shelf Research, 1, 221-236.
- HUTHNANCE, J.M. 1984 Slope currents and "JEBAR".
Journal of Physical Oceanography, 14, 795-810.
- HUTHNANCE, J.M. 1987 Along-shelf evolution and sea levels across the
continental slope.
Continental Shelf Research, 7, 957-974.

- HUTHNANCE, J.M., LOYNES, J. & EDDEN, A.C. 1988 An investigation of meteorological effects on currents in the shelf and continental slope seas northwest of the U.K. I. Analyses for individual moorings. Proudman Oceanographic Laboratory, Report No. 2, 211pp.
- LARGE, W.G. & POND, S. 1981 Open ocean momentum flux measurements in moderate to strong winds. Journal of Physical Oceanography, 11, 324-336.
- PUGH, D.T. 1987 The global sea-level observing system. Hydrographic Journal, 45, 5-8.

TABLE AND FIGURE CAPTIONS

Table 1.	Current meter moorings.
Table 2.	Other data locations.
Table 3.	Cross-correlations and cross-spectra formed.
Table 4.	Regression results in section 3.7.
Table 5.	Parameter values used in section 3.8.
Table 6.	Distribution in time of algebraic maximum current component to east or north, in 14.75 day cycle beginning day 231.0.
Table 7.	Events analysed in section 4.

Figure 1. Frequency dependence of amplification introduced by HILOW filter (CARTWRIGHT, 1983; L=3, M=5, N=24) on 3-hourly values. Phases are unchanged.

Figure 2. Location of data. . coastal sea level
 + current meters
 x bottom pressure
 o thermistor chain

Figure 3. Representative series for groups of current meter moorings. Only relative signs and line lengths within one plotted mode form are relevant. Forms are for depth average of mooring modes given in Appendix 1. Sense of rotation is from dotted 'imaginary' vector to continuous 'real' vector around common origin.

a) Shelf moorings A1,B1,B2,C2,D1,D2,F1,G1,OS,ST; all frequency bands.

b) Low pass groupings of moorings:

 L2,B3,C2,D2,D5B1,D5T1,E2,G2B,G2T2 (500m);

 B4,C3,E3T2,E3N,E4T,E4B,F3T2,F3B2 (1000m);

 D1,D2,D2T1,D5B1 (Wyville-Thomson Ridge).

Figure 4. Record-average depth-integrated heat fluxes. Double arrows represent large fluxes on one-tenth scale.

Appendix figures are described in the respective appendix.

Table 1: Current meter moorings

Name	Position	Depth(m)	Set	Recovered	Meter depths(m)
L2	51° 41.8'N 14° 57.3'W	758	28-06-82	28-09-82	332,728
	51° 41.4'N 14° 56.3'W	786	25-09-82	14-05-83	352,757
L3	51° 41.1'N 15° 12.7'W	1537	26-06-82	25-09-82	789,1487
L4	51° 42.1'N 15° 18.8'W	2404	26-06-82	25-09-82	2354
A1	57° 20.7'N 9° 7.2'W	145	21-08-82	18-02-83	55,120
PR	57° 5.8'N 9° 23.0'W	1032	27-04-82	22-10-82	130,428,729
A5	57° 18.6'N 9° 40.4'W	1614	21-08-82	17-02-83	209,510,1111,1562
MR	57° 17.6'N 10° 20.2'W	2201	28-04-82	12-12-82	160,570,1070,1820
	57° 16.7'N 10° 18.7'W	2224	16-02-83	22-05-83	156,567,1068
FR	57° 28.4'N 12° 15.3'W	1815	08-05-82	23-10-82	89,500,1001,1752
	57° 27.4'N 12° 14.3'W	1818	23-10-82	16-02-83	103,1016,1765
	57° 27.4'N 12° 14.3'W	1820	16-02-83	18-05-83	53,804,1305,1715
B1	57° 56.3'N 8° 51.0'W	155	28-08-82	25-10-82	55,130
	57° 56.0'N 8° 51.4'W	152	25-10-82	18-02-83	52
B2	58° 0.7'N 9° 7.7'W	193	28-08-82	27-10-82	43,168
	58° 0.8'N 9° 8.9'W	194	12-12-82	11-02-83	43,169
B3	58° 6.5'N 9° 33.1'W	504	28-08-82	11-02-83	104,257,457
B4	58° 8.3'N 9° 41.2'W	1082	28-08-82	11-02-83	169,477,784,1035
C2	59° 5.4'N 7° 27.0'W	514	24-08-82	12-02-83	115,266,468
C3	59° 8.5'N 7° 42.4'W	998	23-08-82	12-02-83	104,403,951
D1	59° 39.8'N 6° 0.5'W	210	27-08-82	03-09-82	60
	59° 39.8'N 6° 2.5'W	237	29-09-82	13-02-83	87,212
D2	59° 46.7'N 6° 10.8'W	370	27-08-82	13-02-83	120,270,345
D5	60° 9.9'N 7° 44.5'W	637	21-11-82	27-05-83	102,510,633
I2	60° 12.3'N 9° 12.6'W	1463	18-03-82	27-03-83	251,654,1055,1440
E2	60° 13.3'N 4° 31.8'W	478	10-10-82	02-08-83	453
E3	60° 31.2'N 4° 56.8'W	1035	09-10-82	23-03-83	120,419,725
E4	60° 46.4'N 4° 49.4'W	1015	23-11-82	26-05-83	95,950
F1	61° 9.3'N 1° 31.7'W	189	03-10-82	16-03-83	39
F3	61° 24.8'N 2° 6.1'W	995	04-10-82	16-03-83	79,388,694,945
G1	61° 30.7'N 0° 2.5'E	191	05-10-82	31-01-83	41,166
	61° 31.7'N 0° 2.0'E	186	31-01-83	24-02-83	161
G2	62° 6.1'N 0° 3.9'E	550	05-10-82	17-03-83	151,299,500
G4	63° 8.8'N 0° 0.9'E	1611	04-10-82	18-03-83	195,496,1104,1554
ST	61° 19.5'N 1° 55.1'E	150	01-12-82	09-03-83	30,70,147
OS	60° 33.9'N 2° 47.7'E	102	07-10-82	12-02-83	2,12,25,50,99
			21-02-83	27-04-83	

Table 2. Other Data Locations

Temperature was recorded on all current meters except at ST and OS, see table 1.

Thermistor Chains

Name	Position	Water depth (m)	Set	Recovered	Thermistor depths(m)
B2	58° 0.6'N 9° 7.6'W	201	28-08-82	11-02-83	120(5)170
G1	61° 30.0'N 0° 2.0'E	192	05-10-82	31-01-83	85(7½)160
	61° 29.6'N 0° 2.0'E	192	31-01-83	17-03-83	

Bottom Pressure and Temperature

Name	Position	Water depth (m)	Set	Recovered
A6	57° 19.0'N 9° 52.5'W	1984	22-08-82	17-02-83
B1	57° 56.3'N 8° 51.4'W	152	28-08-82	25-10-82
	58° 0.8'N 9° 33.4'W	213	25-10-82	11-02-83
B5	58° 11.5'N 9° 57.5'W	1870	23-08-82	11-02-83
C1	58° 59.2'N 7° 23.9'W	205	24-08-82	25-10-82
C4	59° 11.6'N 7° 41.5'W	1086	23-08-82	12-02-83
D1	59° 39.3'N 6° 1.8'W	213	27-08-82	16-11-82
	59° 38.3'N 6° 0.5'W	190	03-02-83	13-02-83
E3	60° 31.7'N 4° 58.8'W	1027	09-10-82	23-03-83
F1	61° 8.5'N 1° 32.0'W	185	03-10-82	16-03-83
F3	61° 24.2'N 2° 5.6'W	1045	04-10-82	16-03-83
G1	61° 30.0'N 0° 2.0'E	192	05-10-82	17-03-83
G4	63° 7.9'N 0° 0.4'W	1574	04-10-82	18-03-83

Coastal Sea level

Name	Position	Set	Recovered	Comments
Aughris Head	54°16.4'N 8°45.5'W	25-07-82	16-07-83	dries out, low water springs
Malin Head	55°22.5'N 7°24.0'W	23-07-82	15-07-83	
Griminish Point	57°38.7'N 7°27.9'W	06-07-82	08-08-83	dries out, low water springs pressure point moved; suspect datum
Walls	60°13.5'N 1°34.1'W	08-09-82	04-08-83	late start after faulty tape.
Newlyn	50° 6.1'N 5°32.5'W	Permanent Installations		
Portpatrick	54°50.5'N 5° 7.1'W			
Millport	55°45.0'N 4°54.2'W			
Ullapool	57°53.7'N 5°10.4'W			gaps
Stornoway	58°12.0'N 6°23.0'W			gaps

Table 2 (continued)

Wick 58°26.5'N 3° 5.1'W
Lerwick 60° 9.0'N 1° 8.0'W

Torshavn 62° 01'N 6° 46'W

courtesy of Danish
Meteorological Office

Atmospheric Pressure (P) and Winds (W)

Name	Position	Variables used	Comments
Sule Skerry	59° 05'N 4° 24'W	W	
Torshavn	62° 01'N 6° 46'W	P,W	courtesy of Danish Meteorological Office
OWS Lima	57° 00'N 20° 00'W	P	
Lerwick	60° 08'N 1° 11'W	P,W	
Cape Wrath	58° 37'N 5° 00'W	P	
Wick	58° 27'N 3° 05'W	P	
Stornoway	58° 13'N 6° 20'W	P,W	
Benbecula	57° 28'N 7° 22'W	P,W	
Tiree	56° 30'N 6° 53'W	P,W	
Abbotsinch	55° 52'N 4° 26'W	P	
Mull of Galloway	54° 38'N 4° 51'W	P	
Gwennap Head	50° 02'N 5° 40'W	P	
Shannon	52° 41'N 8° 55'W	P	six-hourly values
Belmullet	54° 14'N 10° 00'W	P	(only) from Daily
Malin Head	55° 22'N 7° 20'W	P	Weather Reports

Table 3.

Cross-correlations(C) and cross-spectra (S) formed.
All entries imply inclusion of meteorological data.
Qualification refers to the heading above.

	Bottom Temperature	Thermistor Chains	Coastal sub-surface Pressure	Bottom Pressure	Currents
Bottom Temperature	S				S nearest
Thermistor Chains	S nearest	C,S			C } S } nearest
Coastal sub-surface Pressure			C,S		
Bottom Pressure			C nearest	C groups, S	C groups
Currents			C nearest		C groups, S

Table 4. Regression results in section 3.7, 3.8

Values given are regression coefficients (fraction of variance accounted for in brackets below).

* - Significant coefficient.

Dependent	Independent	Frequency band	(2 independent variables)			
			Along-shelf means	Along-shelf mean	Longshore wind	Along-shelf trends
Coastal Pressure	Oceanic Pressure	LP	-1.8* (0.12)	-0.33	-0.78* (0.7)	0.51 (0.01)
		BP	0.27 (0.01)	0.38	-0.34* (0.15)	0.65 (0.02)
		HP	1.04* (0.20)	1.06*	-0.11 (0.22)	0.32 (0.01)
Oceanic Pressure	Coastal Pressure	LP	-0.06* (0.12)	-0.04	0.03 (0.08)	0.09 (0.01)
		BP	0.04 (0.01)	0.06	0.05 (0.03)	0.02 (0.02)
		HP	0.19* (0.20)	0.20*	0.04 (0.21)	0.03 (0.01)
Coastal Pressure	Shelf Edge Pressure	LP	2.0* (0.55)	1.2*	-0.56* (0.85)	-0.12 (0.01)
		BP	0.87* (0.15)	0.81*	-0.31* (0.28)	0.20 (0.02)
		HP	0.96* (0.31)	0.95*	-0.08 (0.32)	0.14 (0.01)
Shelf Edge Pressure	Coastal Pressure	LP	0.28* (0.55)	0.43*	0.16* (0.62)	-0.11 (0.01)
		BP	0.17* (0.15)	0.19*	0.04 (0.16)	0.09 (0.02)
		HP	0.32* (0.31)	0.32*	0.01 (0.31)	0.11 (0.01)
Shelf Edge Pressure	Oceanic Pressure	LP	-0.53 (0.06)	-0.11	-0.20* (0.35)	0.13 (0.02)
		BP	0.78* (0.56)	0.80*	-0.07* (0.61)	0.68* (0.32)
		HP	1.03* (0.66)	1.03*	-0.04 (0.66)	0.86* (0.48)
Oceanic Pressure	Shelf Edge Pressure	LP	-0.13 (0.06)	-0.04	0.06 (0.13)	0.18 (0.02)
		BP	0.73* (0.56)	0.75*	0.06* (0.60)	0.47* (0.32)
		HP	0.64* (0.66)	0.64*	0.03 (0.66)	0.57* (0.48)
Coastal -Shelf Edge Pressure	Scaled Transport along shelf	LP	0.45* (0.67)	0.46*	-0.90* (0.69)	0.08 (0.02)
		BP	0.19* (0.06)	0.17	-1.08* (0.15)	-0.007 (0.0001)
		HP	-0.05 (0.01)	-0.02	0.46 (0.02)	-0.10 (0.02)
Scaled Transport along shelf	Coastal -Shelf Edge Pressure	LP	1.49* (0.67)	1.49*	1.93* (0.70)	0.20 (0.02)
		BP	0.34* (0.06)	0.34*	0.01 (0.06)	-0.01 (0.0001)
		HP	-0.22 (0.01)	-0.07	-3.51* (0.20)	-0.24 (0.02)
Shelf Edge -Oceanic Pressure	Scaled Transport along slope	LP	-0.72* (0.67)	-0.73*	-0.30 (0.68)	-0.10* (0.12)
		BP	-0.03 (0.003)	-0.03	-0.94 (0.02)	-0.01 (0.002)
		HP	-0.009 (0.001)	-0.006	3.02* (0.08)	0.002 (0.0001)
Scaled Transport along slope	Shelf Edge -Oceanic Pressure	LP	-0.94* (0.67)	-0.94*	-3.3 (0.69)	-1.23 (0.12)
		BP	-0.10 (0.003)	-0.10	0.07 (0.003)	-0.13 (0.002)
		HP	-0.09 (0.001)	-0.06	-0.97 (0.002)	0.04 (0.0001)

Table 5. Parameter values used in section 3.8

Locations	cross-shelf distance Δx , km
A1	116
B1,B2	104
D1	122
F1	52
G1	85
OS	244
ST	173

Average $\Delta x_2 = 128\text{km}$

Locations	cross-slope distance Δx , km
A5	29
B3	32
B4	19
C2	16
C3	11
D2	22
E2	33
E3	19
F3	40
G2	179

Average $\Delta x_2 = 57\text{km}$

ρ	density	1027 kg/m ³
f	Coriolis parameter	$1.26 \times 10^{-4} \text{ s}^{-1}$
h	depth: shelf	150m
	slope	500m

Wind was converted to the same units through multiplication by

$$\frac{\Delta x_2}{h} 0.0012 | \underline{W} | \rho a$$

where the latter factors from LARGE et al. (1981) with typical $| W | = 10\text{ms}^{-1}$, $\rho a = 1.25 \text{ kg/m}^3$ were used to derive wind stress units from the cross-shelf wind series.

Table 6. Distribution in time of algebraic maximum
current component to east or north, in 14.75 day
cycle beginning day 231.0

Time (days)	Number of occurrences
0- 1	9
1- 2	9
2- 3	11
3- 4	3
4- 5	5
5- 6	0
6- 7	9
7- 8	3
8- 9	7
9-10	19
10-11	14
11-12	18
12-13	27
13-14	12
> 14	8

Table 7. Events analysed in section 4
Variables concerned (meteorological variables always)

Number	Period (days, 1982)	currents	current meter temperature	thermistor chain	bottom temperature	bottom pressure	coastal pressure	Character
4	277-291	A1,B1,B2, C2,D1,D2		B2	B1,D1	A6,B1,B5,C1,C4 D1,E3,F1,F3,G1,G4	TO,LE,WA,WI,GR, MI,PO,MA,AU,NE	extensive relaxation
25	393-410	A1,A5,B1,B2,B3,C2,C3, D1,D2,D5T1,D5B1,I2,F1, F3T2,F3B2,G2T2,G2B,		B2	B1,F1,F3	A6,B1,C4,E3, F1,F3,G1,G4	TO,LE,WA,WI,UL,GR, MI,PO,MA,AU,NE	of slope current
27	410-440	E2,E3T2,E3N,E4T,E4B F1,F3T2,F3B2,I2, G2T2,G2B,C4T1,C4B3			E3 F1,F3 G4	E3 F1,F3 G1,G4	TO,LE,WA,ST,UL,GR, MI,PO,MA,AU,NE	extensive strong fluctuations (Faeroe-Shetland Channel)
10	329-334					A6,B1,B5,C4, E3,F1,F3,G1,G4	LE,WA,WI,MI, PO,MA,AU,NE	low pressure at F1,G1; WI
1	260-280	B4						<u>Individual fluctuations</u>
7	310-340	F1,F3B2,F3T2			F1,F3	A6,B1,B5,C4,D1, E3,F1,F3,G1,G4	TO,LE,WA,WI,GR, MI,PO,MA,AU,NE	sharp southward peak flow reverses to southwest
11	339-350	C2,C3				A6,B1,B5,C4, E3,F1,F3,G1,G4	TO,LE,WA,WI,UL, MI,PO,MA,AU,NE	flow reverses to southwest at C2; C3 oscillatory
13	348-353	G2T2,G2B						peak in G2T2 eastward flow
15	350-370	E2,E3T2,E3N,E4T,E4B			E3	A6,B1,B5,C4, E3,F1,F3,G1,G4	TO,LE,WA,WI,UL, MI,PO,MA,AU,NE	strong reversals
20	370-390	E3T2,E3N,E4T,E4B			E3	A6,B1,B5,C4, E3,F1,F3,G1,G4	TO,LE,WA,WI,UL,GR, MI,PO,MA,AU,NE	strong reversals
23	380-395	C3						strong flow to southwest then northeast
26	400-415	ST				A6,C4, E3,F1,F3,G1,G4	TO,LE,WA,WI,UL,GR, MI,PO,MA,AU,NE	strong flow to northwest
5	295-305	A1,B1,B3			B1	A6,B1,B5,C4,D1, E3,F1,F3,G1,G4	TO,LE,WA,WI,GR, MI,PO,MA,AU,NE	<u>near-diurnal oscillations</u>

Table 7. (continued)

Number	Period (days, 1982)	currents	current meter temperature	thermistor chain	bottom temperature	bottom pressure	coastal pressure	Character	
12	341-351	I2(bottom 2)							near-
14	348-362	ST,OS				A6,B1,B5,C4, E3,F1,F3,G1,G4	TO,LE,WA,WI,UL, MI,PO,MA,AU,NE	and flow to north/northwest	diurnal
16	353-362	C2,C3				A6,B1,B5,C4, E3,F1,F3,G1,G4	TO,LE,WA,WI,UL, MI,PO,MA,AU,NE		oscillations
18	365-380	B1,B2,B3		B2	B1	A6,B1,B5,C4, E3,F1,F3,G1,G4	TO,LE,WA,WI,UL, MI,PO,MA,AU,NE		
22	379-390	ST,OS				A6,B1,B5,C4, E3,F1,F3,G1,G4	TO,LE,WA,WI,UL,GR, MI,PO,MA,AU,NE	and change of LP flow	
24	390-402	OS				A6,B1,C4,E3, F1,F3,G1,G4	TO,LE,WA,WI,UL,GR, MI,PO,MA,AU,NE		
28	422-447	OS				E3,F1,F3,G1,G4	TO,LE,WA,ST,UL,GR, MI,PO,MA,AU,NE		
2	268-279	B3	B3					top temperature has +ve 'pulses'	
3	272-300	I2	I2					current fluctuates	
6	297-305	F3B2,F3T2	F3B2,F3T2		F3			cold events at bottom two meters	
8	317-322	G1	G1	G1	G1			warm peak at middle two meters	
9	328-350	D5T1,D5B1	D5T1,D5B1					sharp irreversible cooling	
								cold pulse to southwest day 330 and strong fluctuations	
17	357-360	F1	F1		F1			strong oscillation	
19	368-392	G1	G1	G1	G1			large variance at all frequencies	
21	372-388	G4T1,G4B3	G4T1,G4B3		G4			cold trough at top meter	

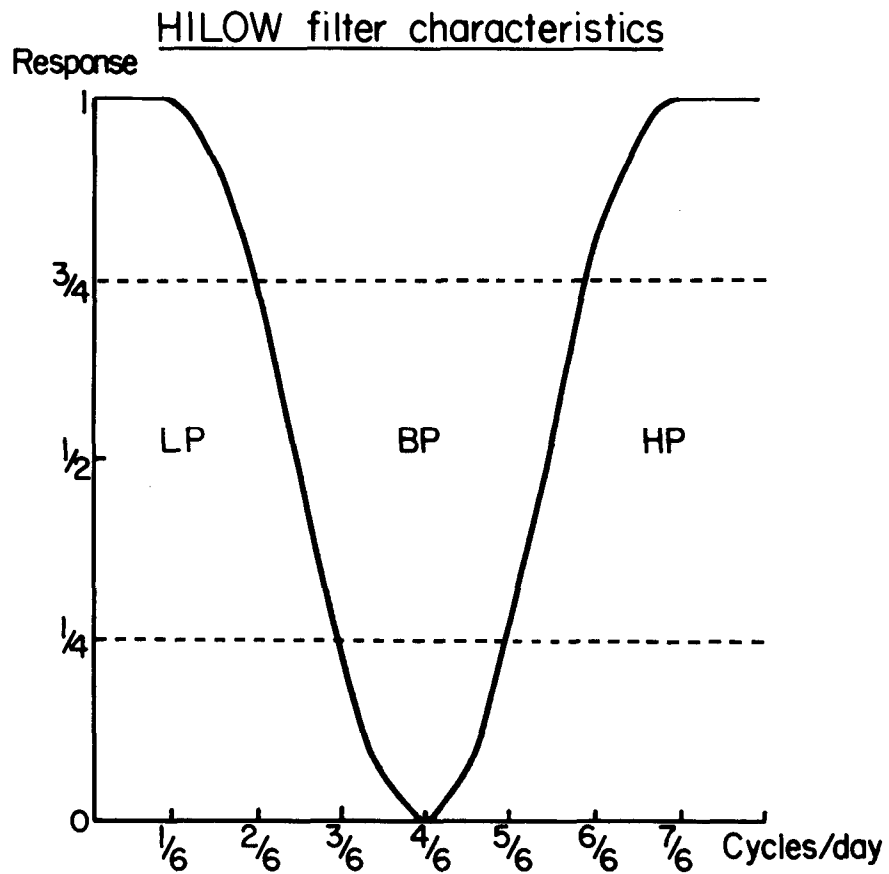


Figure 1. Frequency dependence of amplification introduced by HILOW filter (CARTWRIGHT, 1983; $L=3$, $M=5$, $N=24$) on 3-hourly values. Phases are unchanged.

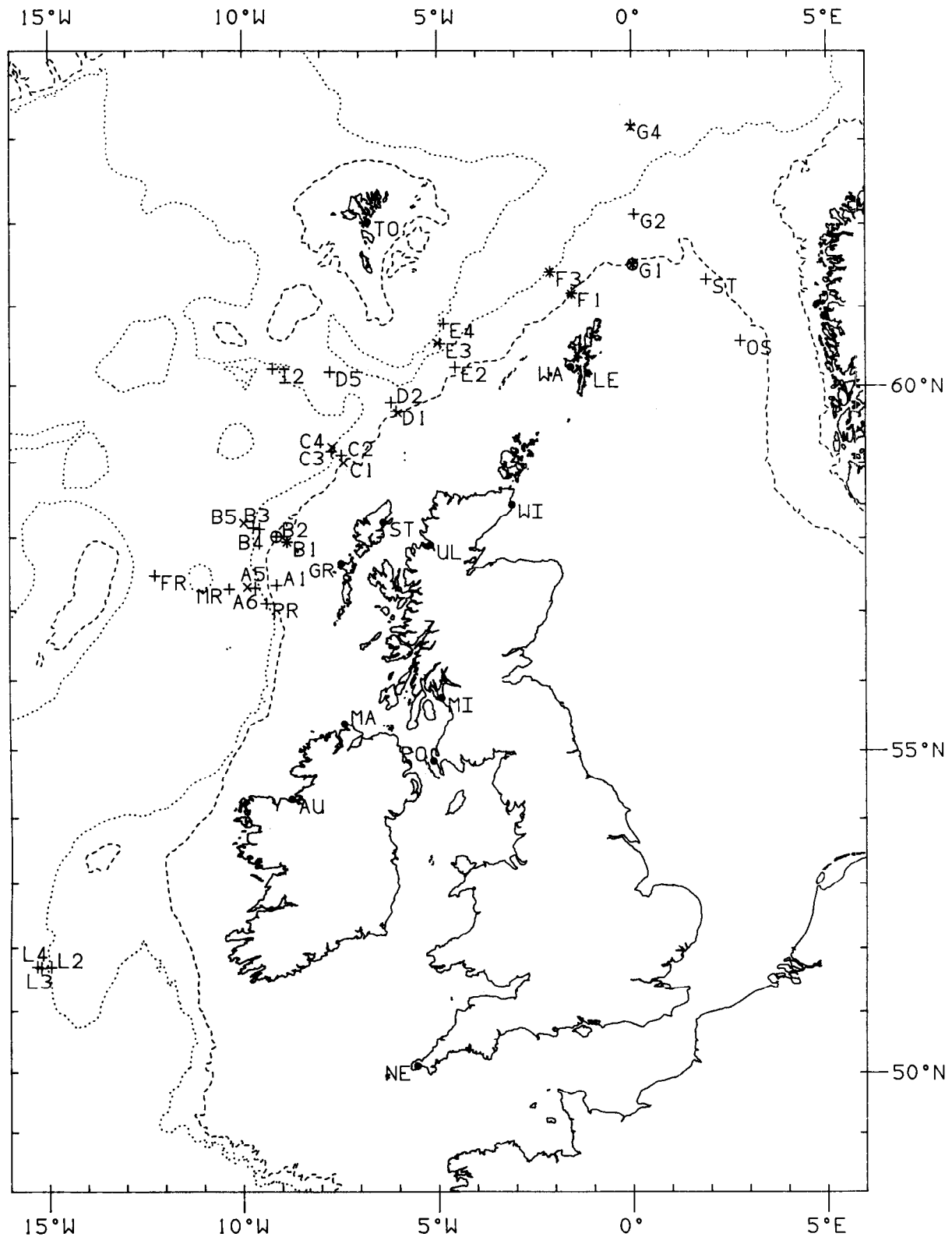


Figure 2. Location of data.

- coastal sea level
- + current meters
- x bottom pressure
- o thermistor chain

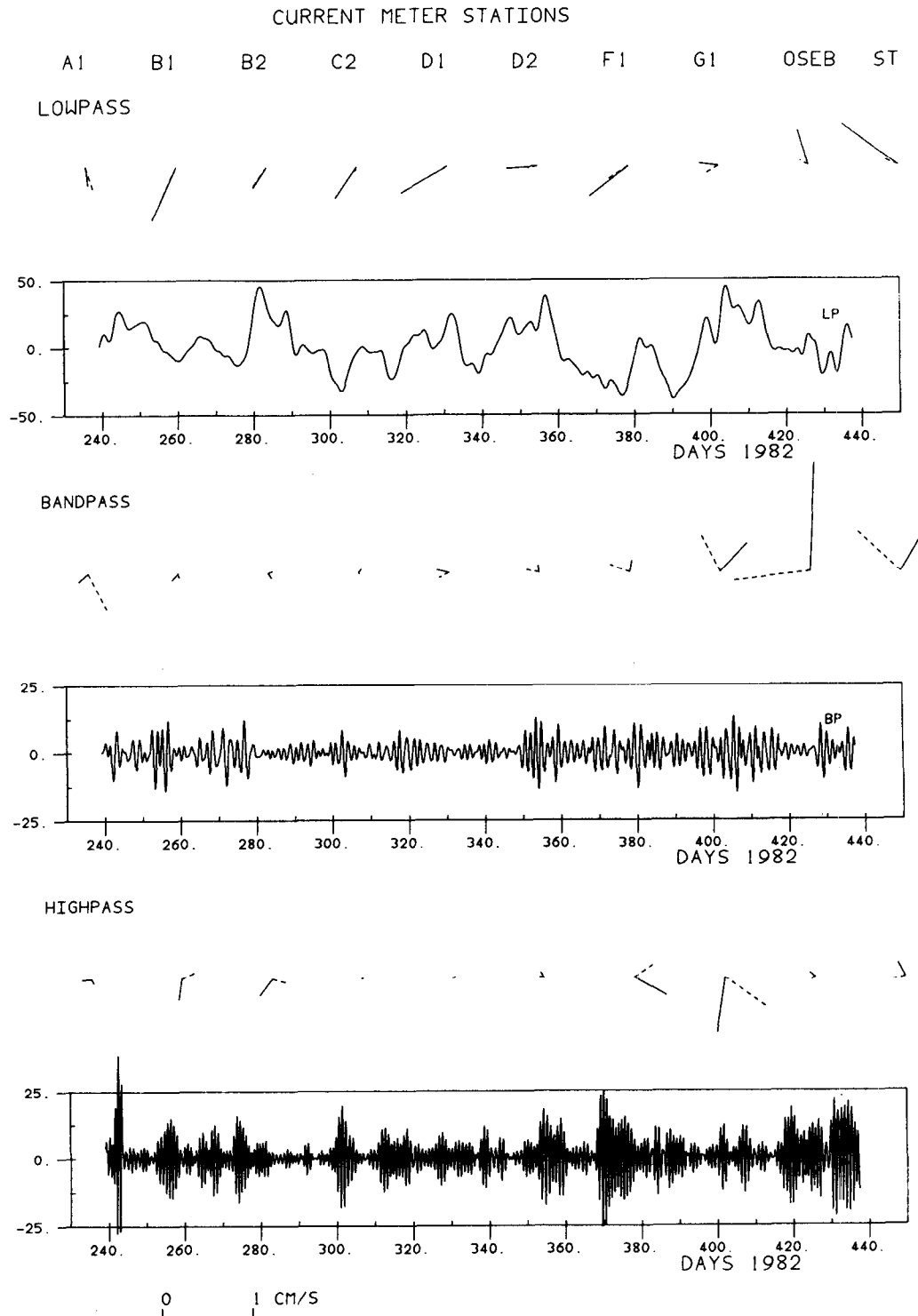


Figure 3. Representative series for groups of current meter moorings. Only relative signs and line lengths within one plotted mode form are relevant. Forms are for depth average of mooring modes given in Appendix. Sense of rotation is from dotted 'imaginary' vector to continuous 'real' vector around common origin.

a) Shelf moorings A1,B1,B2,C2,D1,D2,F1,G1,OS,ST; all frequency bands.

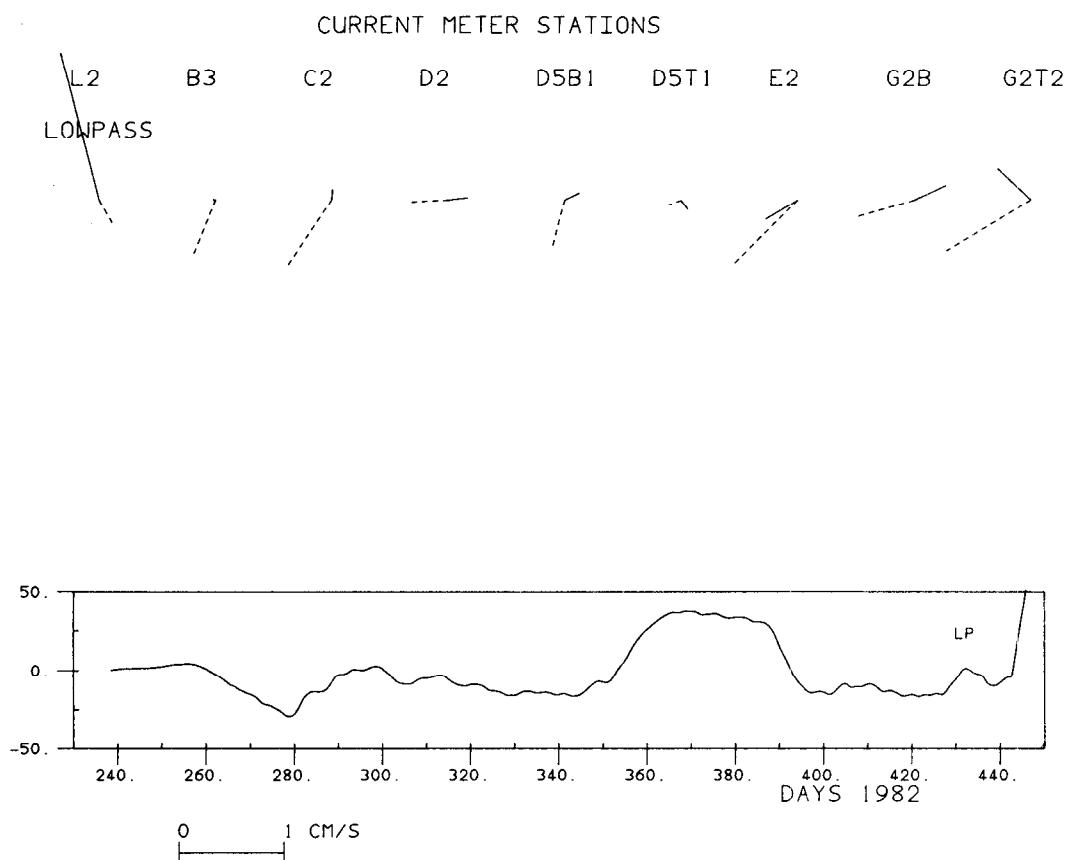


Figure 3. Representative series for groups of current meter moorings. Only relative signs and line lengths within one plotted mode form are relevant. Forms are for depth average of mooring modes given in Appendix. Sense of rotation is from dotted 'imaginary' vector to continuous 'real' vector around common origin.

b) Low pass groupings of moorings:

L2,B3,C2,D2,D5B1,D5T1,E2,G2B,G2T2 (500m);

B4,C3,E3T2,E3N,E4T,E4B,F3T2,F3B2 (1000m);

D1,D2,D2T1,D5B1

(Wyville-Thomson Ridge).

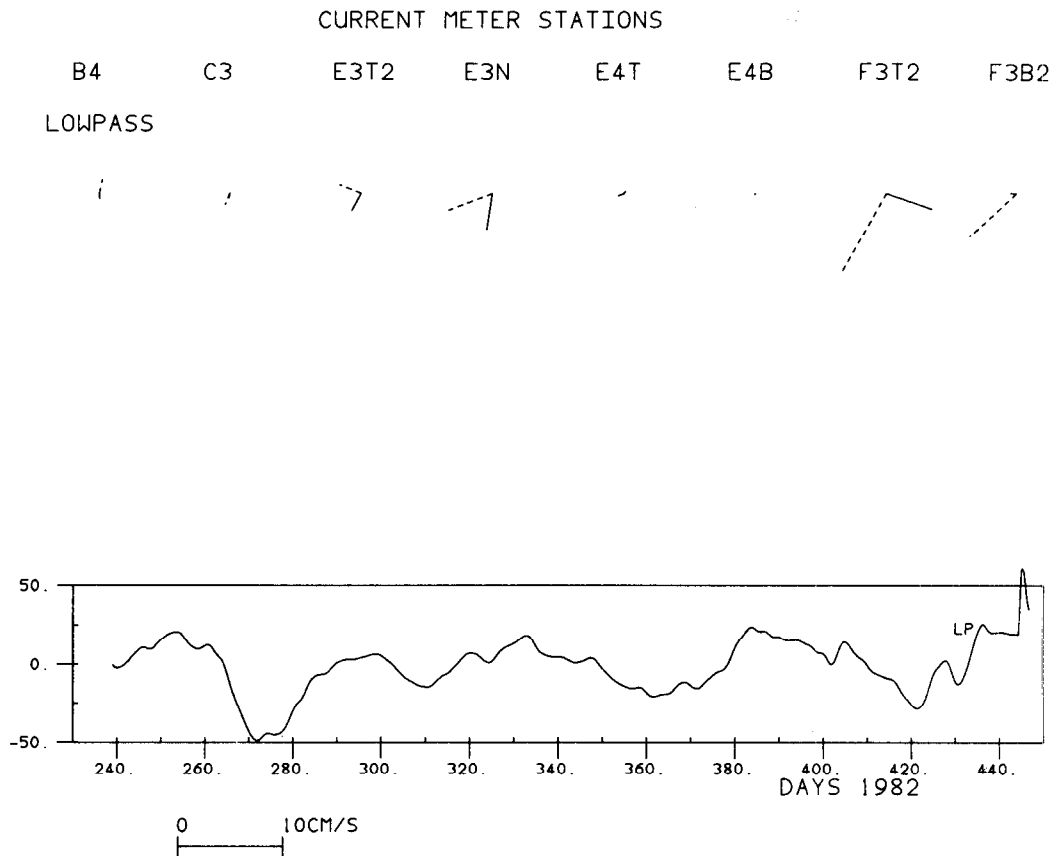


Figure 3. Representative series for groups of current meter moorings. Only relative signs and line lengths within one plotted mode form are relevant. Forms are for depth average of mooring modes given in Appendix. Sense of rotation is from dotted 'imaginary' vector to continuous 'real' vector around common origin.

b) Low pass groupings of moorings:

L2,B3,C2,D2,D5B1,D5T1,E2,G2B,G2T2 (500m);

B4,C3,E3T2,E3N,E4T,E4B,F3T2,F3B2 (1000m);

D1,D2,D2T1,D5B1 (Wyville-Thomson Ridge).

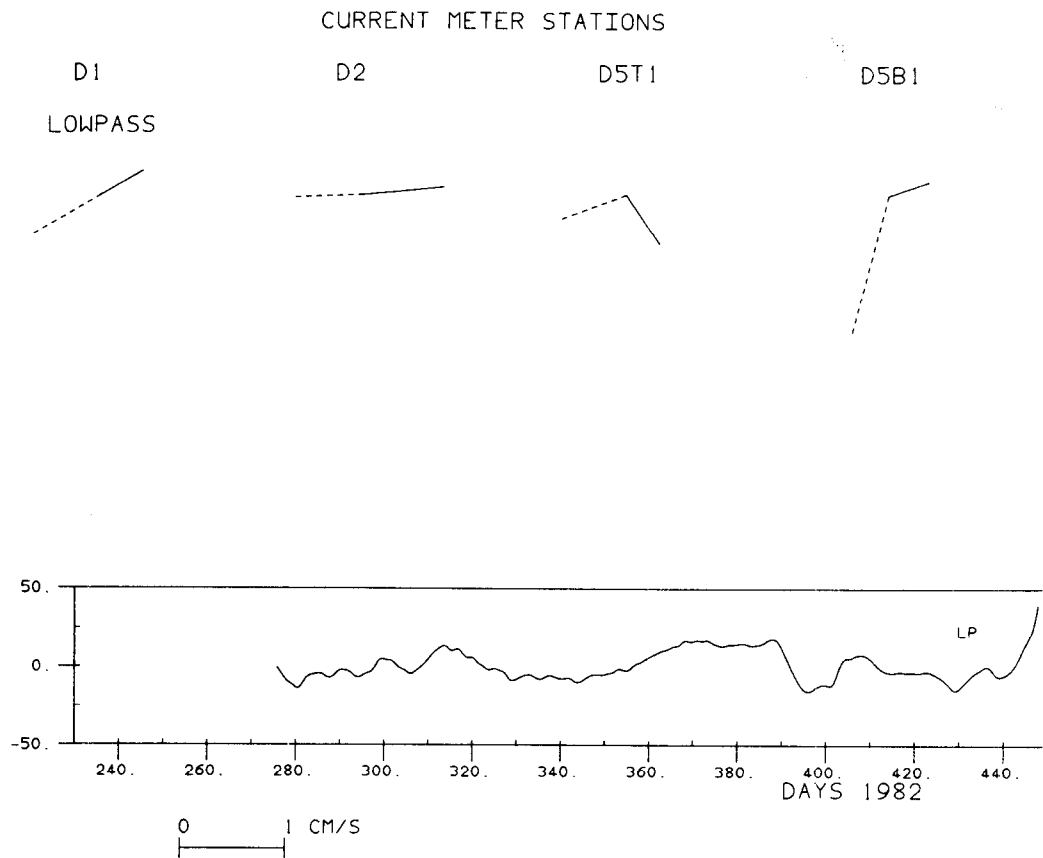


Figure 3. Representative series for groups of current meter moorings. Only relative signs and line lengths within one plotted mode form are relevant. Forms are for depth average of mooring modes given in Appendix. Sense of rotation is from dotted 'imaginary' vector to continuous 'real' vector around common origin.

b) Low pass groupings of moorings:

L2,B3,C2,D2,D5B1,D5T1,E2,G2B,G2T2 (500m);

B4,C3,E3T2,E3N,E4T,E4B,F3T2,F3B2 (1000m);

D1,D2,D2T1,D5B1 (Wyville-Thomson Ridge).

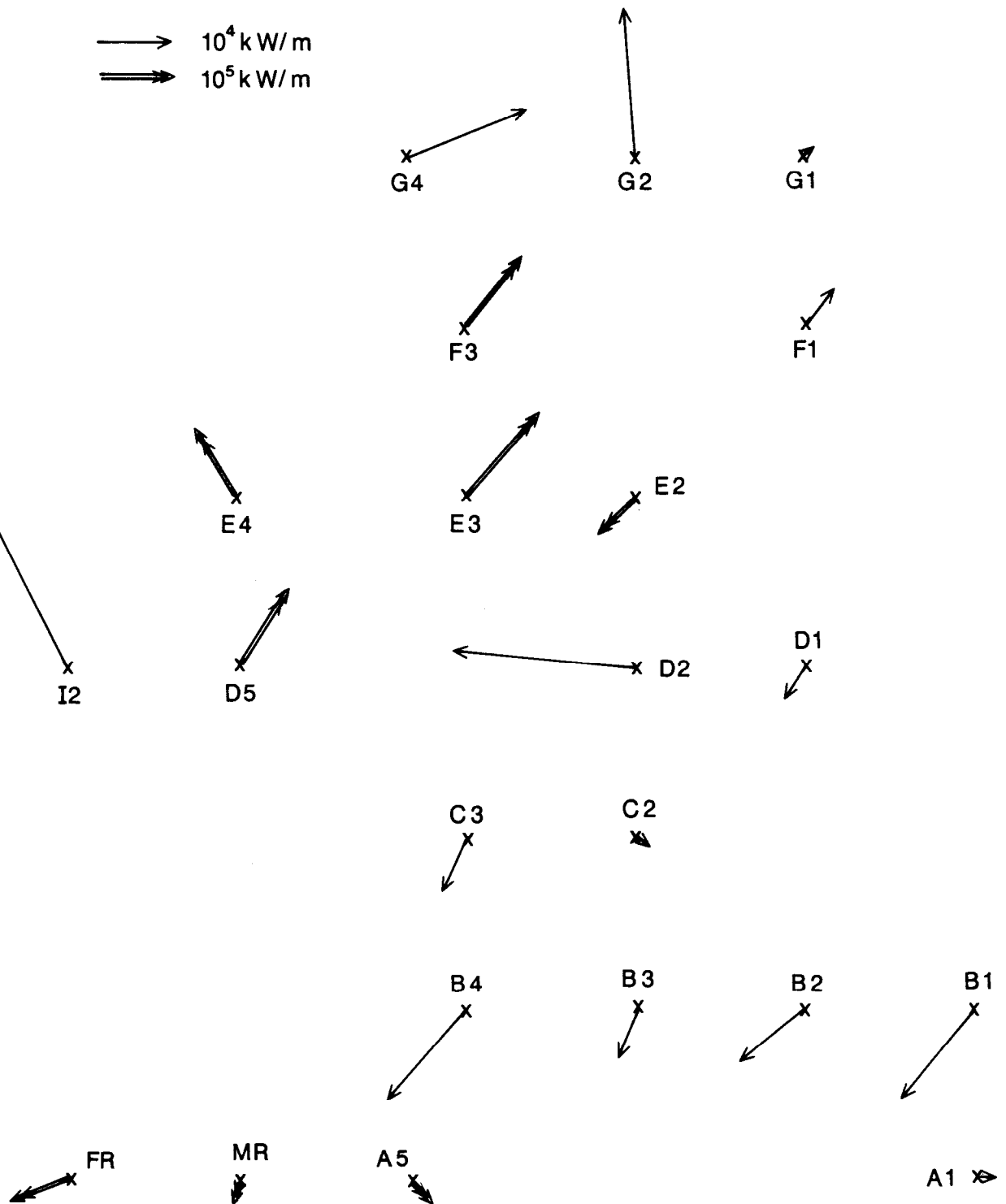


Figure 4. Record-average depth-integrated heat fluxes. Double arrows represent large fluxes on one-tenth scale.

APPENDICES. REPRESENTATIVE SERIES

The reduction of data to these series is described in section 2. Their representations together with the associated structure of the phenomena are shown in the following appendices, one for each source of data.

APPENDIX A. CURRENT MOORINGS AND TEMPERATURE

One plot follows for each mooring, except that deeper moorings in the Faeroe-Shetland Channel have a plot each for those meters above the thermocline and for those below. Series and corresponding forms for each frequency band (LP, BP, HP) are shown. The convention for current forms is as in figure 3. Thus the sense of rotation of the current vector is from the dotted 'imaginary' vector to the continuous 'real' vector around their common origin. The 'real' vector direction and relative strengths are taken up simultaneously at the various depths as $\underline{a}_1\varphi(t)$ in section 2.2, while the 'imaginary' vector shows the direction and relative magnitude of $\underline{a}_2(\varphi(t+\Delta t)-\varphi(t))$ 'on average' through the record, as determined by mean variance. The scales shows \underline{a}_1 corresponding to dimensionless $\varphi(t)$ numerically as plotted.

Flow direction and strength correlating with maximum temperatures are indicated by the position of the asterisk as a vector from the common origin. The corresponding elevation of temperature is printed.

L2

FREQUENCY BANDS

LOWPASS

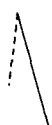
BANDPASS

HIGHPASS



C/M DEPTH

*



*



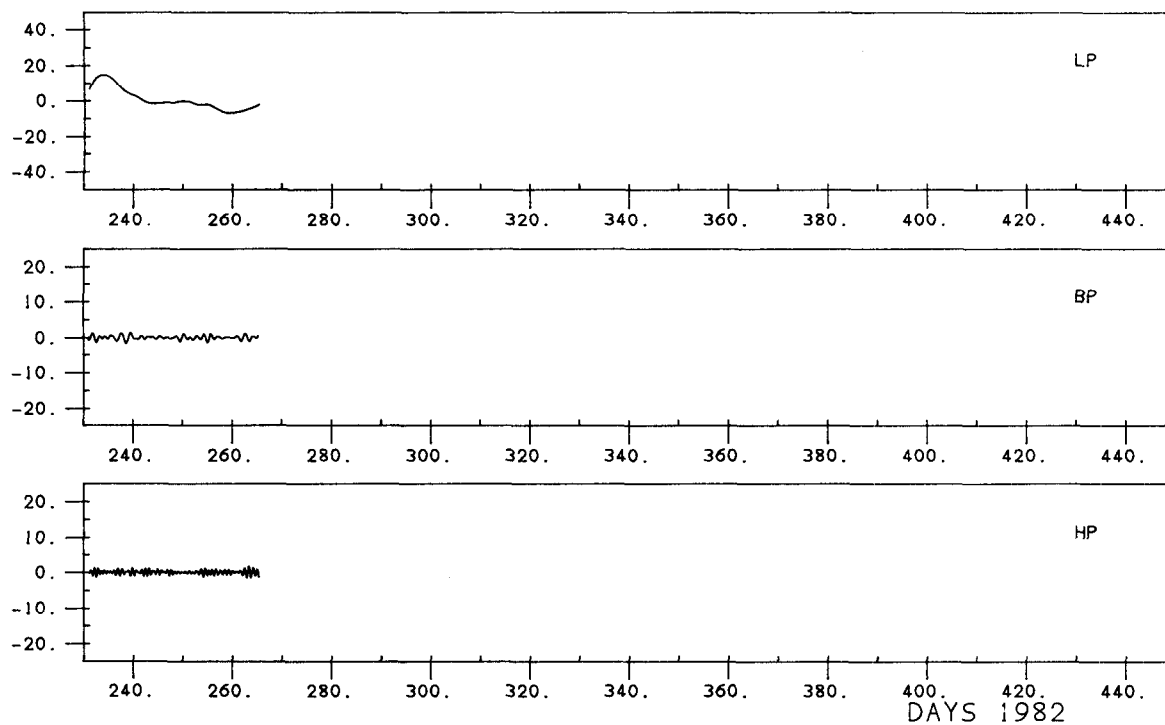
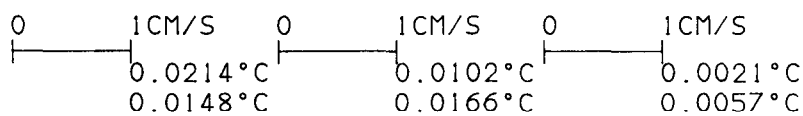
*

332



*

728



L3

↑ N

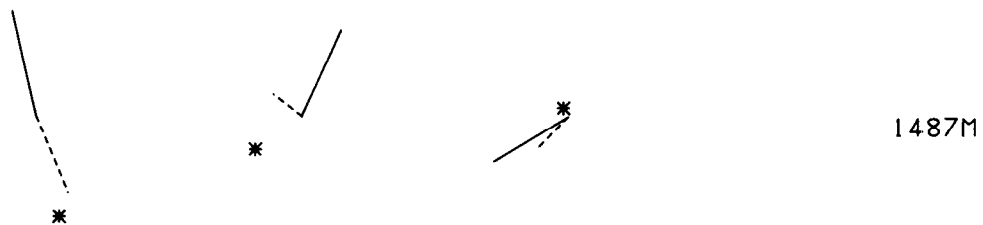
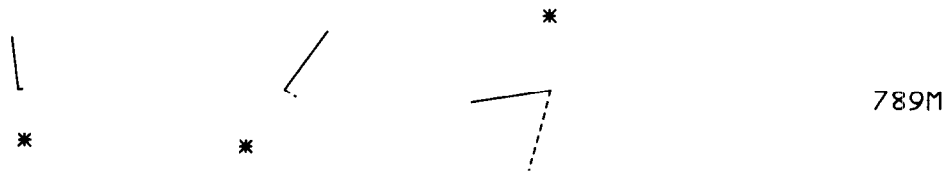
FREQUENCY BANDS

LOWPASS

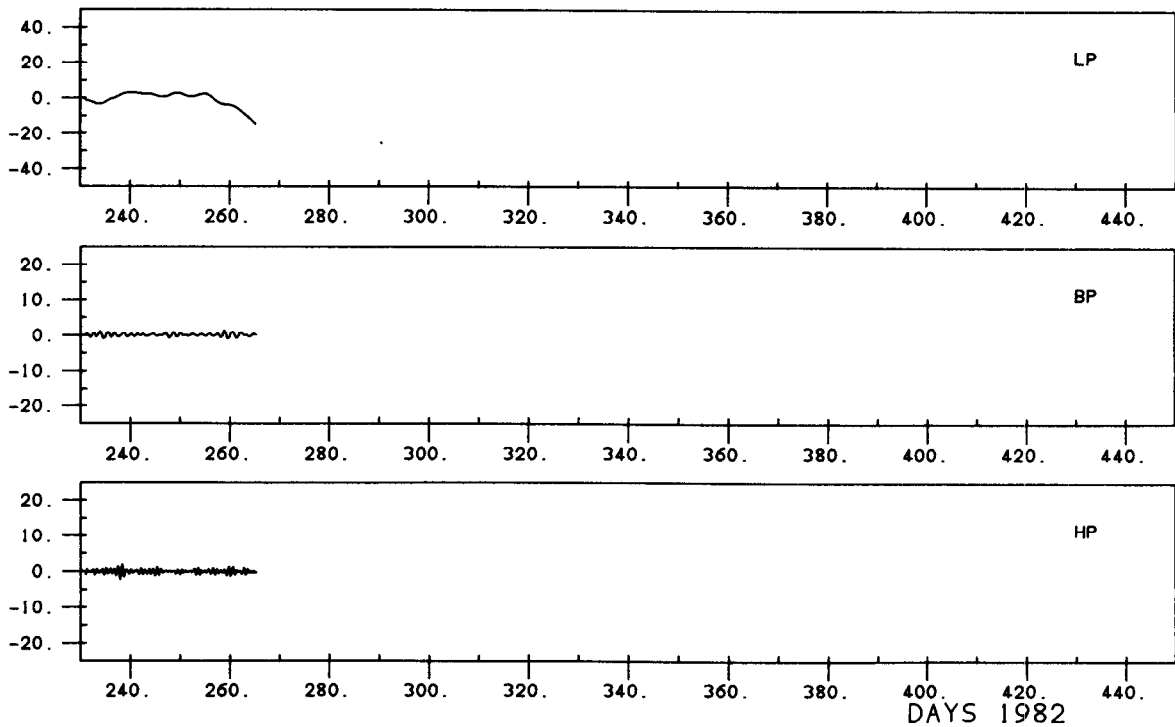
BANDPASS

HIGHPASS

C/M DEPTH



ρ ——— CM/S	ρ ——— CM/S	ρ ——— CM/S
0.0018°C	0.0282°C	0.0037°C
0.0046°C	0.0117°C	0.0066°C



L4

FREQUENCY BANDS

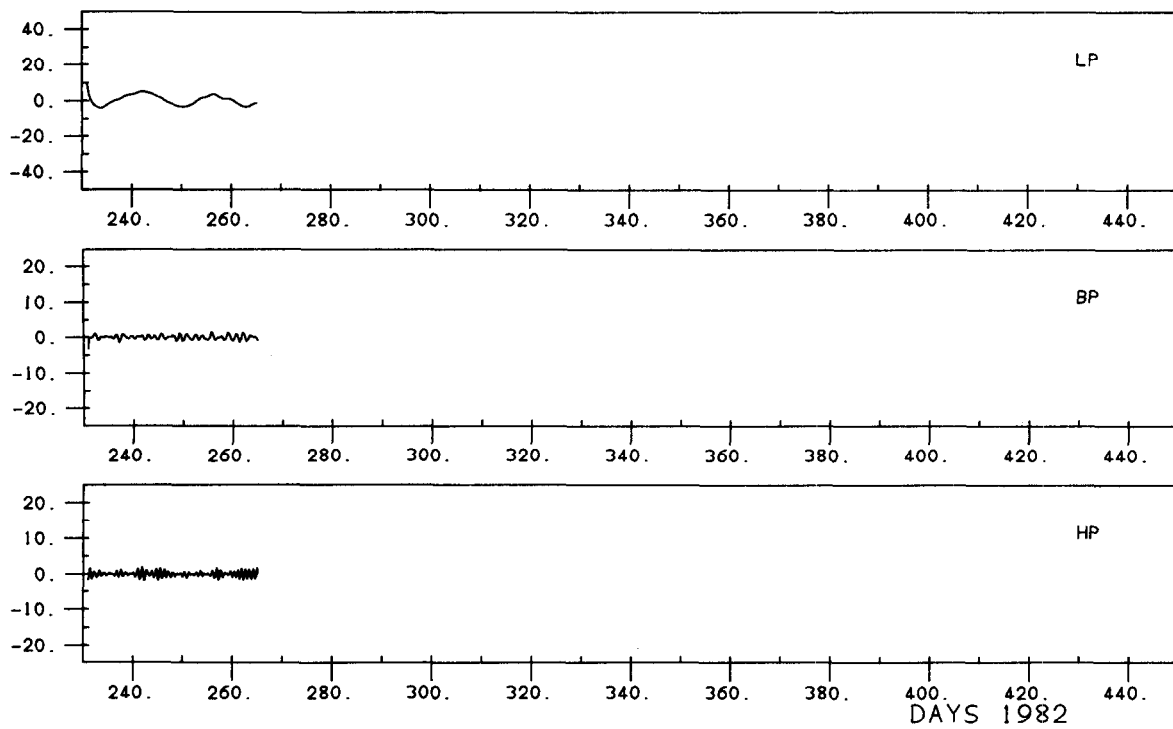
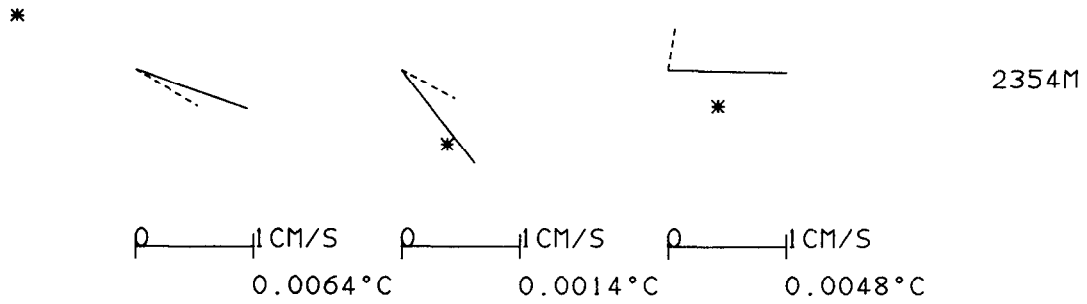
LOWPASS

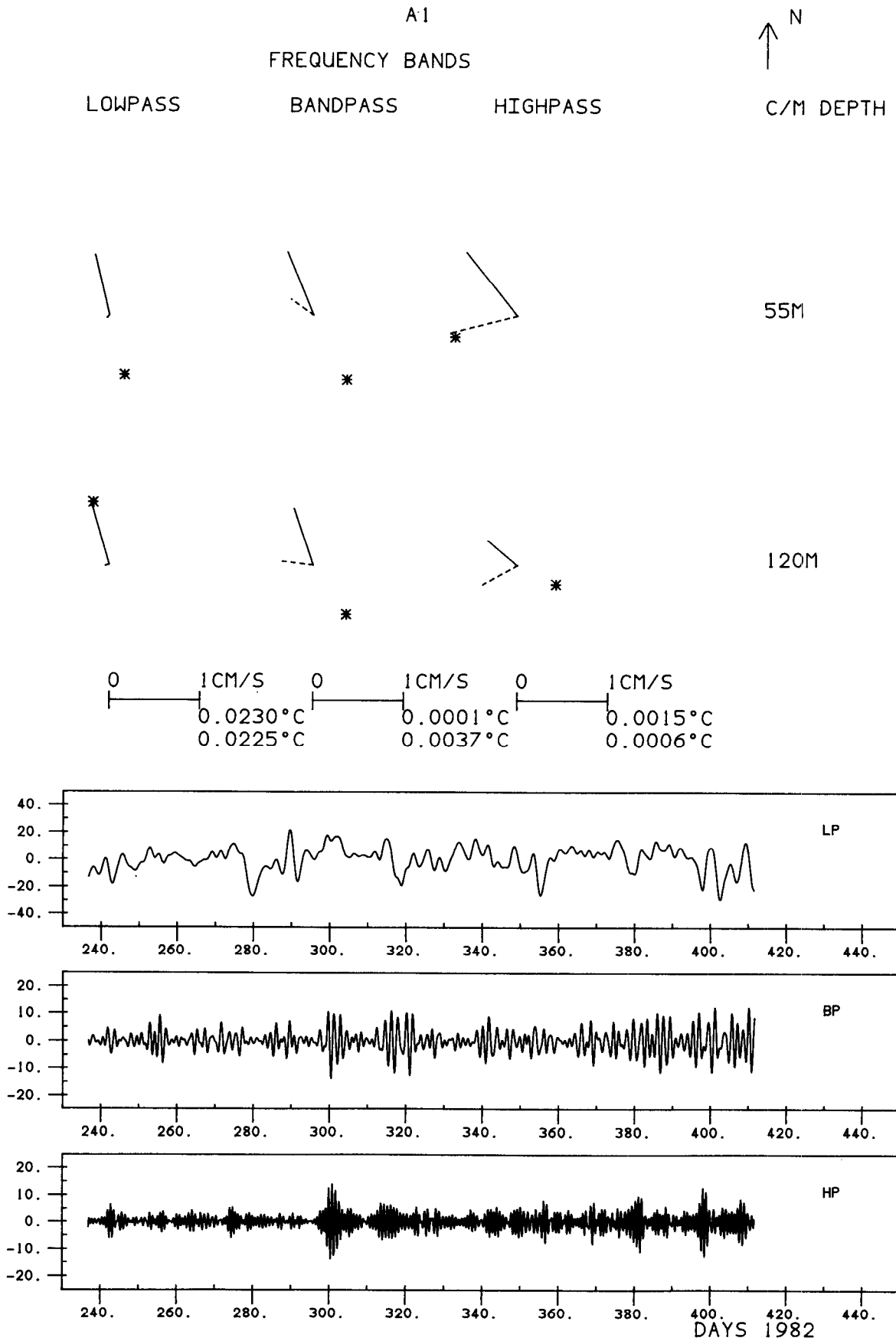
BANDPASS

HIGHPASS

↑ N

C/M DEPTH





A5

↑ N

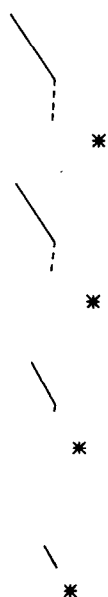
FREQUENCY BANDS

LOWPASS

BANDPASS

HIGHPASS

C/M DEPTH



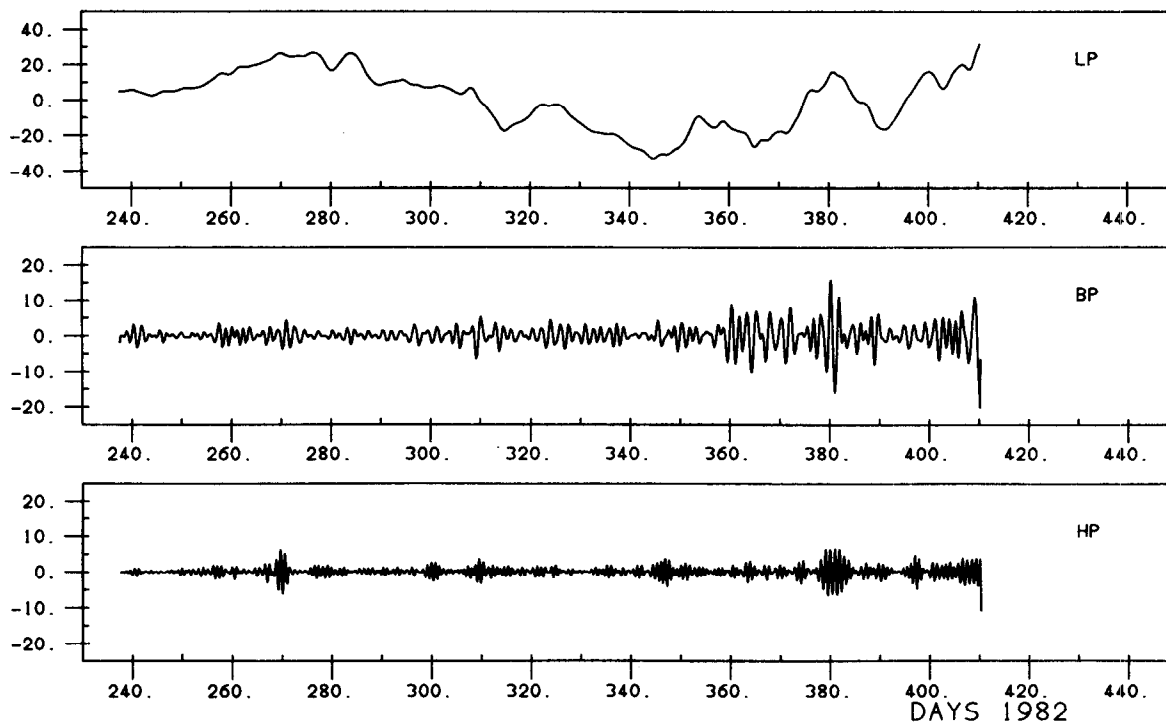
209M

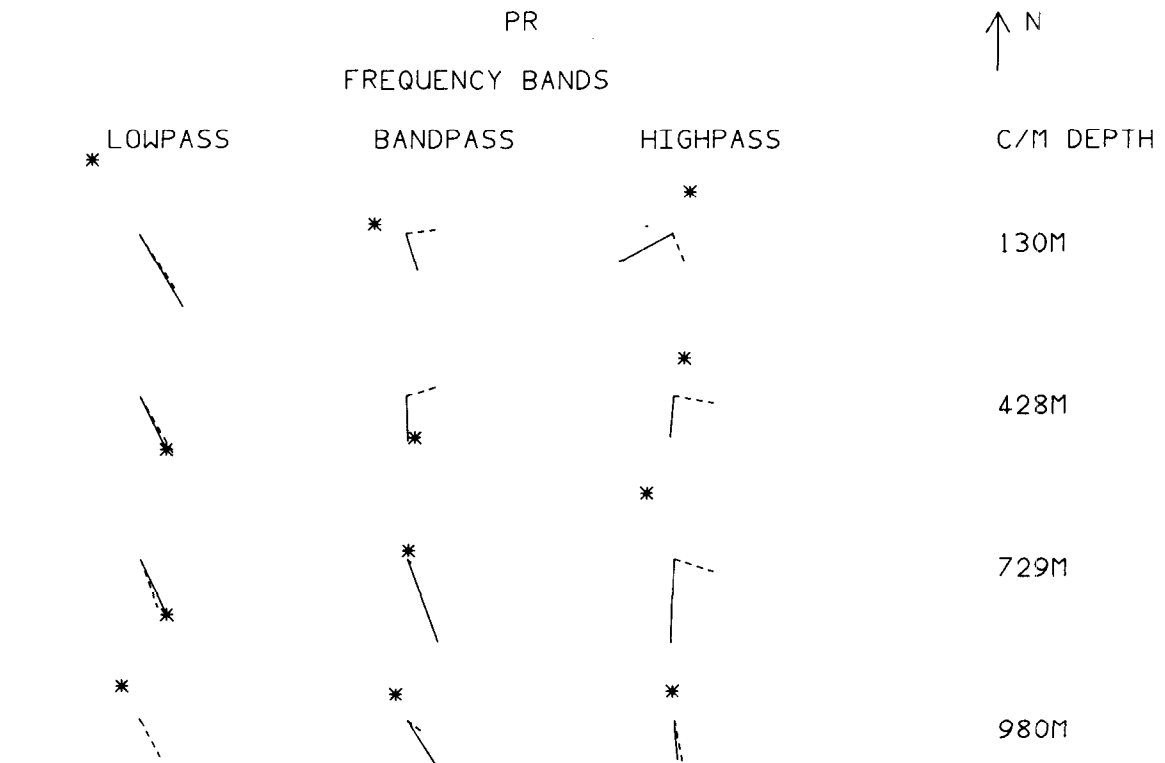
510M

1111M

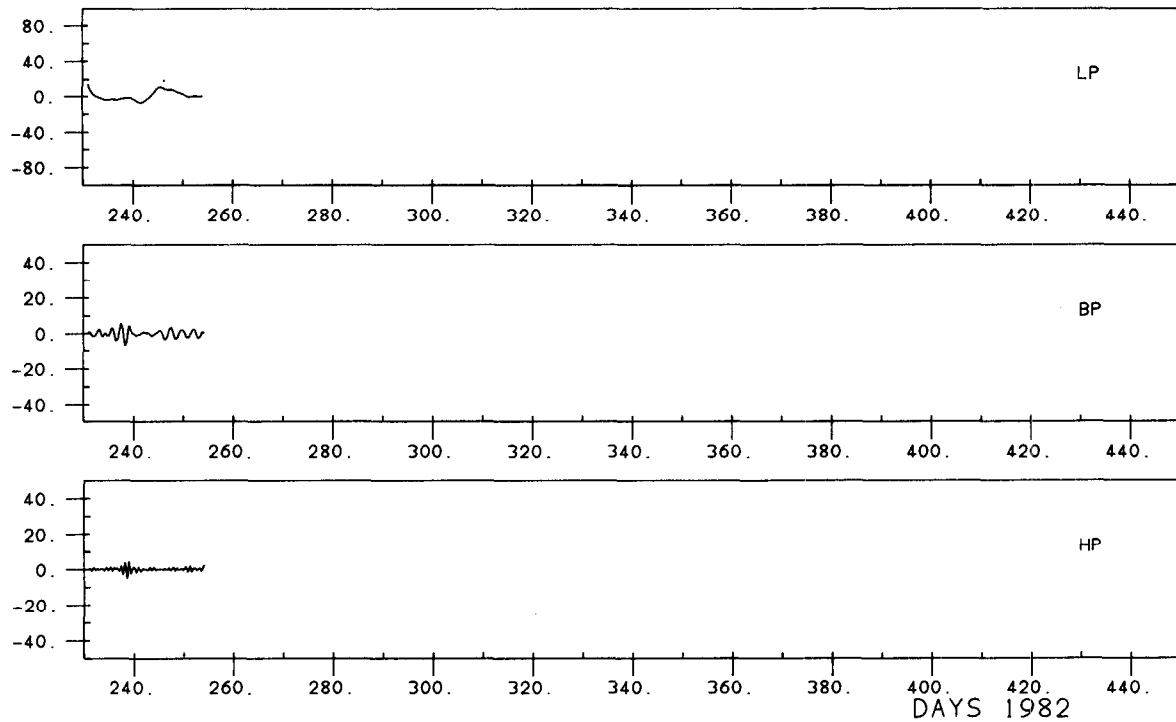
1562M

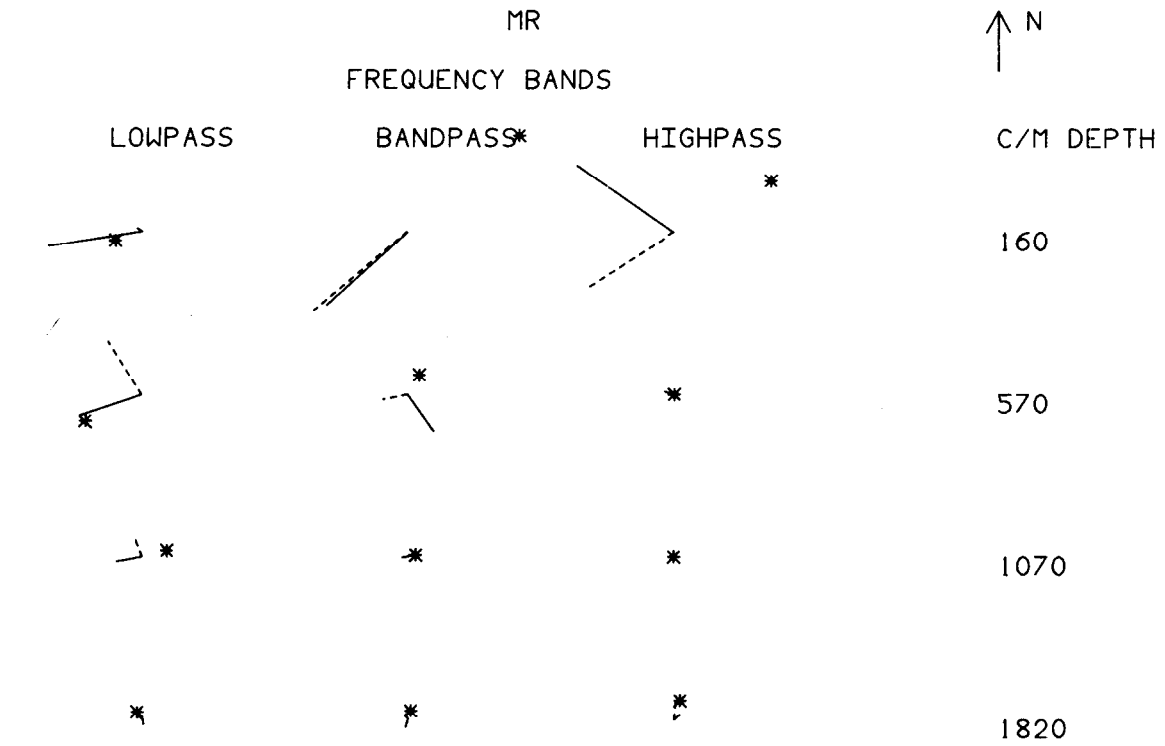
ρ	1 CM/S	ρ	1 CM/S	ρ	1 CM/S
0.0026°C		0.0028°C		0.0030°C	
0.0047°C		0.0052°C		0.0066°C	
0.0116°C		0.0037°C		0.0041°C	
0.0006°C		0.0030°C		0.0019°C	



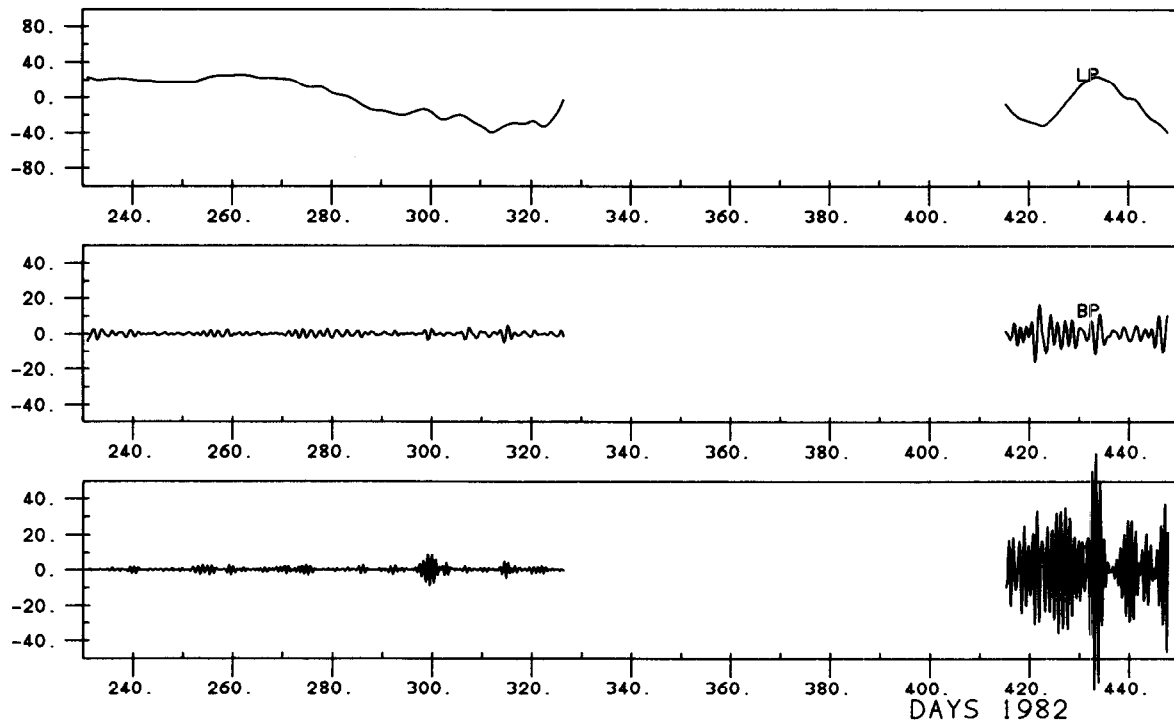


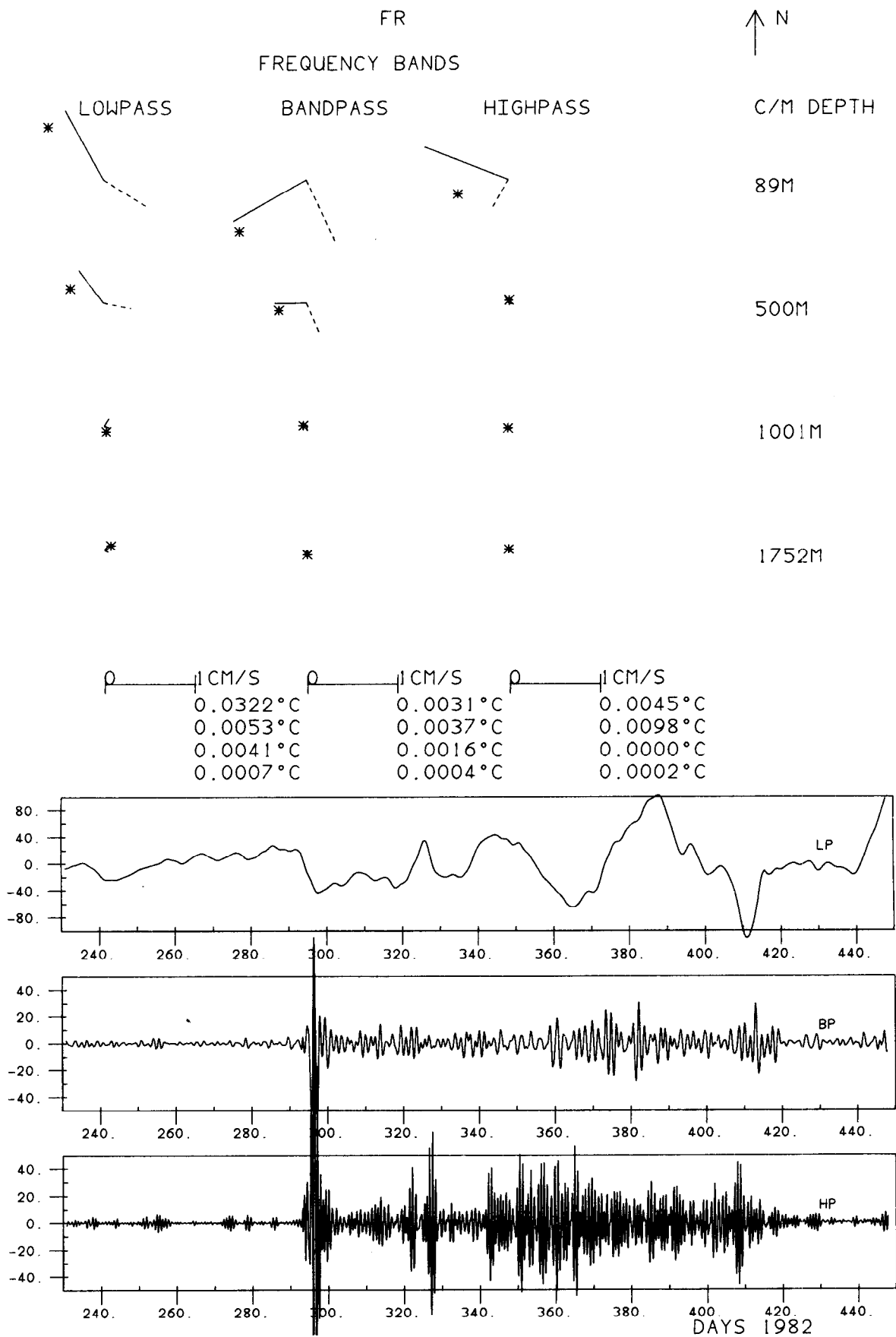
ρ ——— CM/S	ρ ——— CM/S	ρ ——— CM/S
0.0054°C	0.0146°C	0.0078°C
0.0010°C	0.0044°C	0.0015°C
0.0034°C	0.0076°C	0.0031°C
0.0052°C	0.0351°C	0.0040°C





ρ	CM/S	ρ	CM/S	ρ	CM/S
	0.0227°C		0.0163°C		0.0024°C
	0.0057°C		0.0075°C		0.0009°C
	0.0016°C		0.0022°C		0.0002°C
	0.0020°C		0.0002°C		0.0006°C





B1

FREQUENCY BANDS

 N

LOWPASS

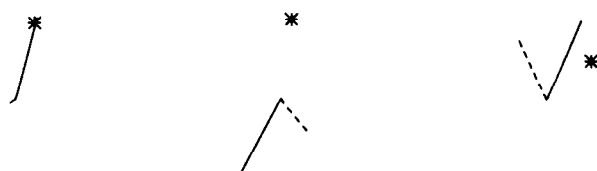
BANDPASS

HIGHPASS

C/M DEPTH

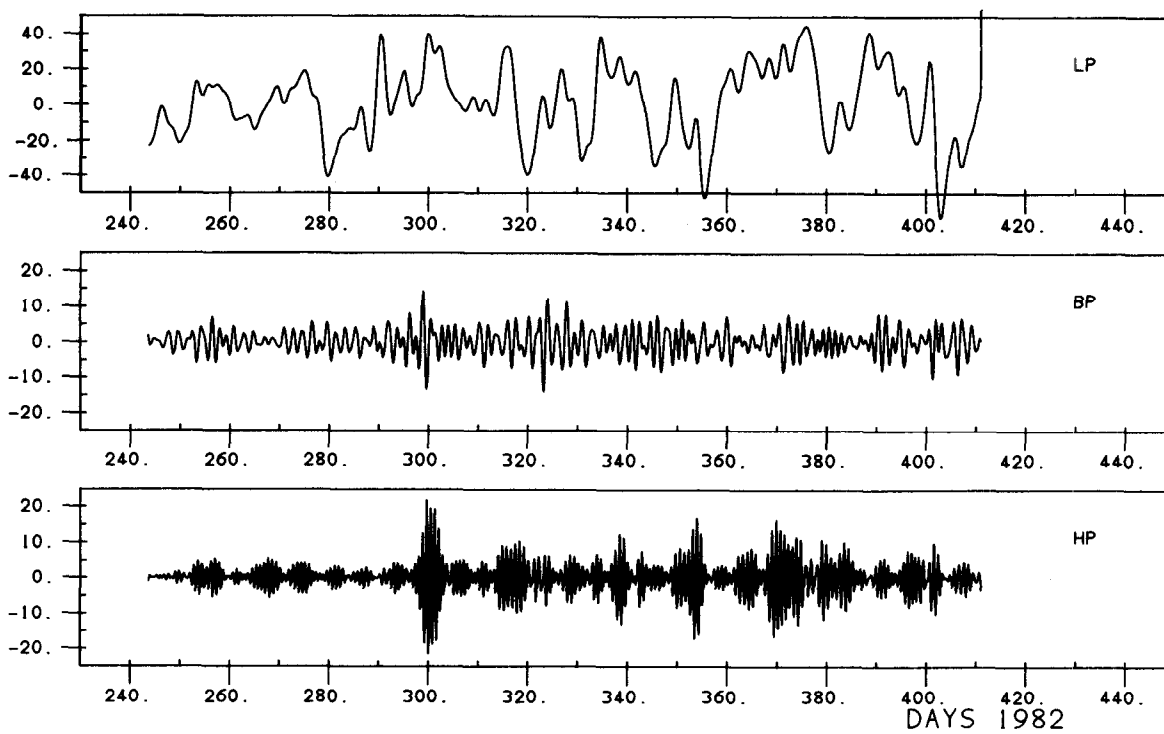


55M



130M

ρ — 1 CM/S	ρ — 1 CM/S	ρ — 1 CM/S
0.0068°C	0.0028°C	0.0021°C
0.0078°C	0.0045°C	0.0017°C



B2
FREQUENCY BANDS

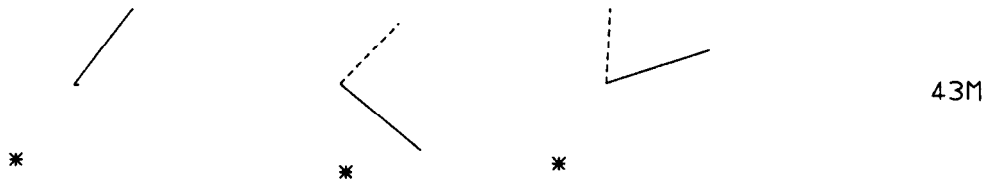
↑ N

LOWPASS

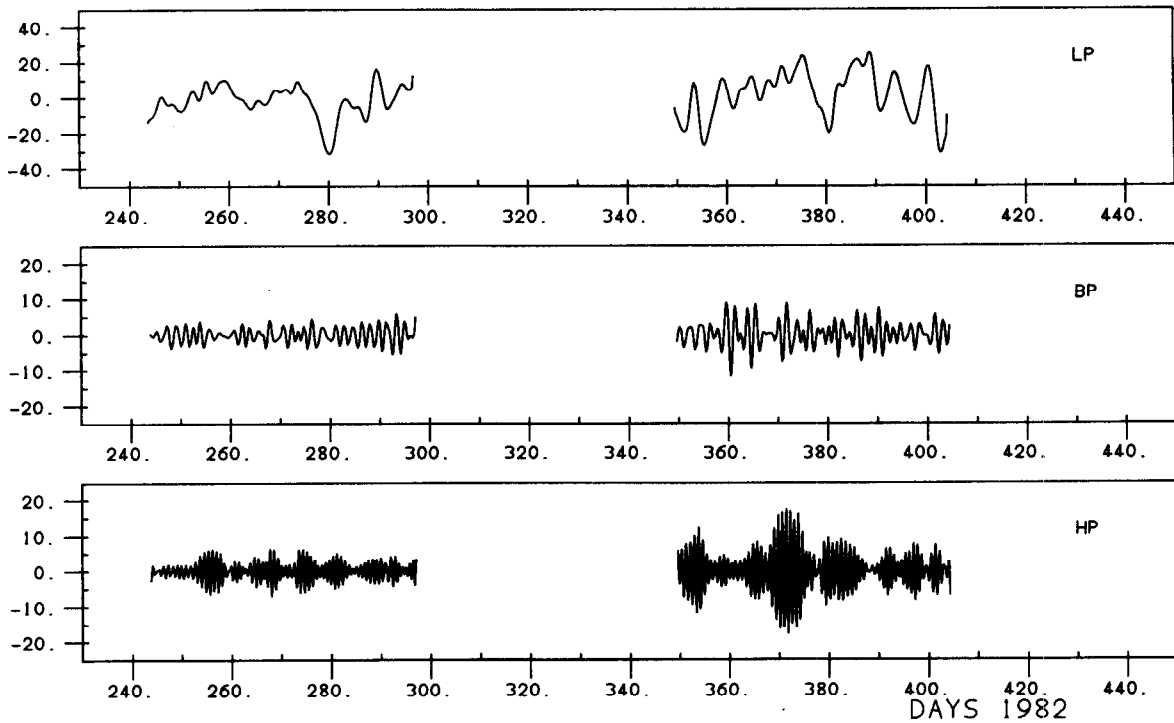
BANDPASS

HIGHPASS

C/M DEPTH



ρ ——— 1 CM/S	ρ ——— 1 CM/S	ρ ——— 1 CM/S
0.0446°C	0.0018°C	0.0009°C
0.0182°C	0.0023°C	0.0009°C



B3

FREQUENCY BANDS

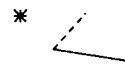
↑ N

LOWPASS

BANDPASS

HIGHPASS

C/M DEPTH



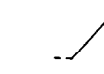
104M

*



257M

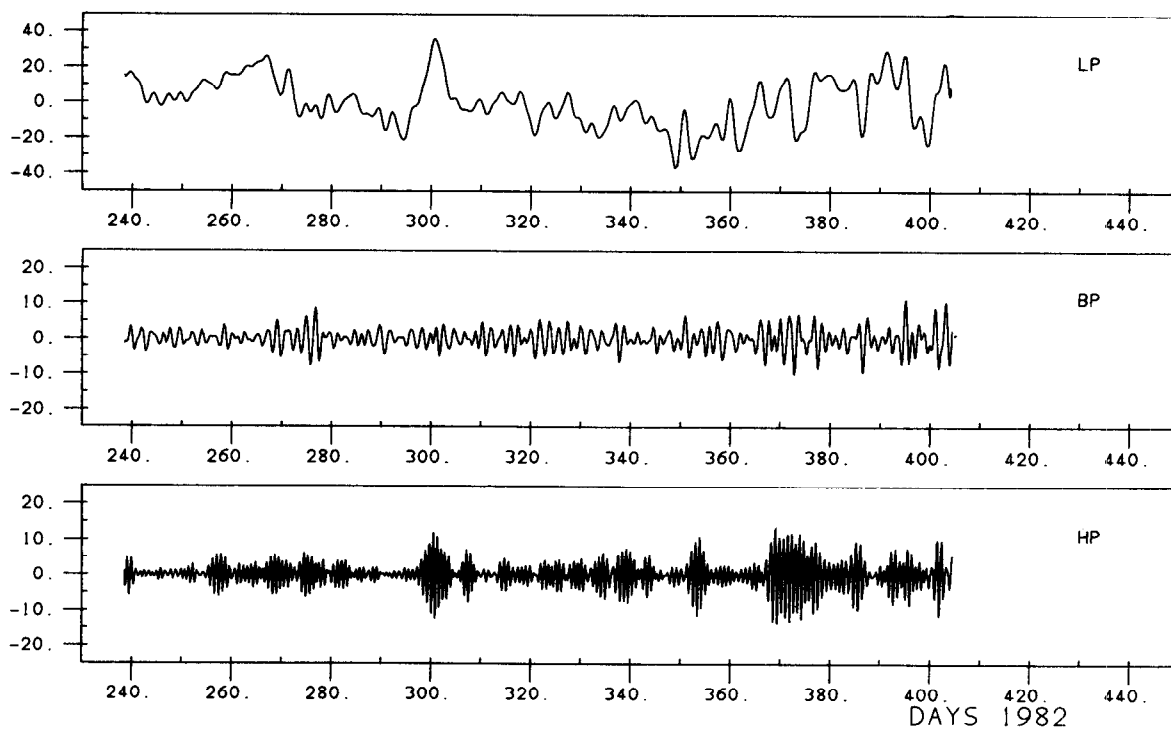
*



504M

*

ρ	1 CM/S	ρ	1 CM/S	ρ	1 CM/S
	0.0098°C		0.0031°C		0.0012°C
	0.0144°C		0.0027°C		0.0019°C
	0.0144°C		0.0018°C		0.0052°C



B4

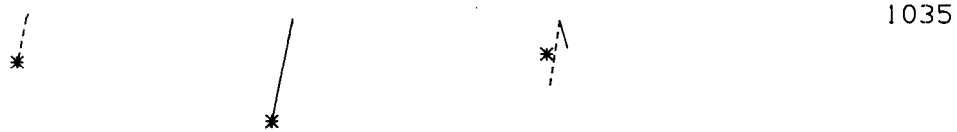
FREQUENCY BANDS

LOWPASS

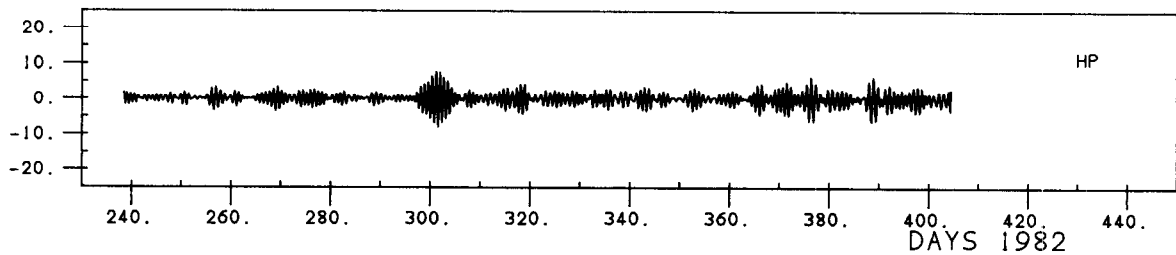
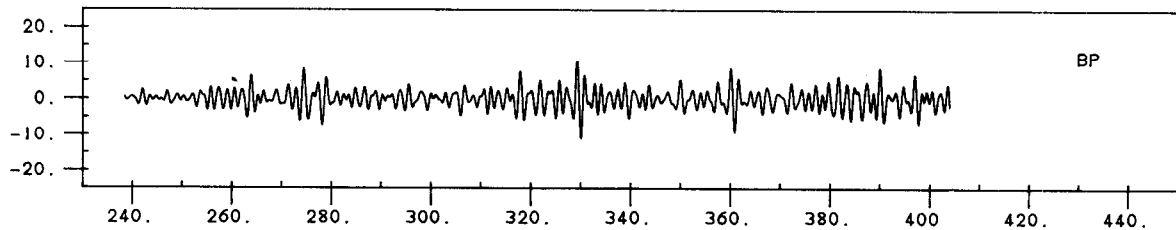
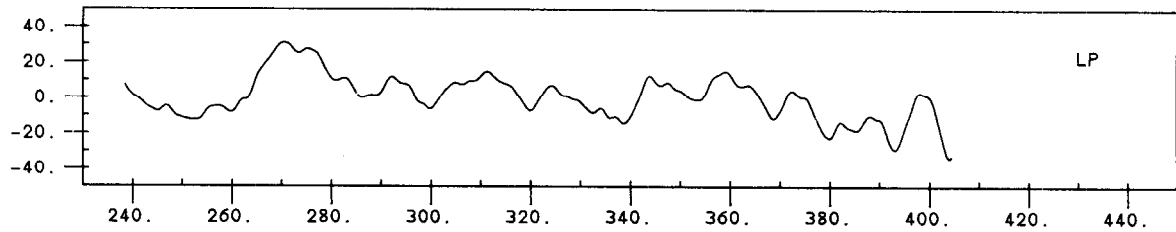
BANDPASS

HIGHPASS

C/M DEPTH



0	1CM/S	0	1CM/S	0	1CM/S
	0.0148°C		0.0020°C		0.0034°C
	0.0034°C		0.0089°C		0.0027°C
	0.0030°C		0.0204°C		0.0105°C



DAYS 1982

C2

↑ N

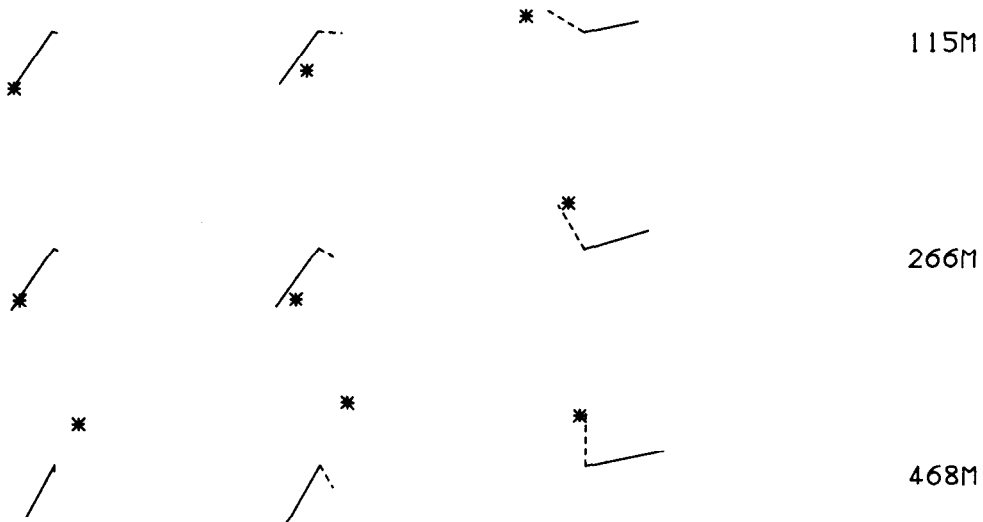
FREQUENCY BANDS

LOWPASS

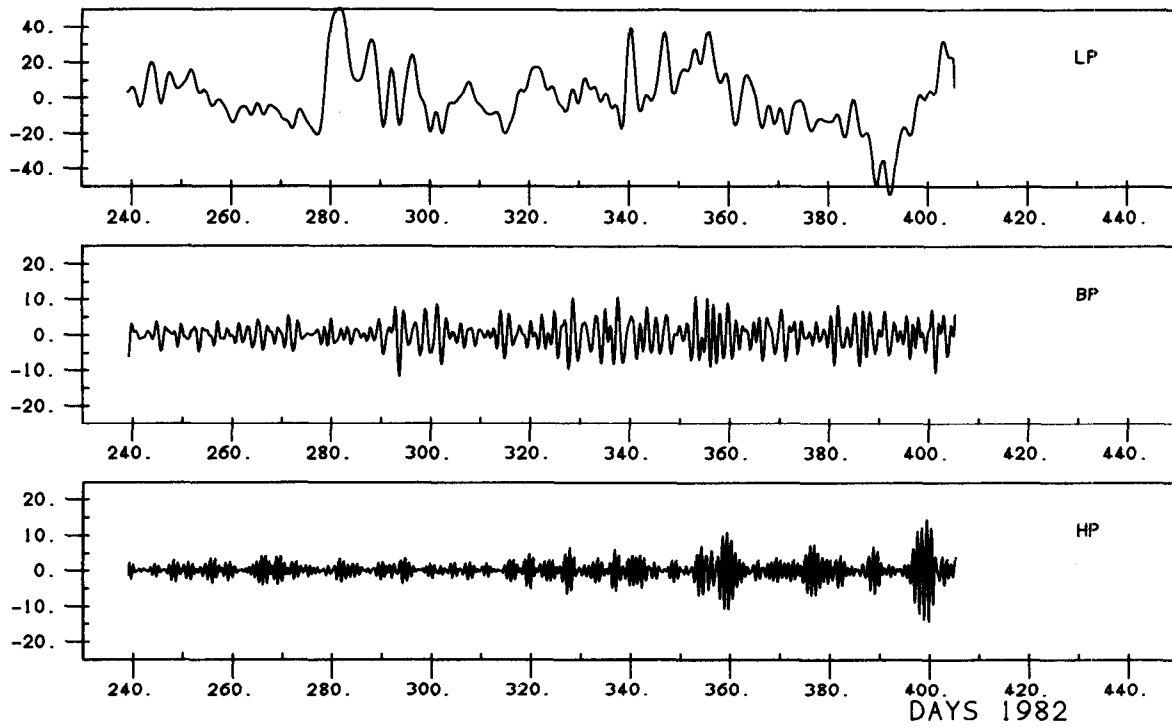
BANDPASS

HIGHPASS

C/M DEPTH



ρ ——— CM/S	ρ ——— CM/S	ρ ——— CM/S
0.0171°C	0.0045°C	0.0032°C
0.0132°C	0.0013°C	0.0062°C
0.0174°C	0.0034°C	0.0103°C



C3

↑ N

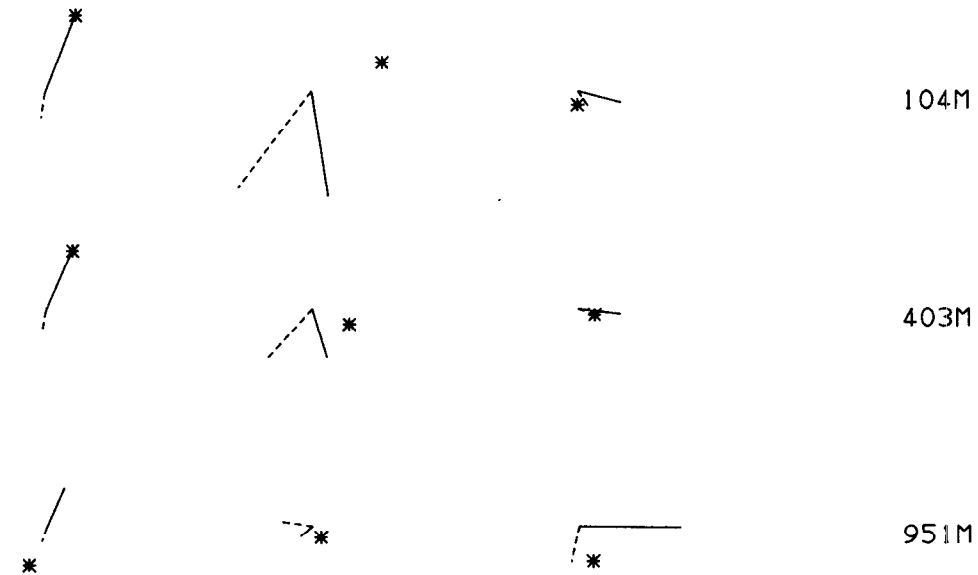
FREQUENCY BANDS

LOWPASS

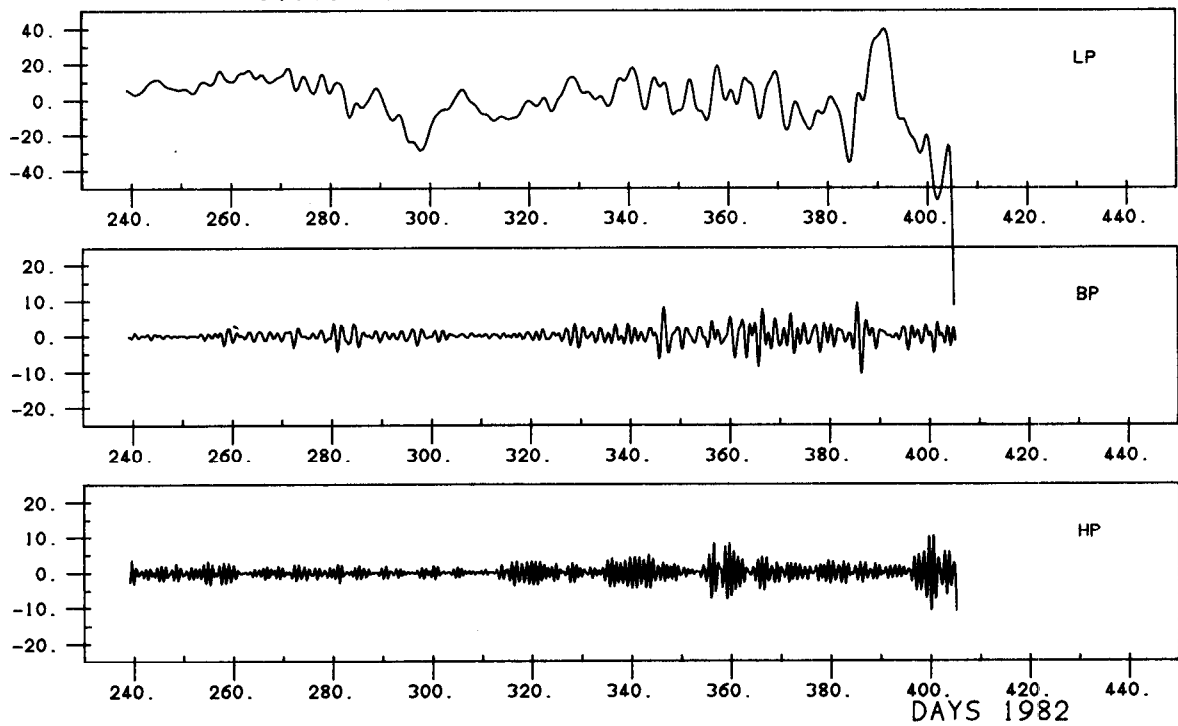
BANDPASS

HIGHPASS

C/M DEPTH



ρ ——— 1 CM/S	ρ ——— 1 CM/S	ρ ——— 1 CM/S
0.0041°C	0.0009°C	0.0018°C
0.0020°C	0.0007°C	0.0040°C
0.0058°C	0.0100°C	0.0520°C



D1

FREQUENCY BANDS

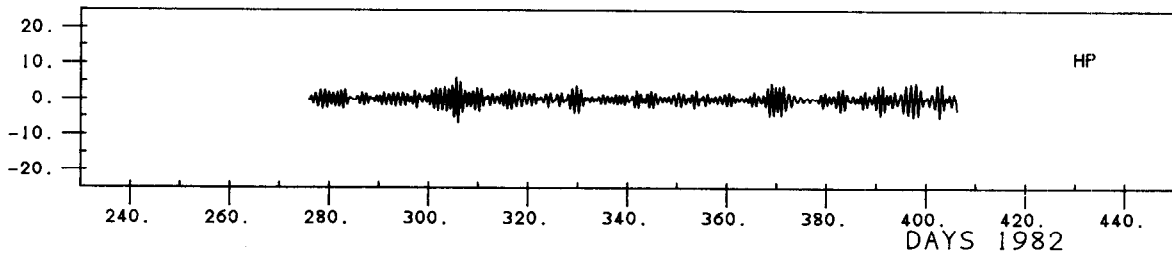
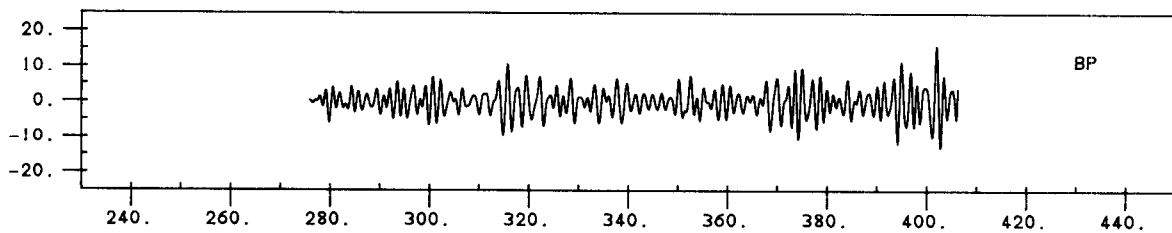
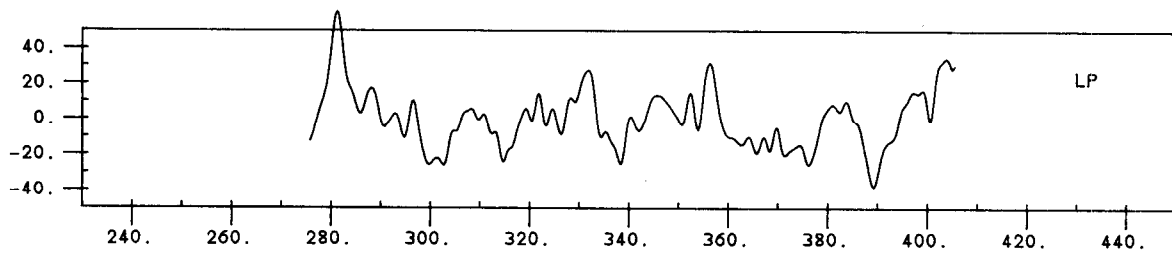
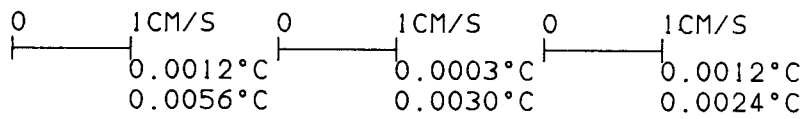
LOWPASS

BANDPASS

HIGHPASS

N
↑

C/M DEPTH



DAYS 1982

D2

FREQUENCY BANDS

N
↑

LOWPASS

BANDPASS

HIGHPASS

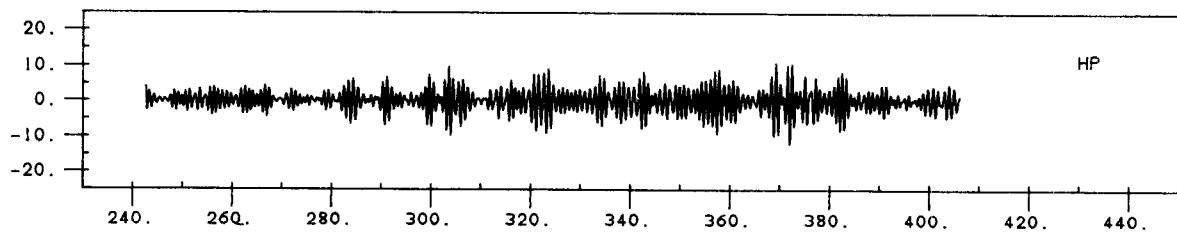
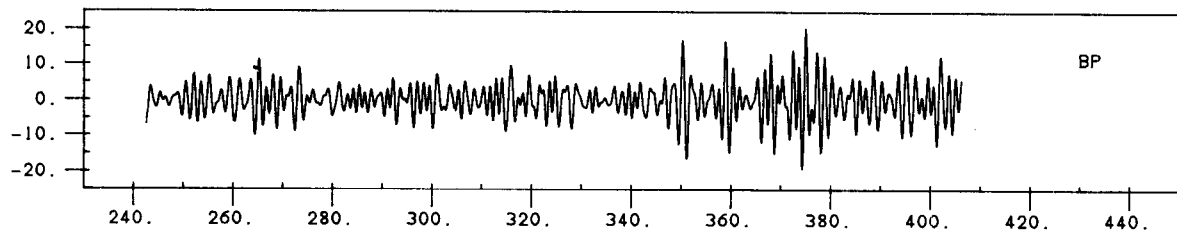
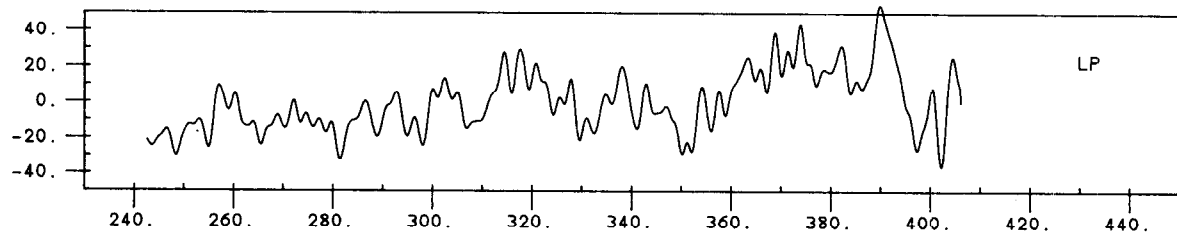
C/M DEPTH

* — * * * 120

* — * * * 270

* — * * * 345

0	1CM/S	0	1CM/S	0	1CM/S
	0.0147°C		0.0084°C		0.0040°C
	0.0087°C		0.0095°C		0.0071°C
	0.0115°C		0.0118°C		0.0144°C



DAYS 1982

D5T1

↑ N

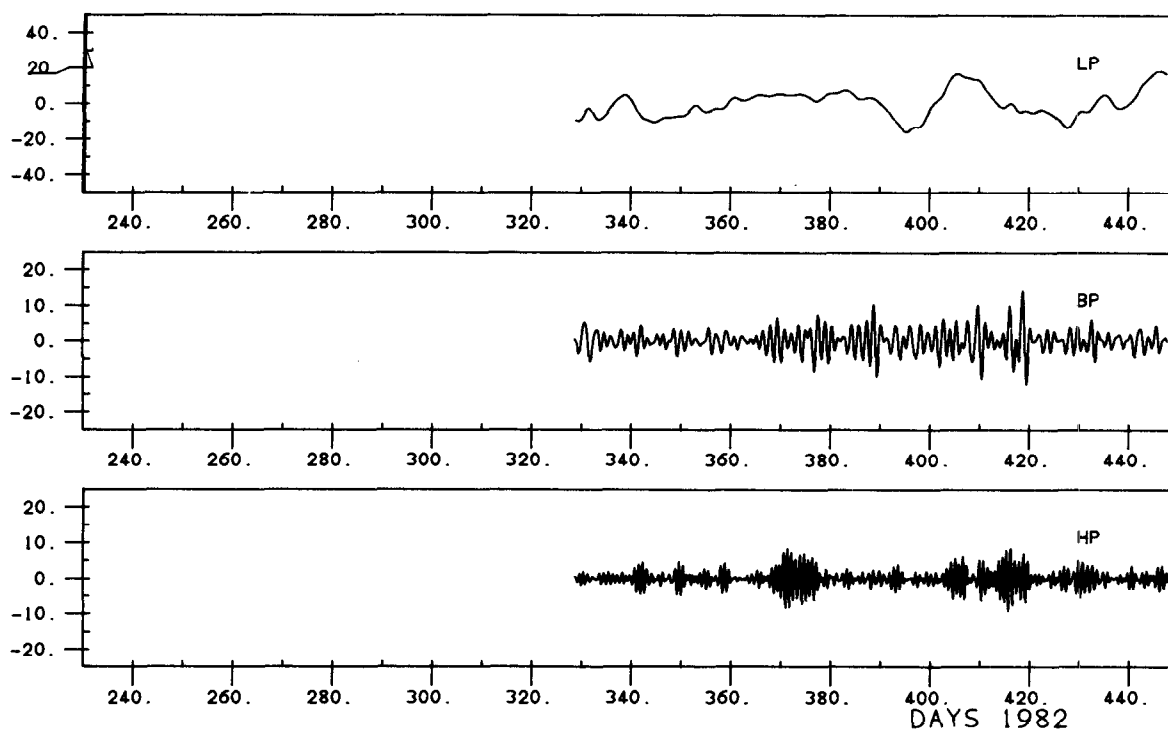
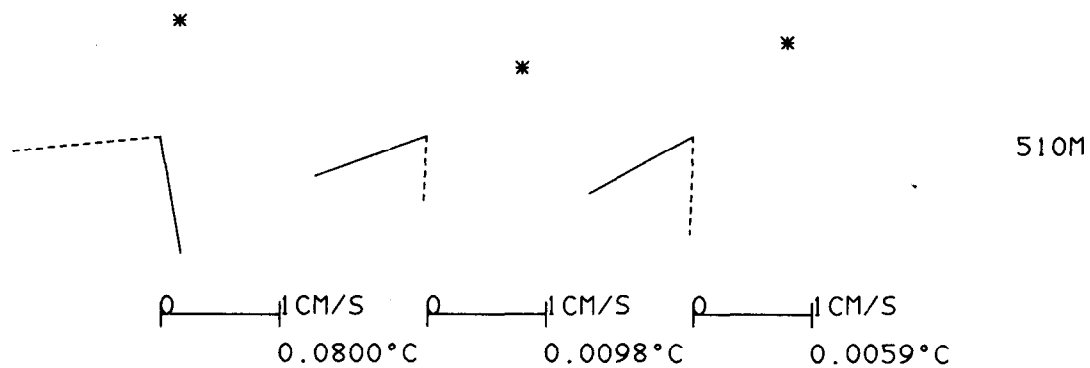
FREQUENCY BANDS

LOWPASS

BANDPASS

HIGHPASS

C/M DEPTH



D5B1

↑ N

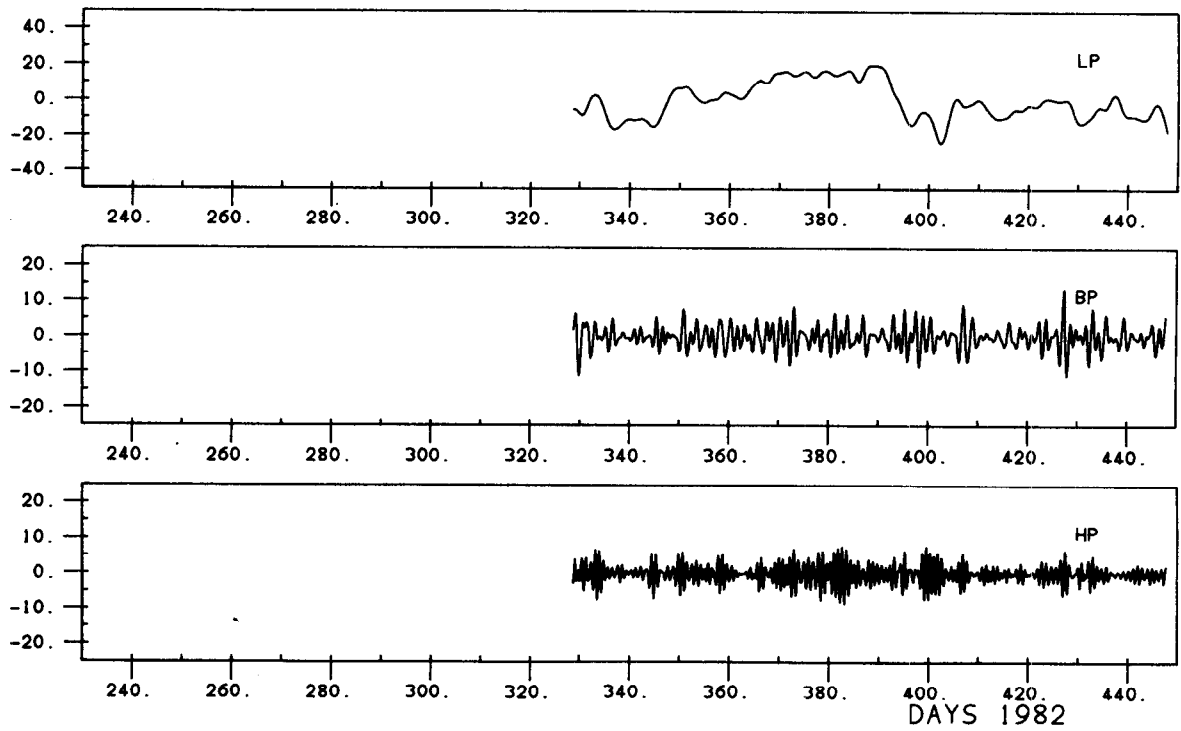
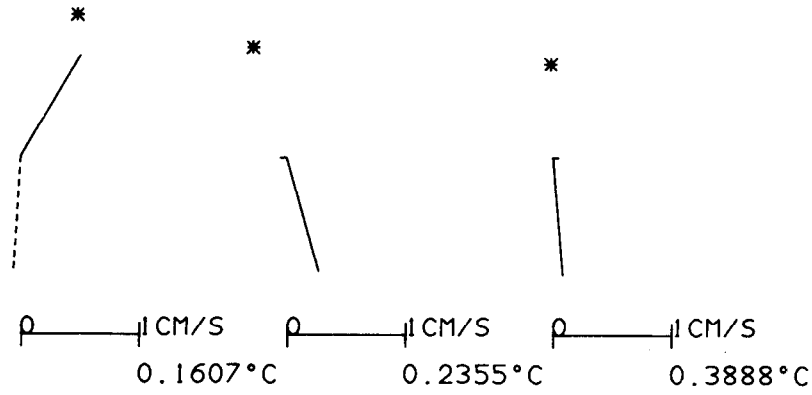
FREQUENCY BANDS

LOWPASS

BANDPASS

HIGHPASS

C/M DEPTH



I2

↑ N

FREQUENCY BANDS

LOWPASS

BANDPASS

HIGHPASS

C/M DEPTH

*

*

*

251M

*

*

*

654M

*

*

*

1055M

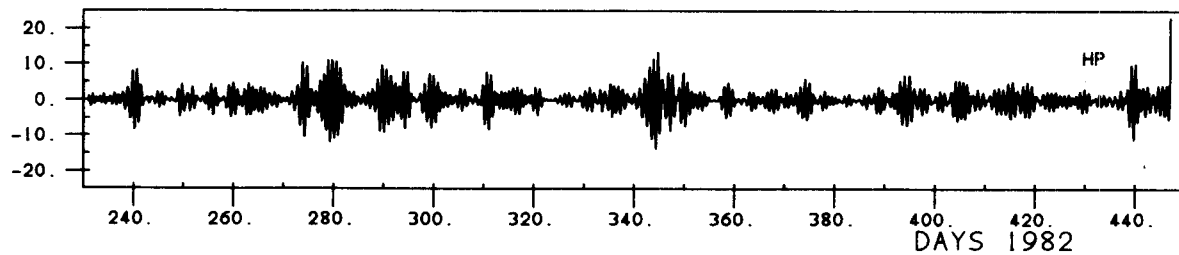
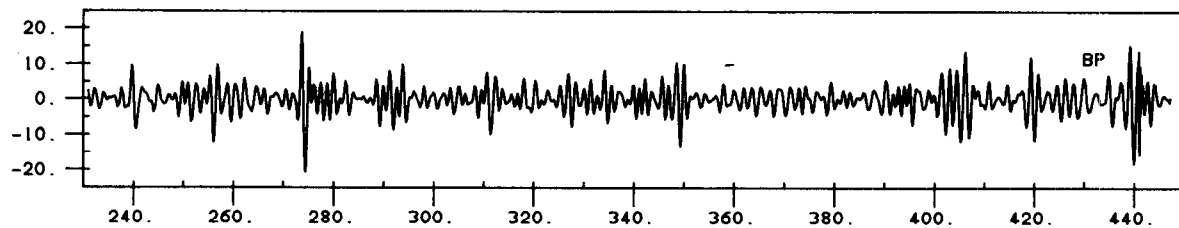
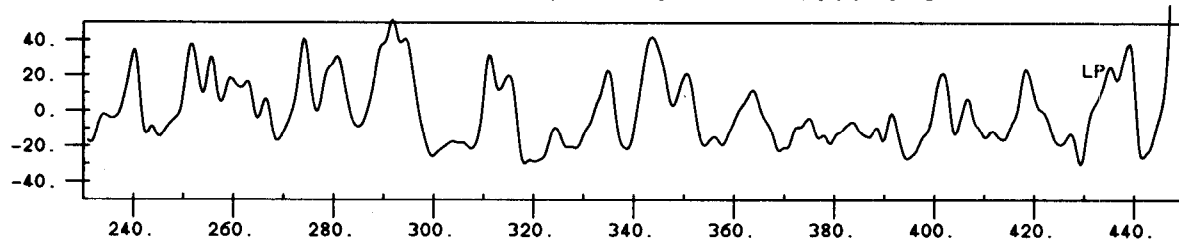
*

*

*

1440M

ρ	1 CM/S	ρ	1 CM/S	ρ	1 CM/S
0.0044°C		0.0028°C		0.0027°C	
0.0052°C		0.0026°C		0.0032°C	
0.0160°C		0.0019°C		0.0109°C	
0.0057°C		0.0085°C		0.0181°C	



DAYS 1982

E2

↑ N

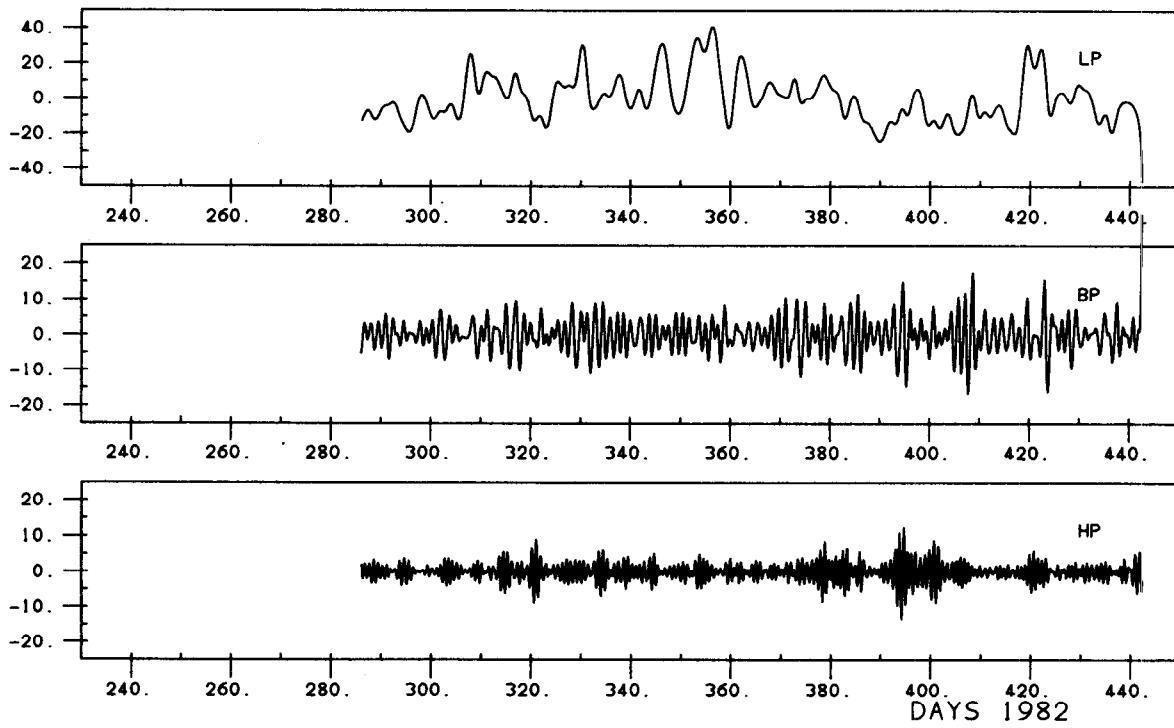
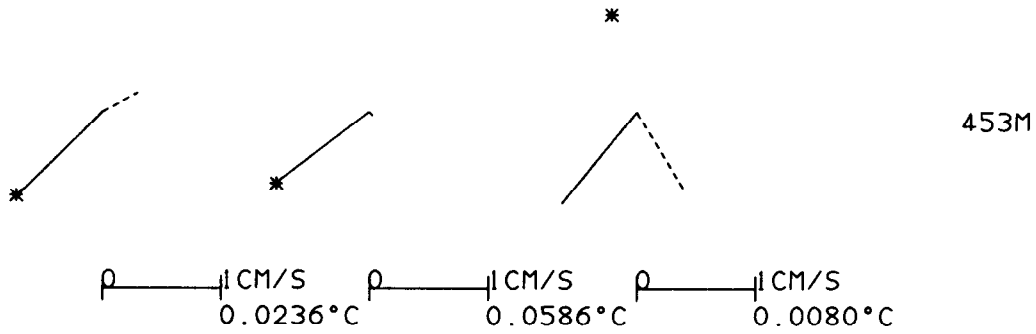
FREQUENCY BANDS

LOWPASS

BANDPASS

HIGHPASS

C/M DEPTH



E3T2

↑ N

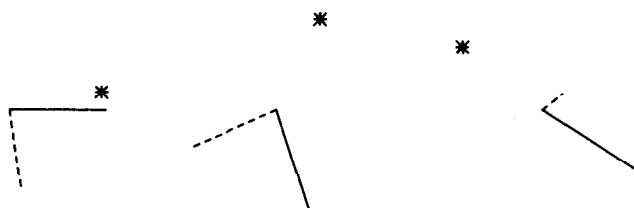
FREQUENCY BANDS

LOWPASS

BANDPASS

HIGHPASS

C/M DEPTH

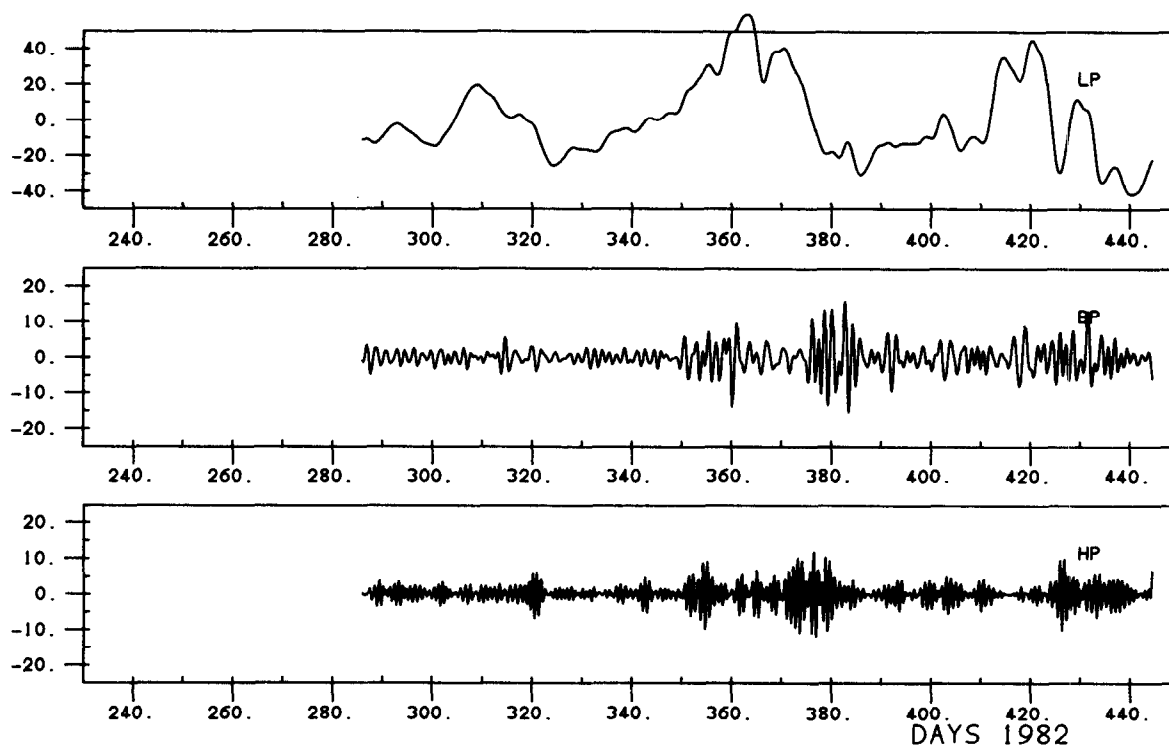


120M



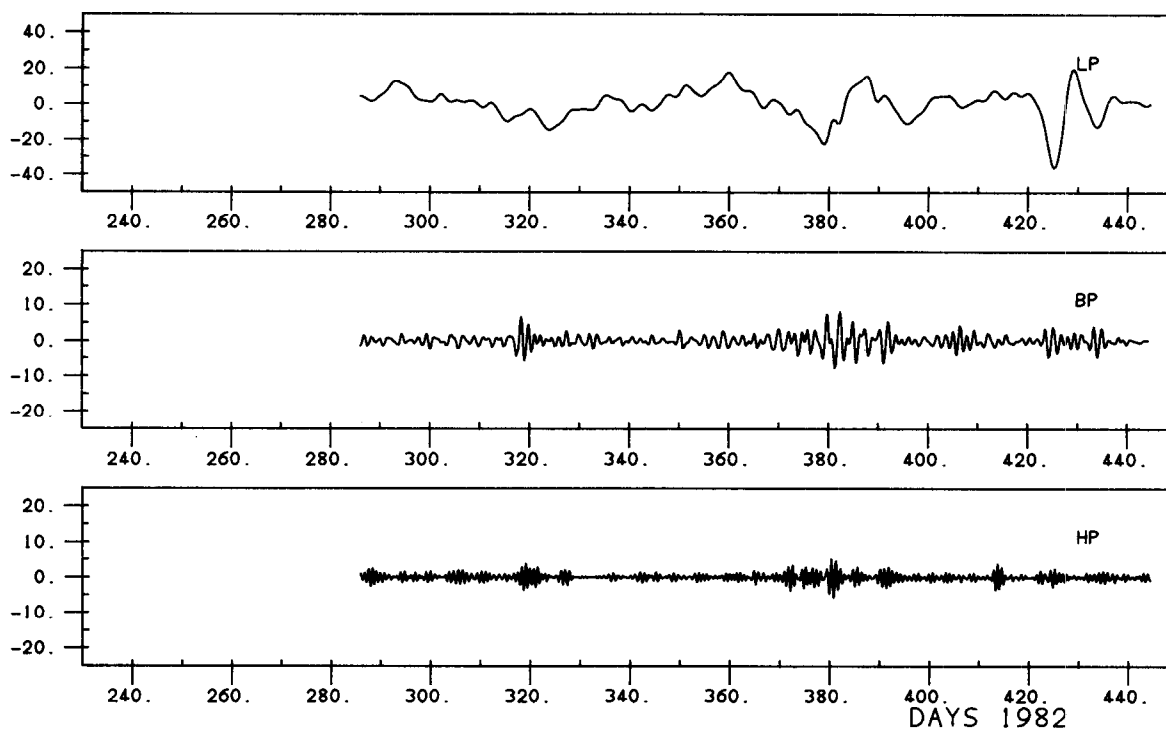
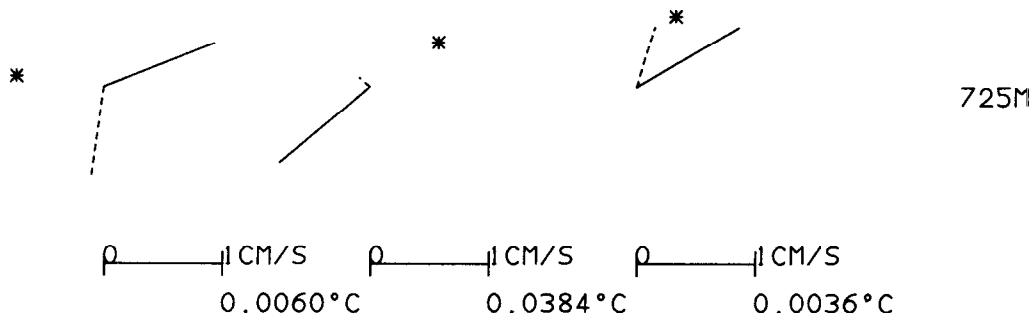
419M

ρ — 1 CM/S ρ — 1 CM/S ρ — 1 CM/S
0.0091°C 0.0104°C 0.0009°C
0.0303°C 0.0144°C 0.0053°C



E3N
FREQUENCY BANDS
LOWPASS BANDPASS HIGHPASS C/M DEPTH

↑ N



E4T

↑ N

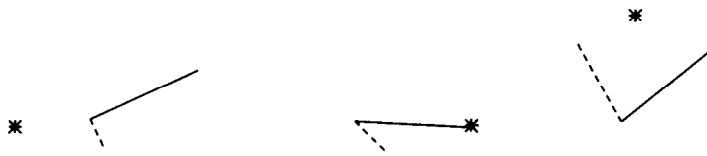
FREQUENCY BANDS

LOWPASS

BANDPASS

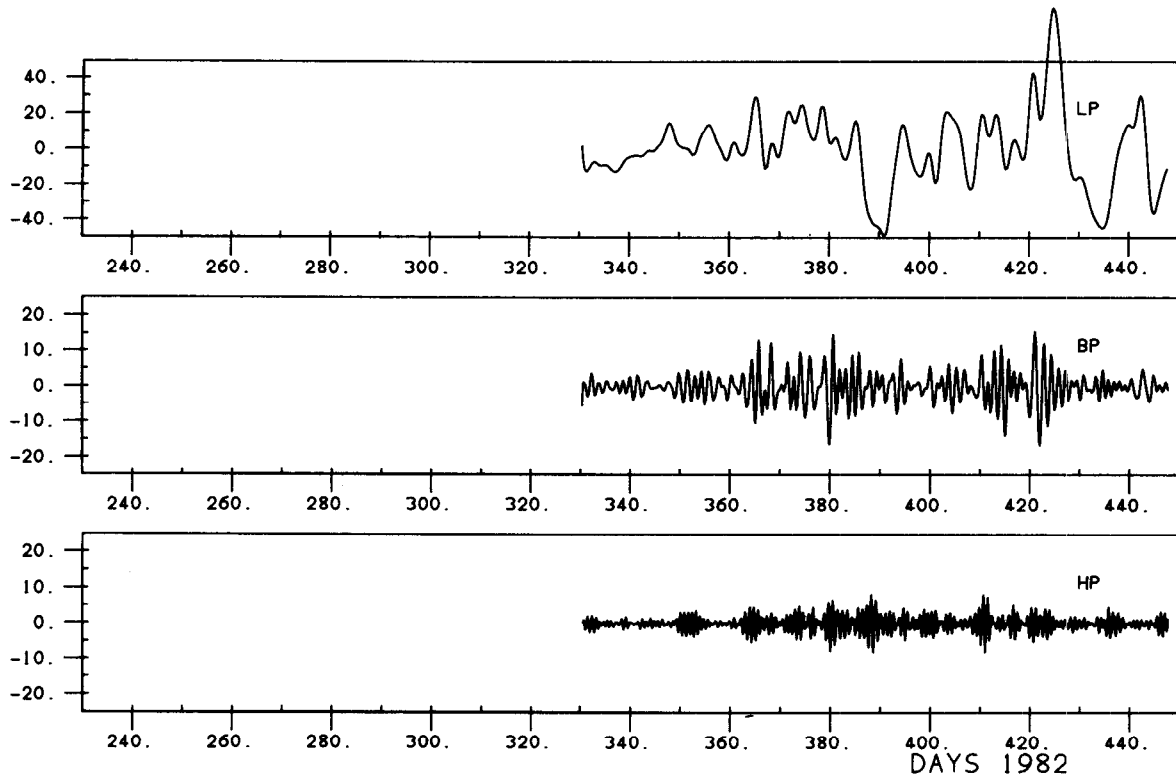
HIGHPASS

C/M DEPTH



95M

ρ — 1 CM/S ρ — 1 CM/S ρ — 1 CM/S
0.0171°C 0.0058°C 0.0004°C



E4B

FREQUENCY BANDS

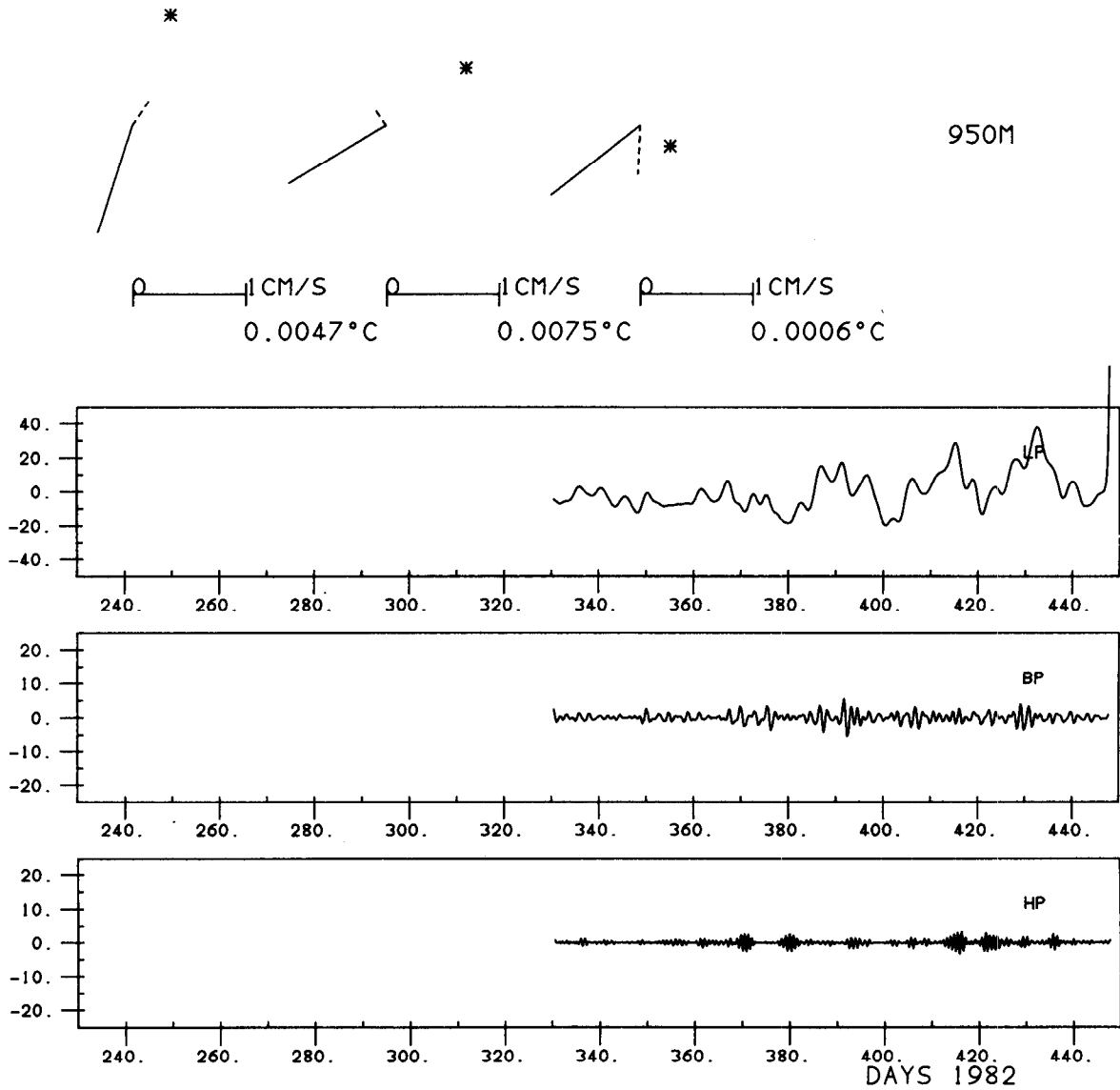
LOWPASS

BANDPASS

HIGHPASS

↑ N

C/M DEPTH



F1

FREQUENCY BANDS

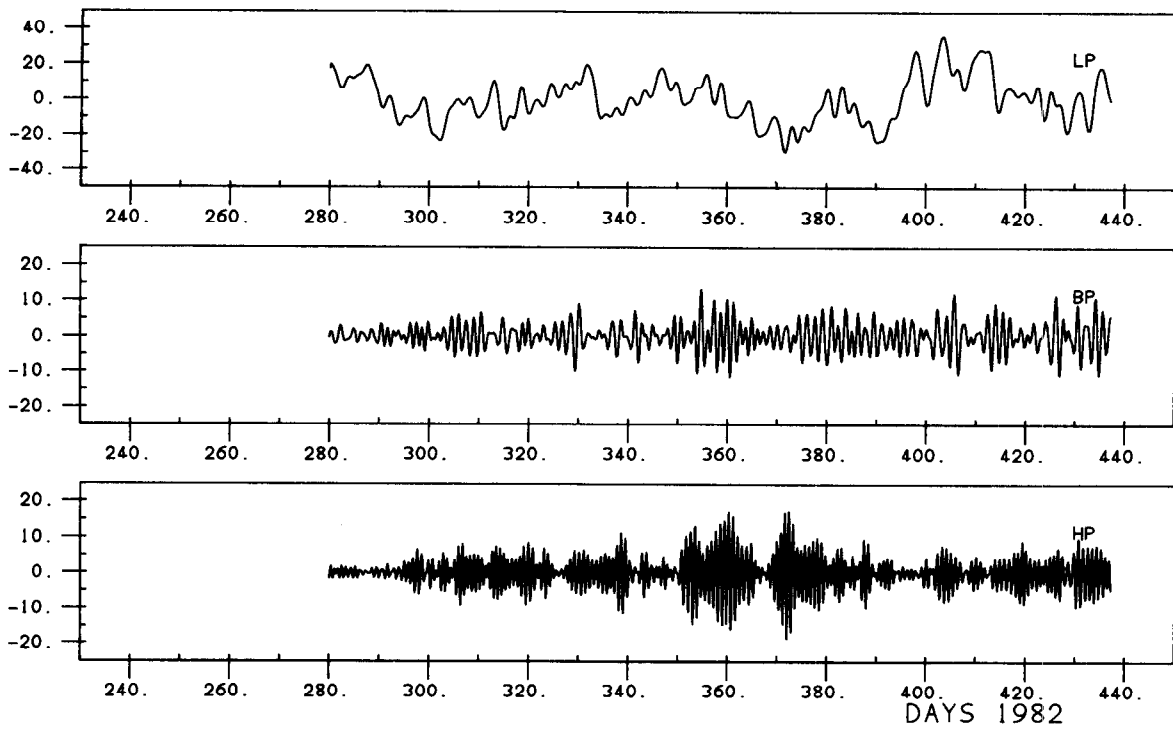
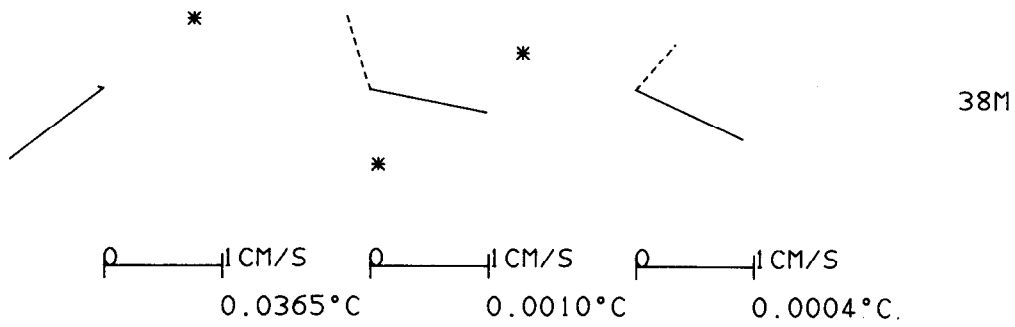
LOWPASS

BANDPASS

HIGHPASS

↑ N

C/M DEPTH



F3T2

FREQUENCY BANDS

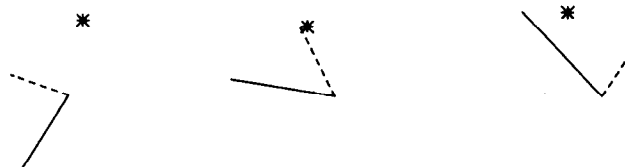
↑ N

LOWPASS

BANDPASS

HIGHPASS

C/M DEPTH

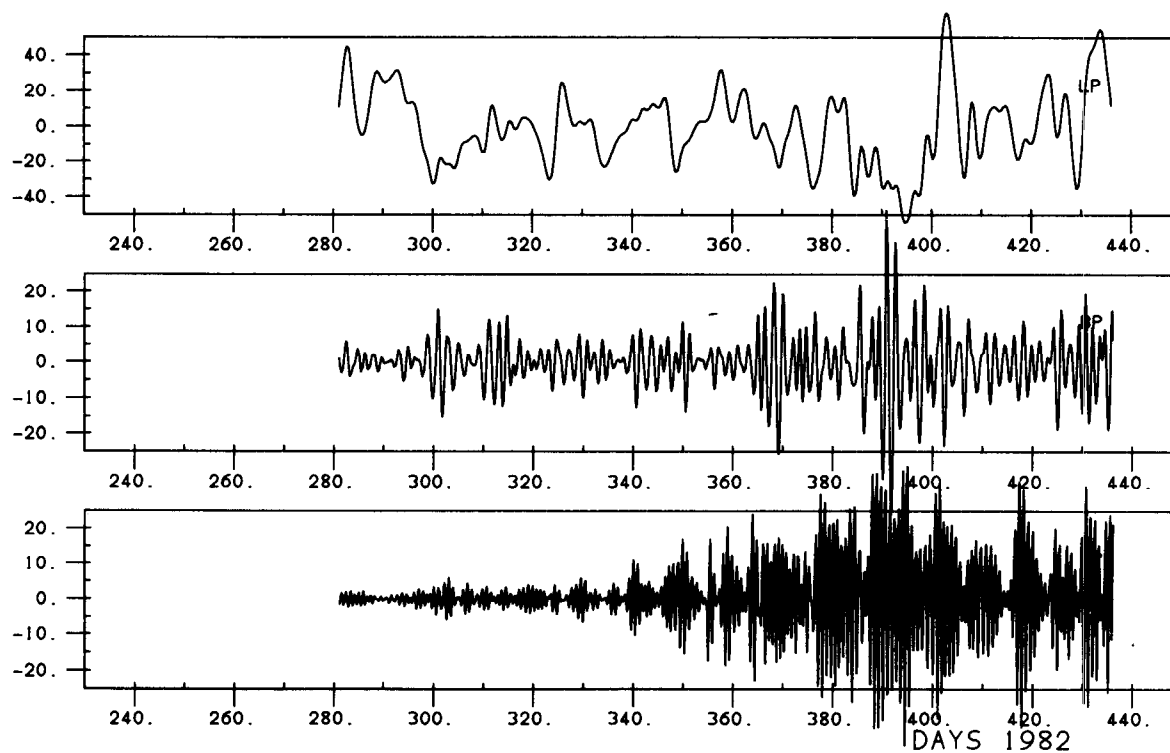


79M



388M

ρ ——— | CM/S ρ ——— | CM/S ρ ——— | CM/S
 0.0033°C 0.0185°C 0.0160°C
 0.0456°C 0.0184°C 0.0037°C



F3B2

↑ N

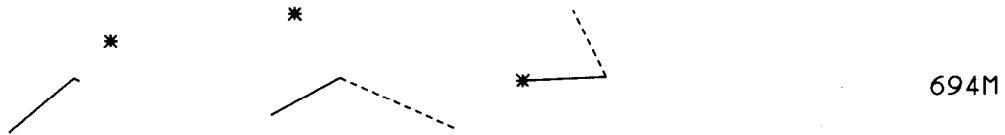
FREQUENCY BANDS

LOWPASS

BANDPASS

HIGHPASS

C/M DEPTH

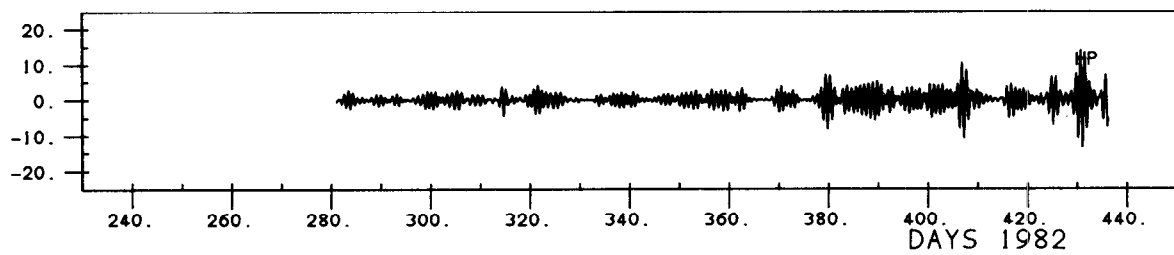
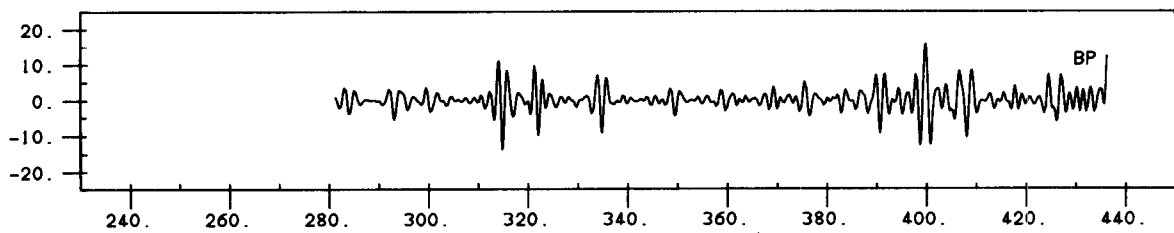
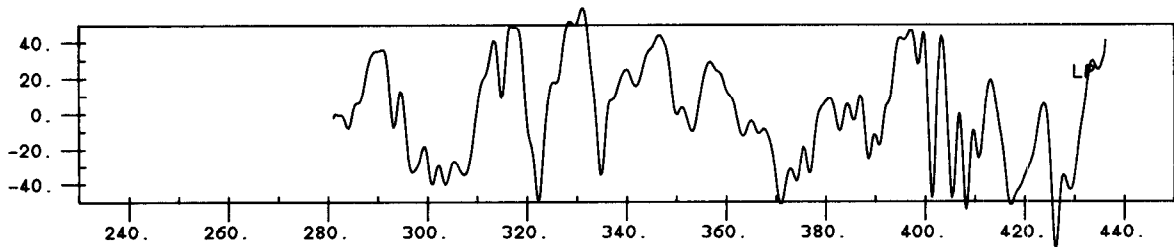


694M



945M

ρ — 1 CM/S ρ — 1 CM/S ρ — 1 CM/S
0.0173°C 0.0135°C 0.0045°C
0.0004°C 0.0011°C 0.0005°C



DAYS 1982

G1

↑ N

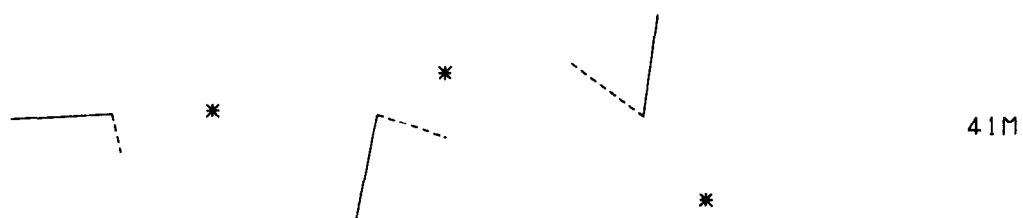
FREQUENCY BANDS

LOWPASS

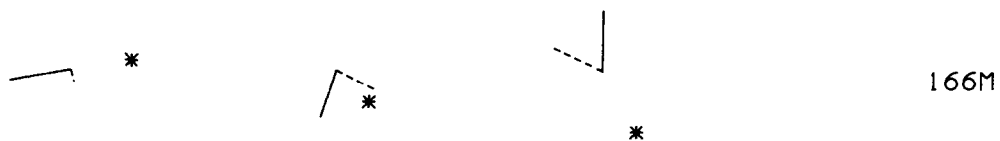
BANDPASS

HIGHPASS

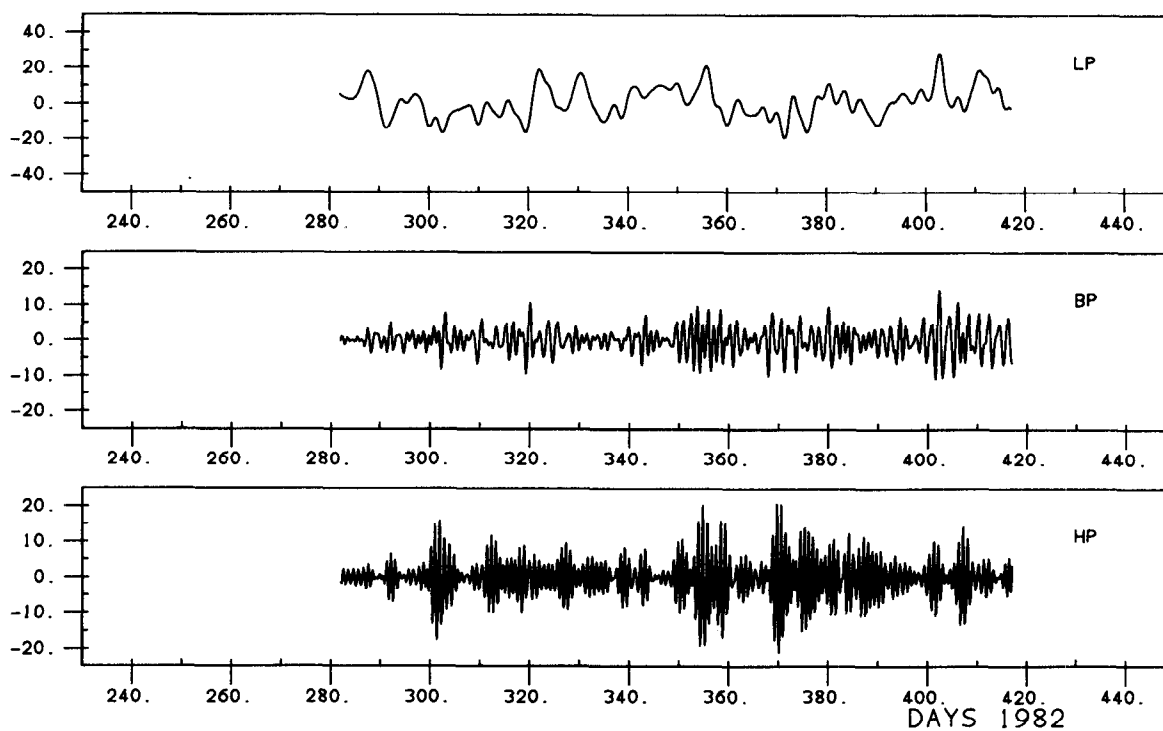
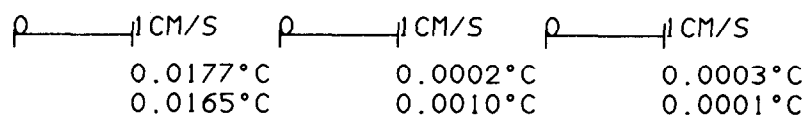
C/M DEPTH



41M



166M



G2T2

↑ N

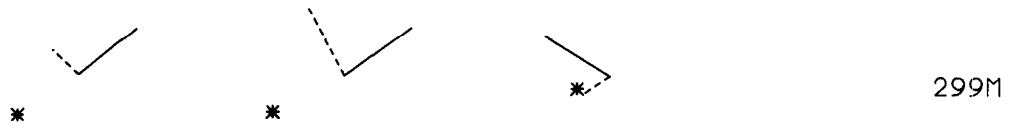
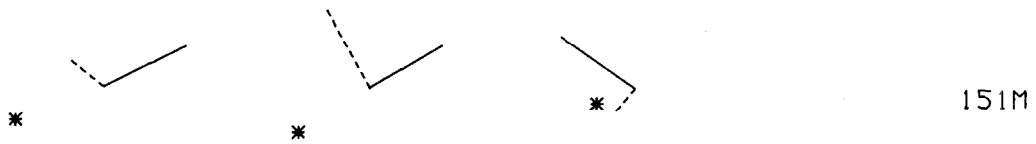
FREQUENCY BANDS

LOWPASS

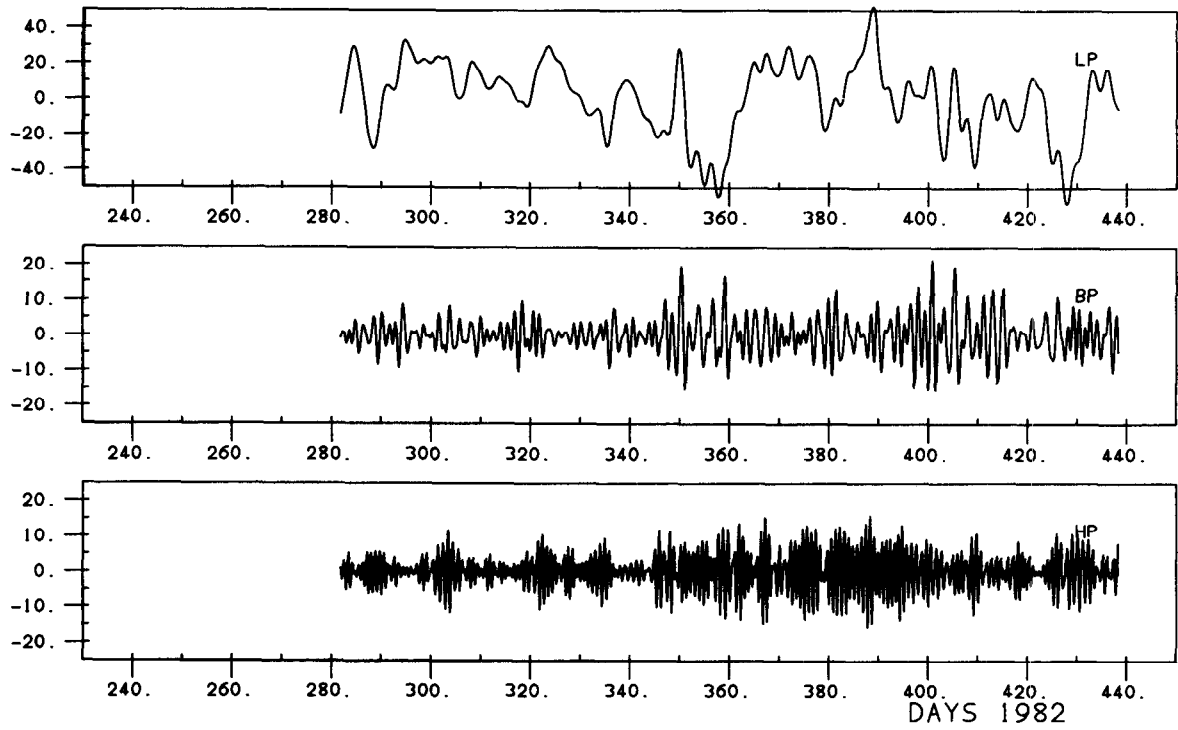
BANDPASS

HIGHPASS

C/M DEPTH



ρ ——— ρ ——— ρ ———
 1 CM/S 1 CM/S 1 CM/S
 0.0072°C 0.0121°C 0.0124°C
 0.0181°C 0.0150°C 0.0113°C



G2B

FREQUENCY BANDS

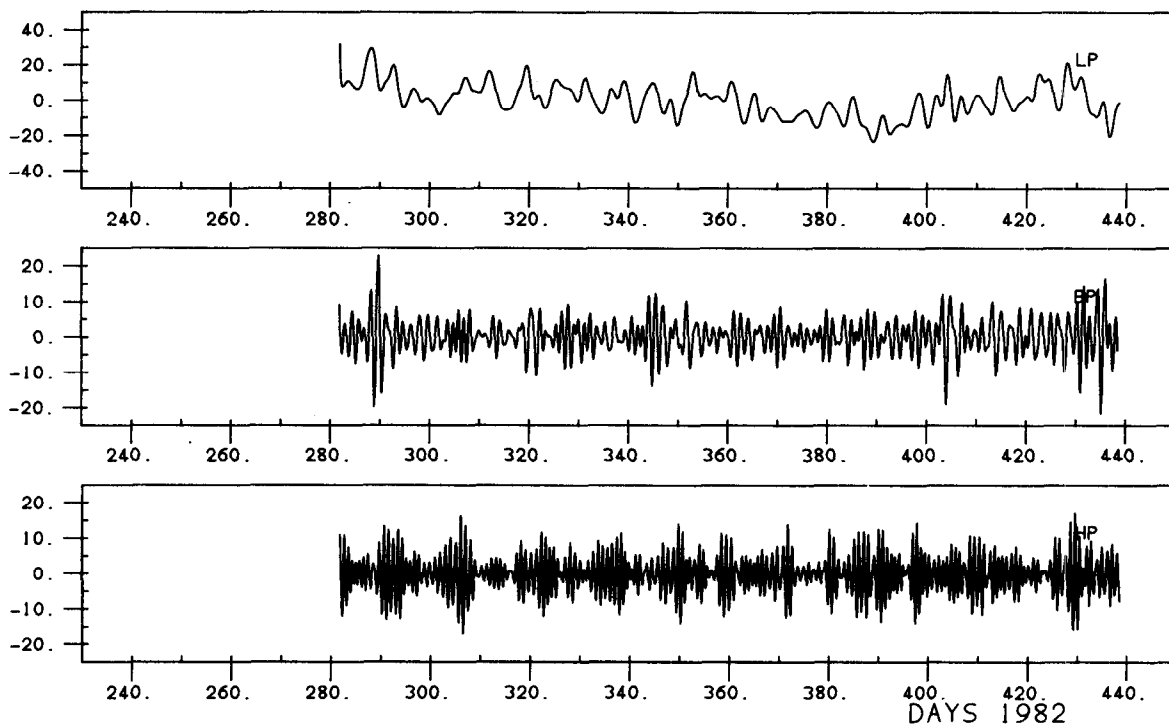
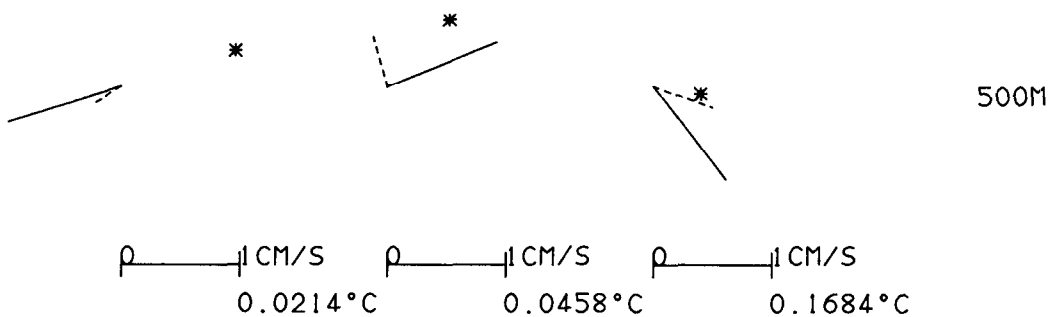
LOWPASS

BANDPASS

HIGHPASS

↑ N

C/M DEPTH



G4T1

↑ N

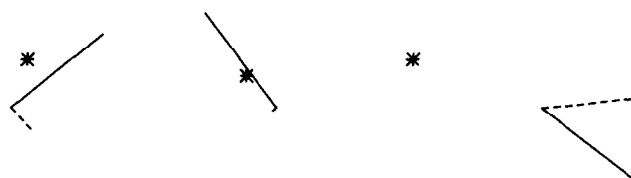
FREQUENCY BANDS

LOWPASS

BANDPASS

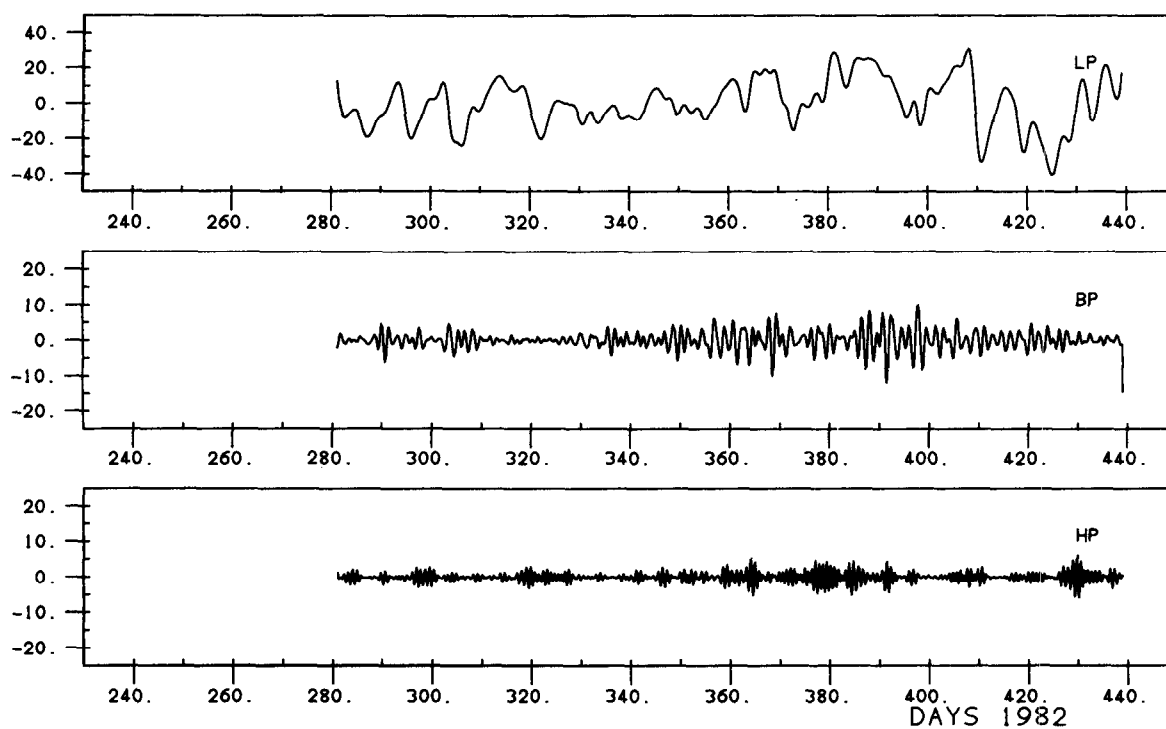
HIGHPASS

C/M DEPTH



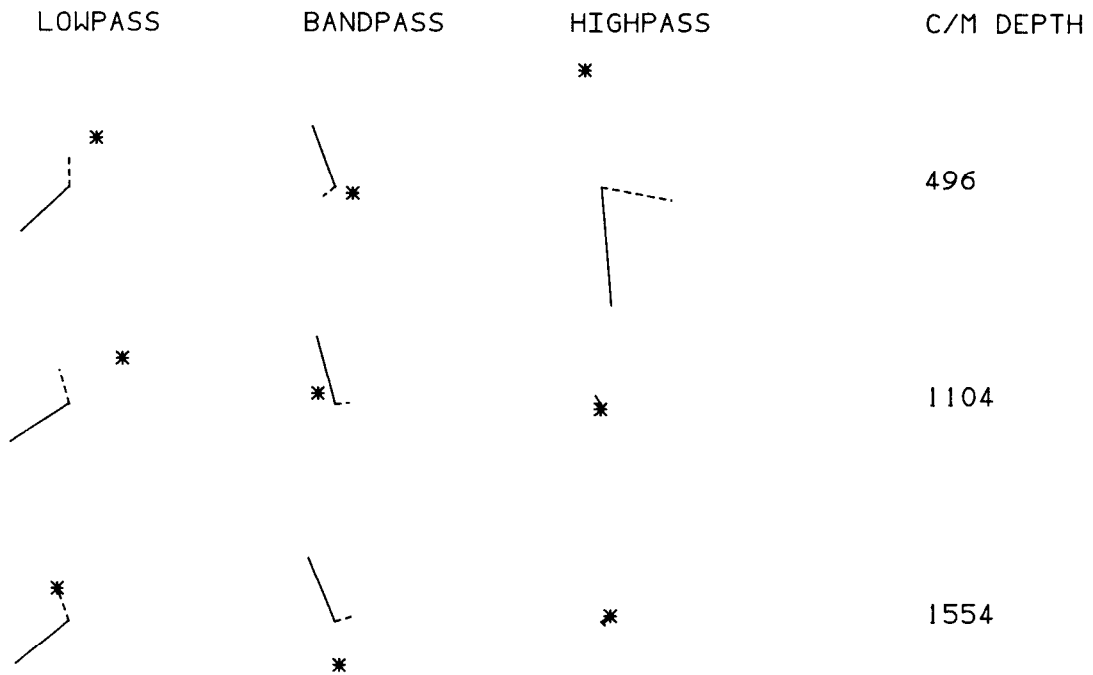
195M

ρ ——— | 1 CM/S ρ ——— | 1 CM/S ρ ——— | 1 CM/S
0.0418°C 0.3163°C 0.0073°C

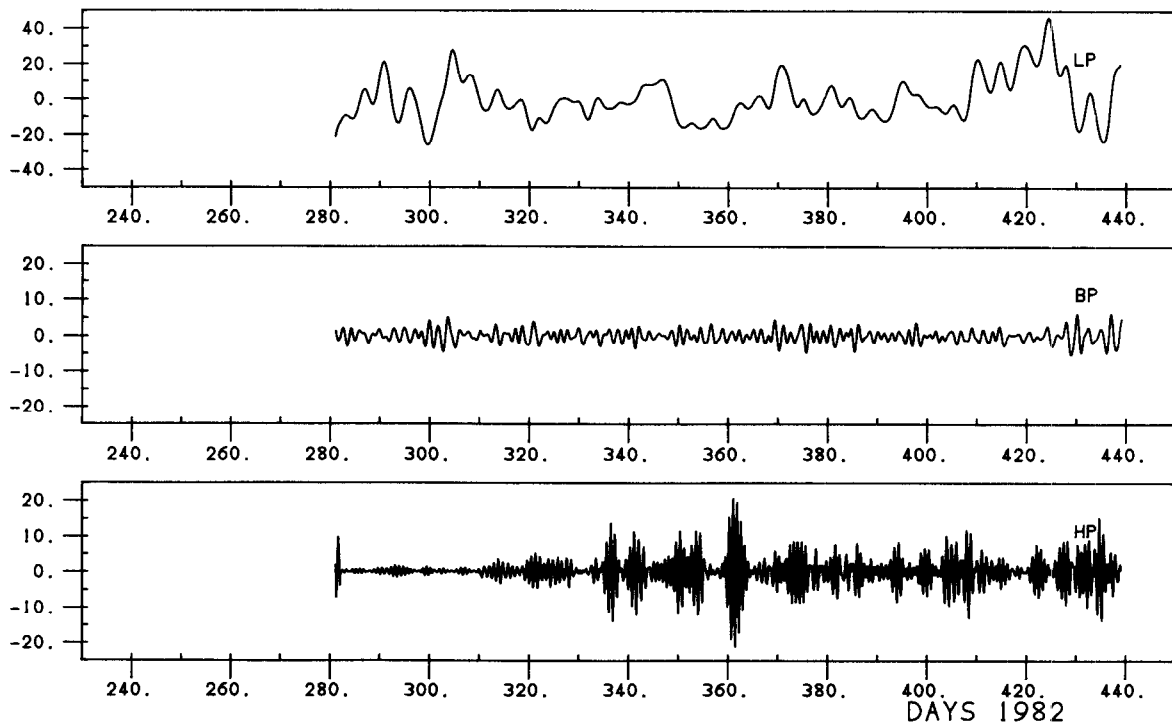


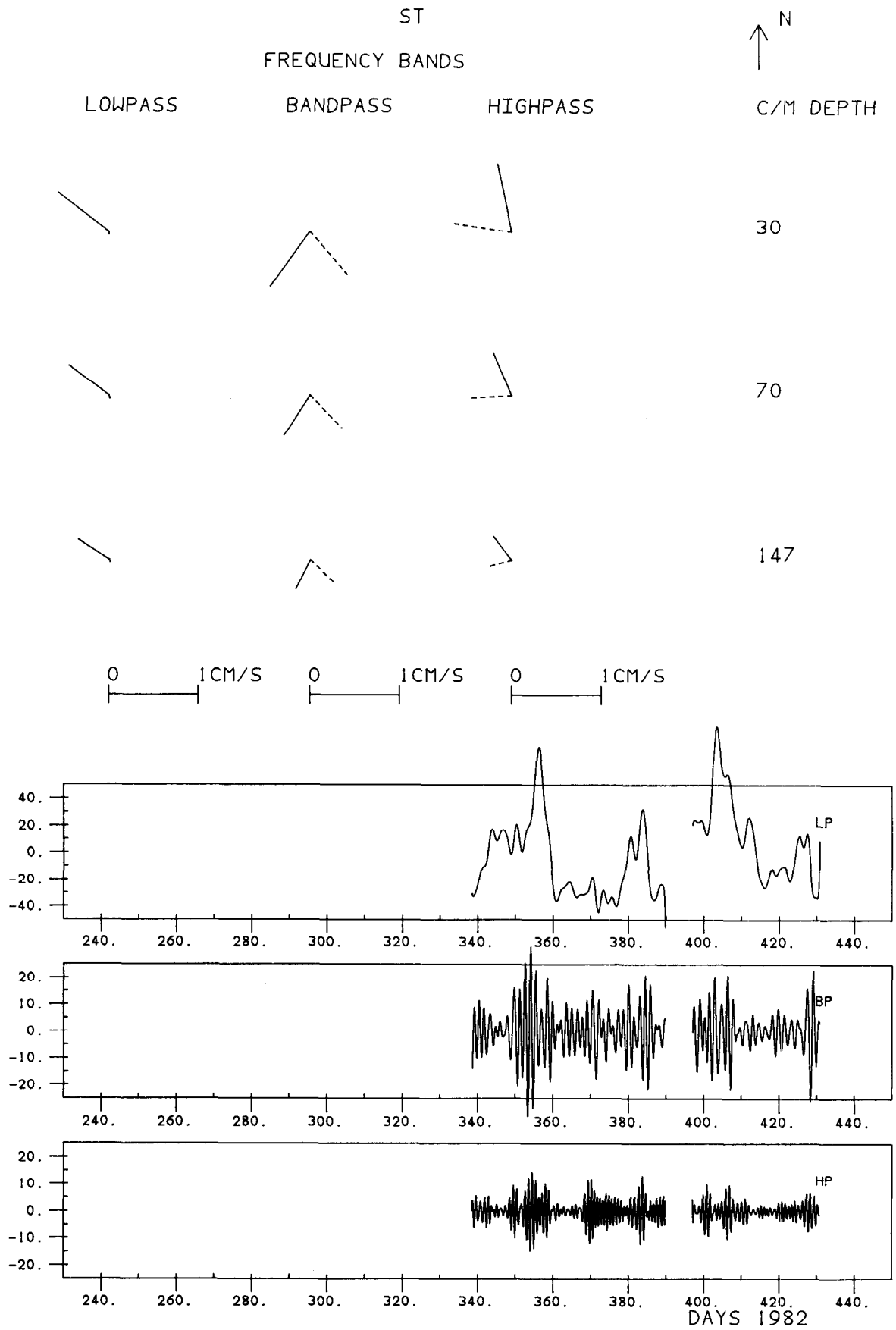
G4B3

FREQUENCY BANDS

N
↑

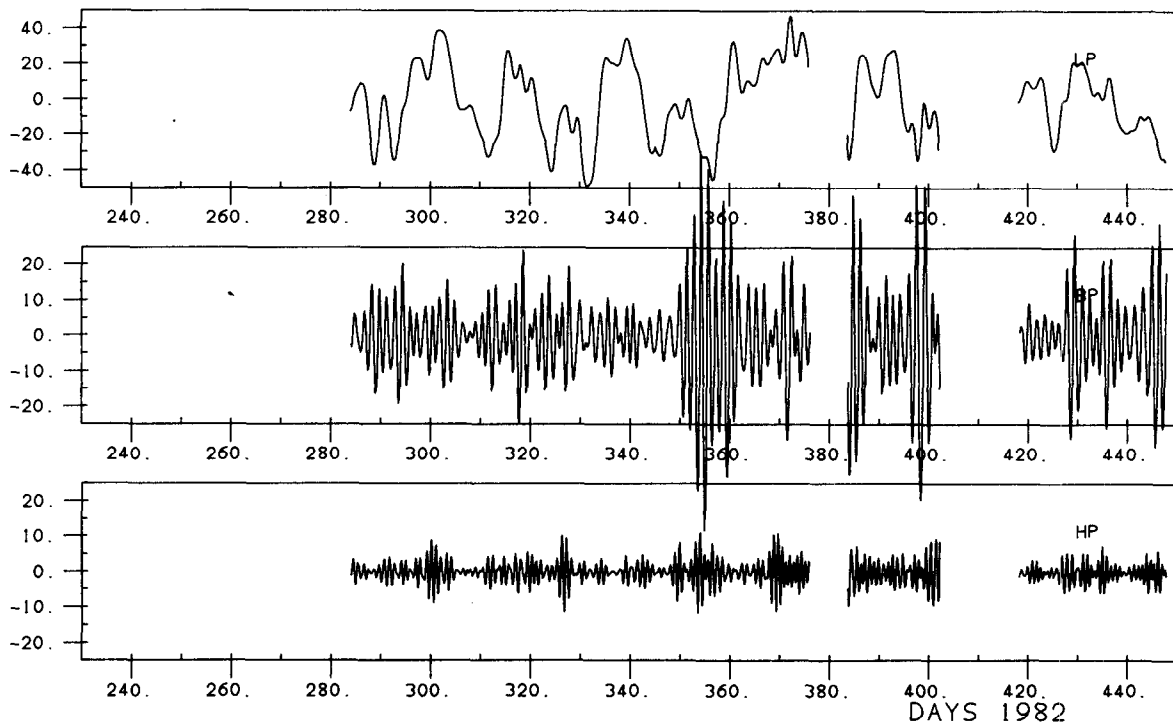
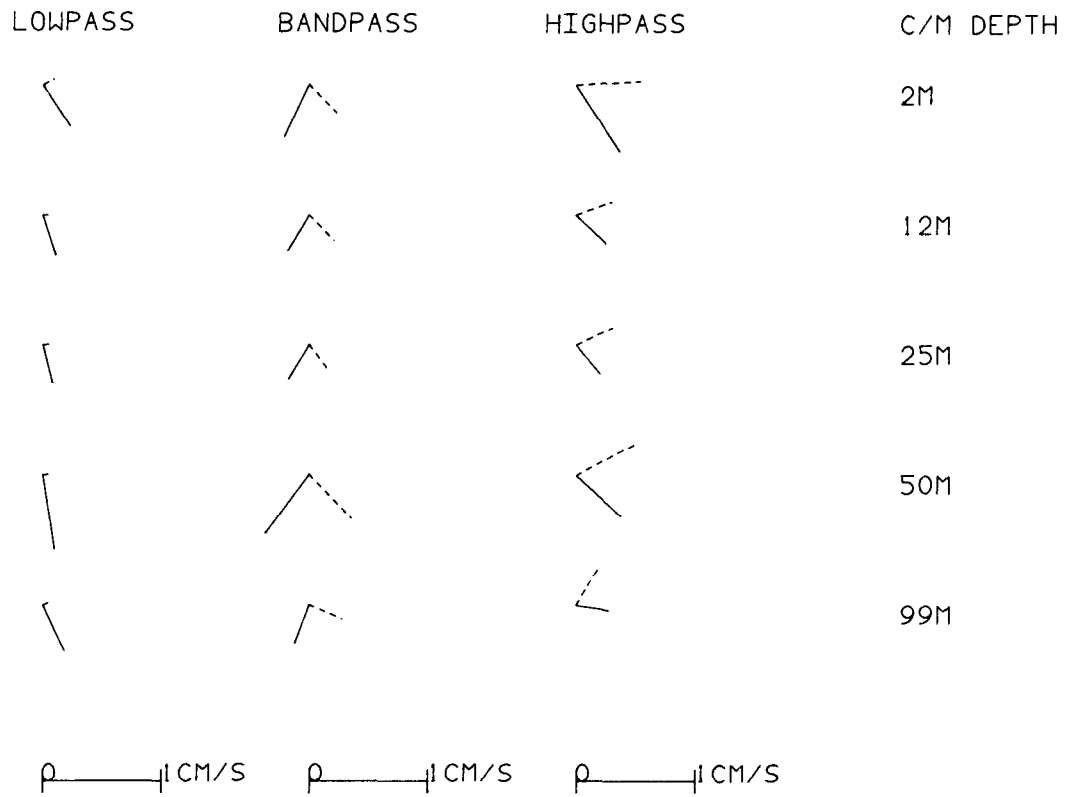
0	1CM/S	0	1CM/S	0	1CM/S
	0.0177°C		0.0393°C		0.0018°C
	0.0011°C		0.0023°C		0.0002°C
	0.0002°C		0.0016°C		0.0002°C





OSEBERG
FREQUENCY BANDS

↑ N



APPENDIX B. THERMISTOR CHAINS

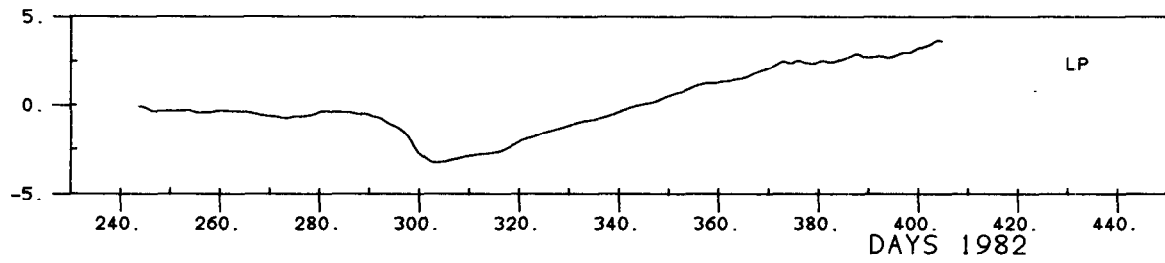
A plot follows for each of the chains B2 and G1, showing series and corresponding forms for each frequency band (LP, BP, HP). The arrows denote the magnitude of temperature variations at the various depths by their respective lengths, while their direction denotes phase. An Argand diagram convention is used; thus the component of $\underline{a}_1 + \sigma i \underline{a}_2$ for the appropriate depth is plotted, where $\sigma^2 = \text{var}[\varphi(t+\Delta t) - \varphi(t)] / \text{var}[\varphi(t)]$. By this convention, a clockwise rotation denotes a phase lag. The scale shows \underline{a}_1 corresponding to dimensionless $\varphi(t)$ numerically as plotted.

THERMISTOR CHAIN AT B2

1 2 3 4 5 6 7 8 9 10 11

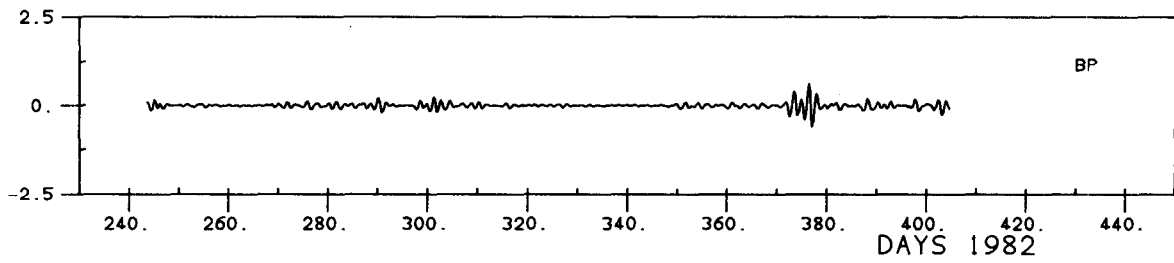
LOWPASS

< < < < < < < < < < <



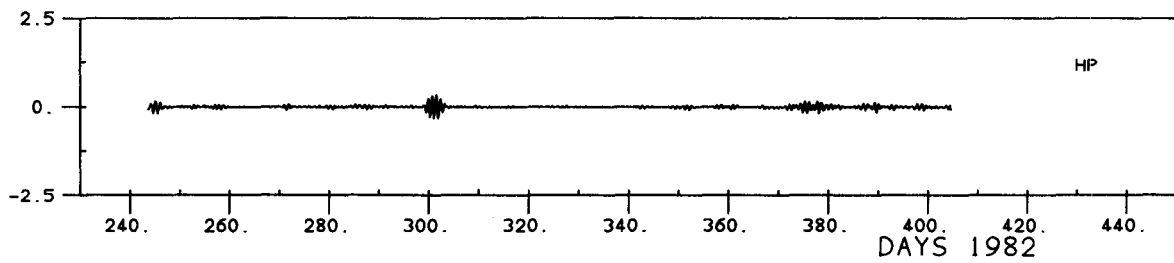
BANDPASS

< < < < < < < < < < <



HIGHPASS

< < < < < < < < < < <



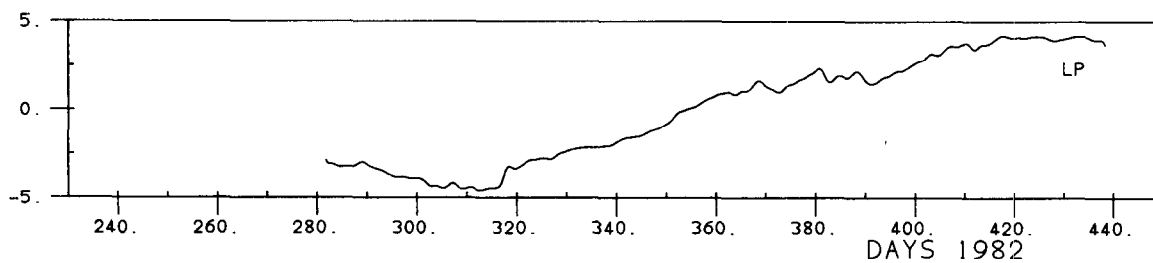
0 1 DEG.C

THERMISTOR CHAIN AT G1

1 2 3 4 5 6 7 8 9 10 11

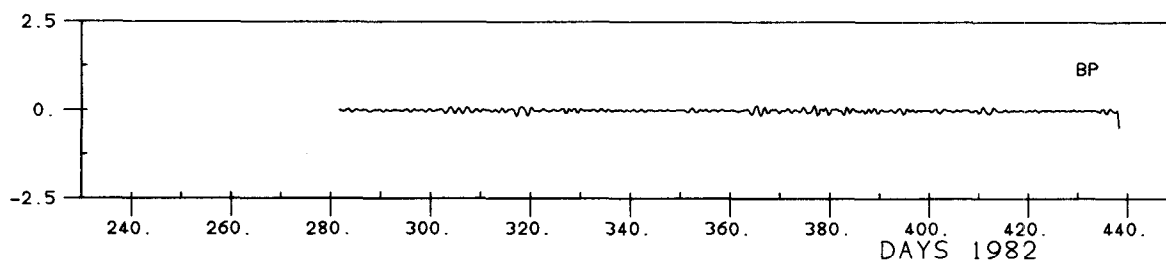
LOWPASS

< < < < < < < < < < <



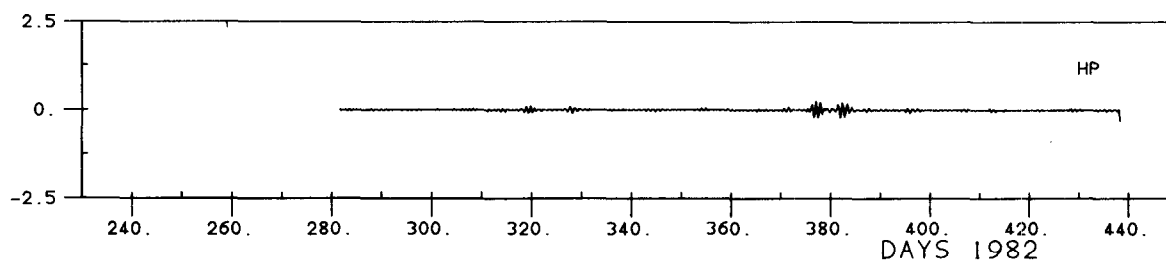
BANDPASS

< < < < < < < < < < <



HIGHPASS

< < < < < < < < < < <



0 1 DEG. C

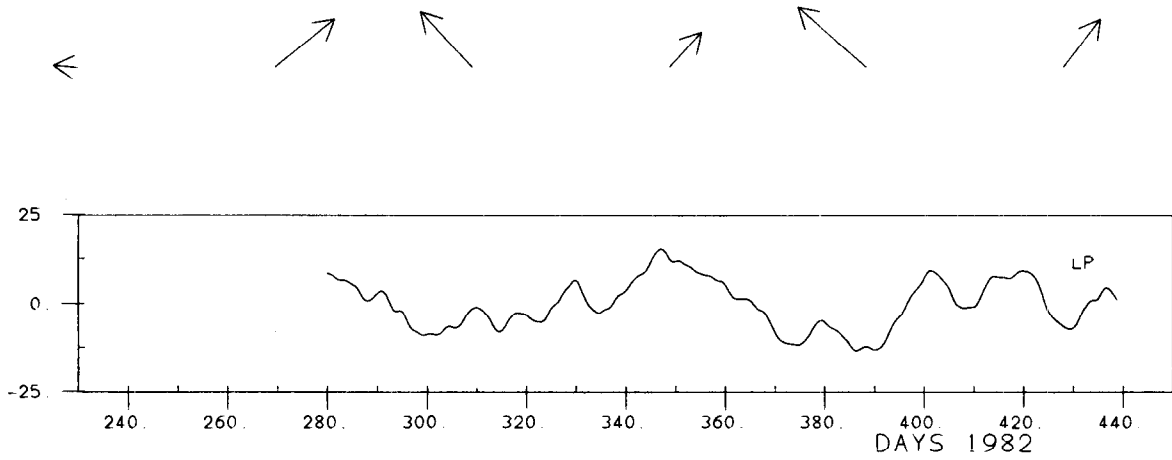
APPENDIX C. BOTTOM PRESSURE AND TEMPERATURE

Plots follow for all locations taken together to form a representative series in each frequency band. There are also plots for sub-groups of bottom pressure location. Diagram conventions are as for Appendix B, with different locations of pressure (or bottom temperature) substituting for the depth on the thermistor chain.

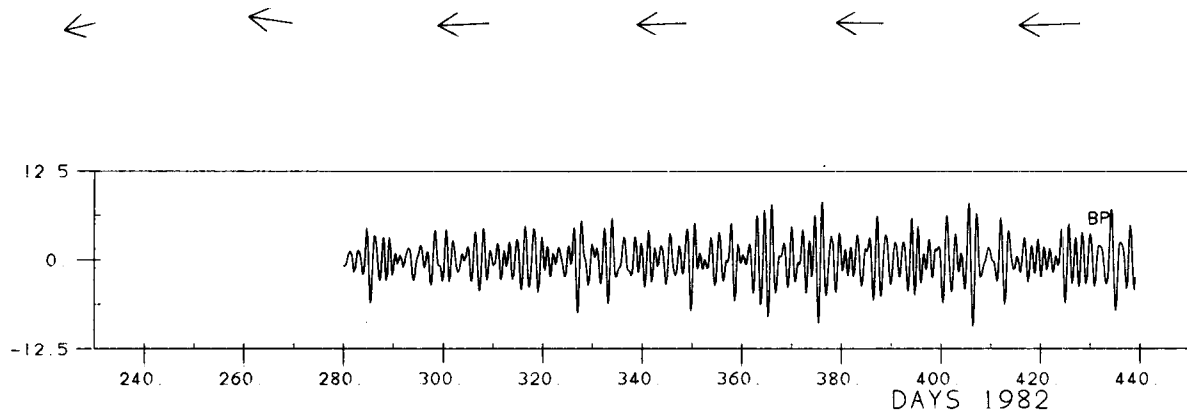
BOTTOM PRESSURES D1, E3, F1, F3, G1, G4

D1 E3 F1 F3 G1 G4

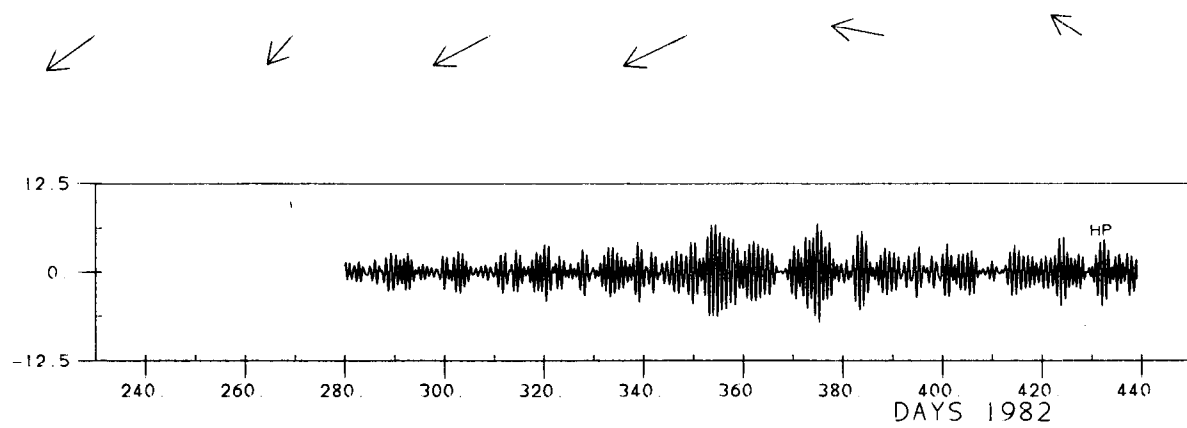
LOWPASS



BANDPASS



HIGHPASS



0 1 MB.

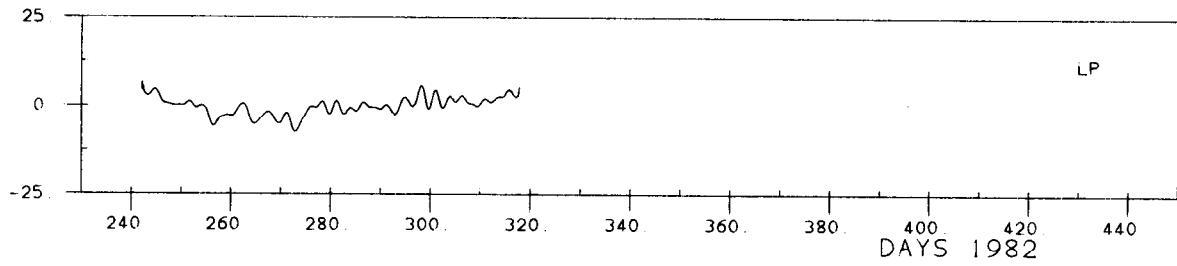
BOTTOM PRESSURES

C1

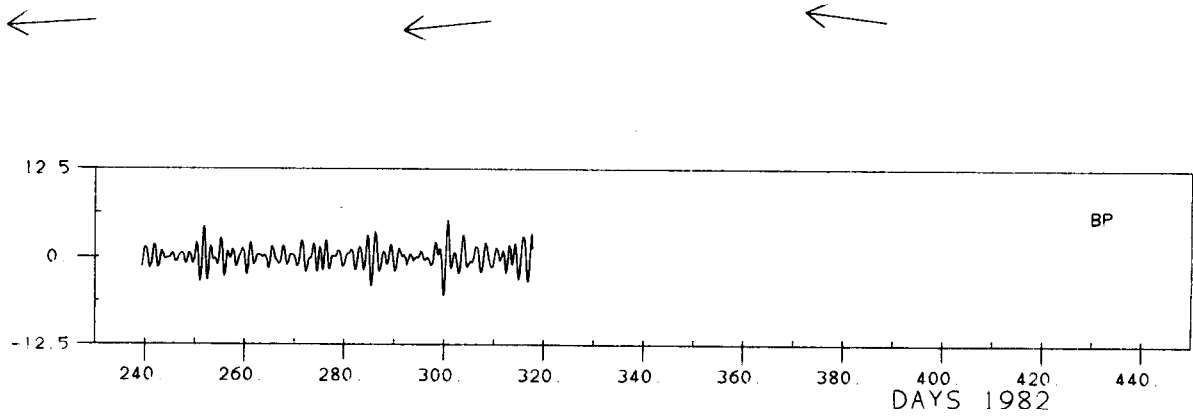
C4

D1

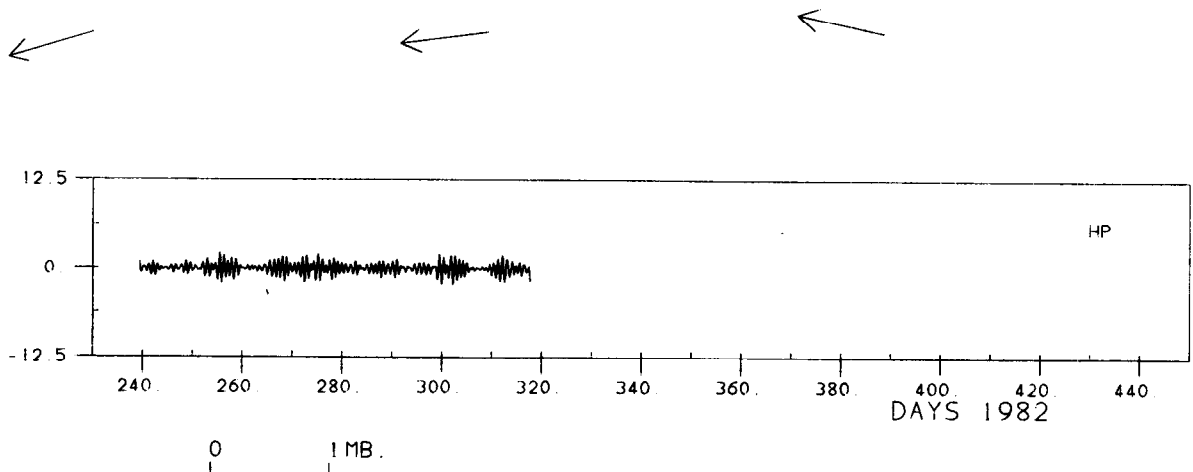
LOWPASS



BANDPASS



HIGHPASS



BOTTOM PRESSURES

B1

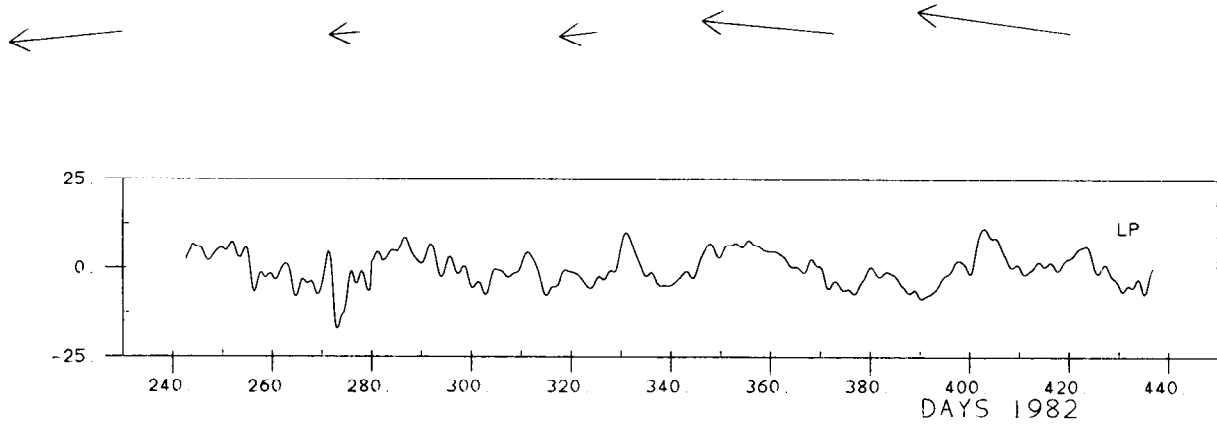
C1

D1

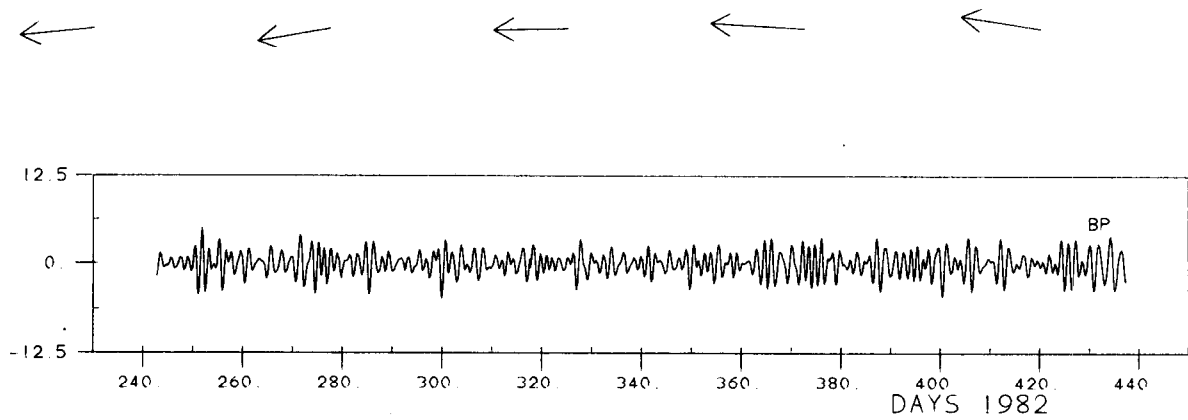
F1

G1

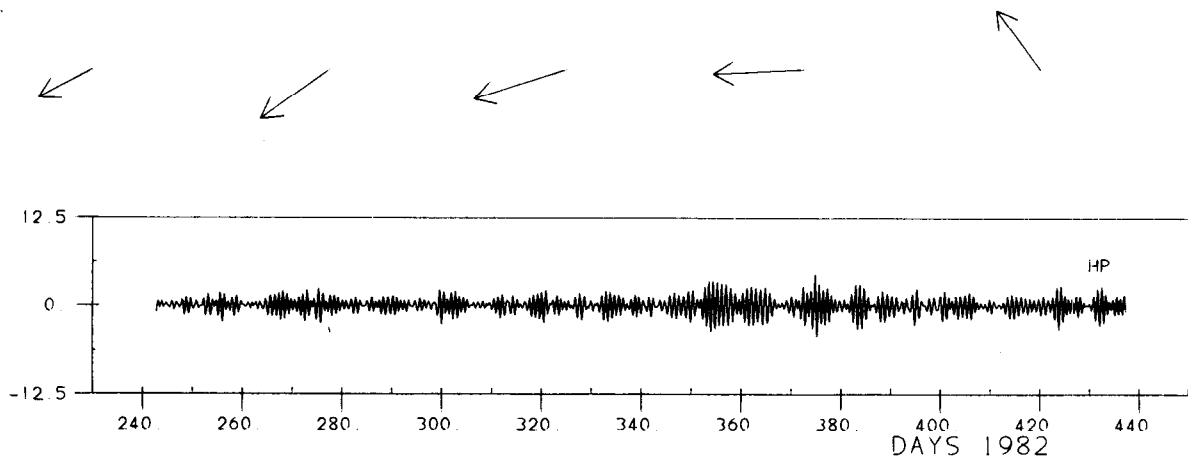
LOWPASS



BANDPASS



HIGHPASS

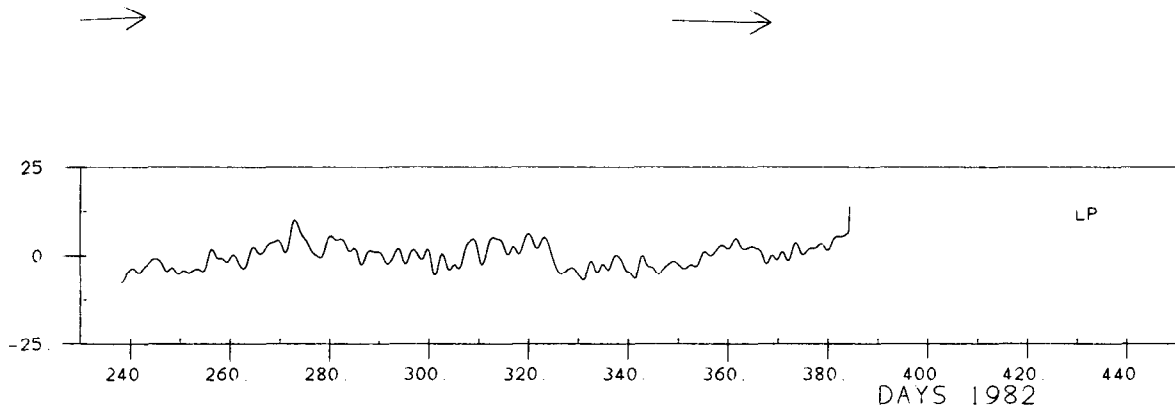


BOTTOM PRESSURES AT A6,B5

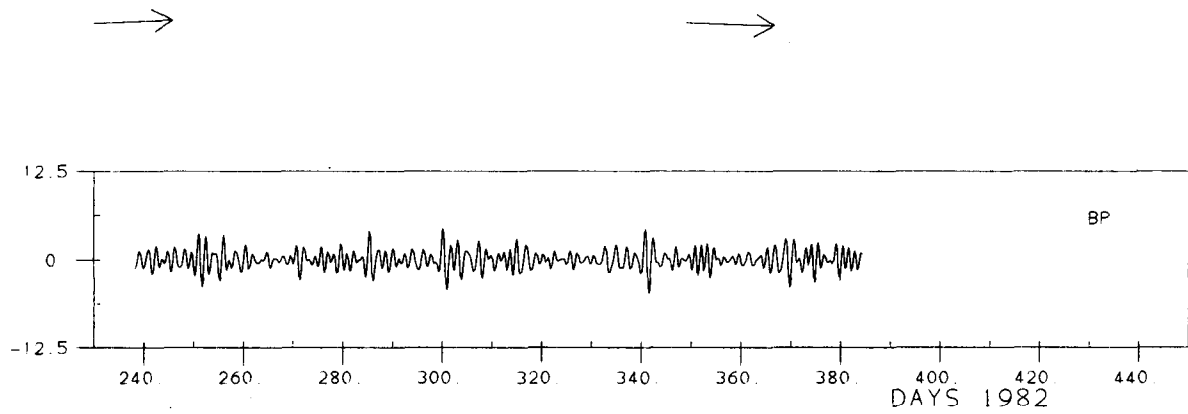
A6

B5

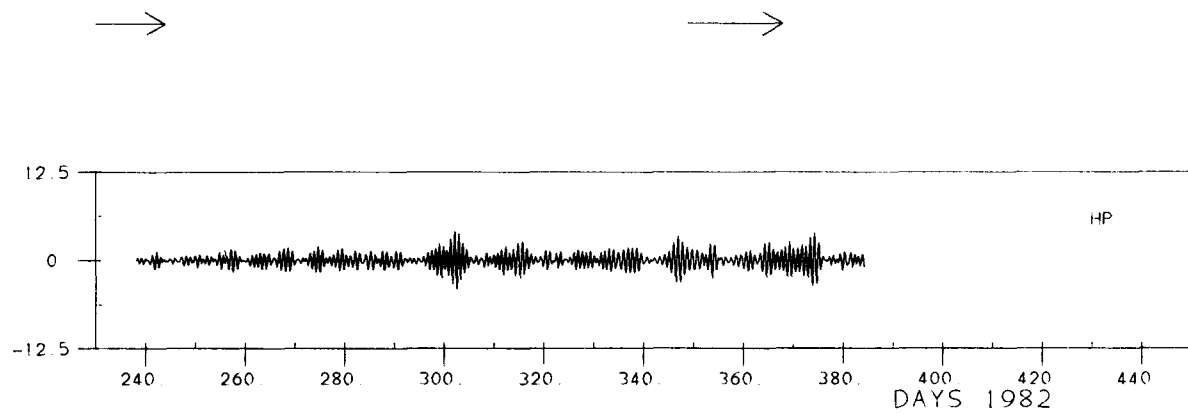
LOWPASS



BANDPASS



HIGHPASS



0 1 MB

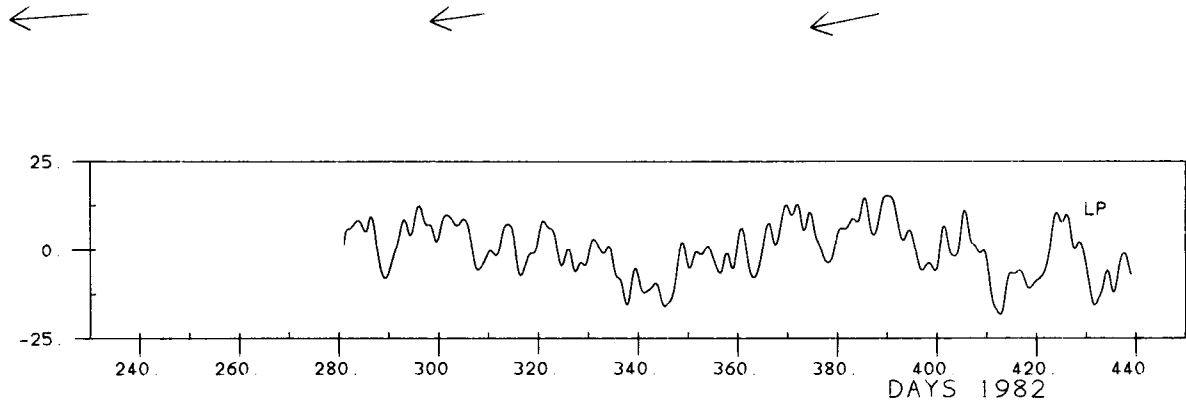
BOTTOM PRESSURES AT E3,F3,G4

E3

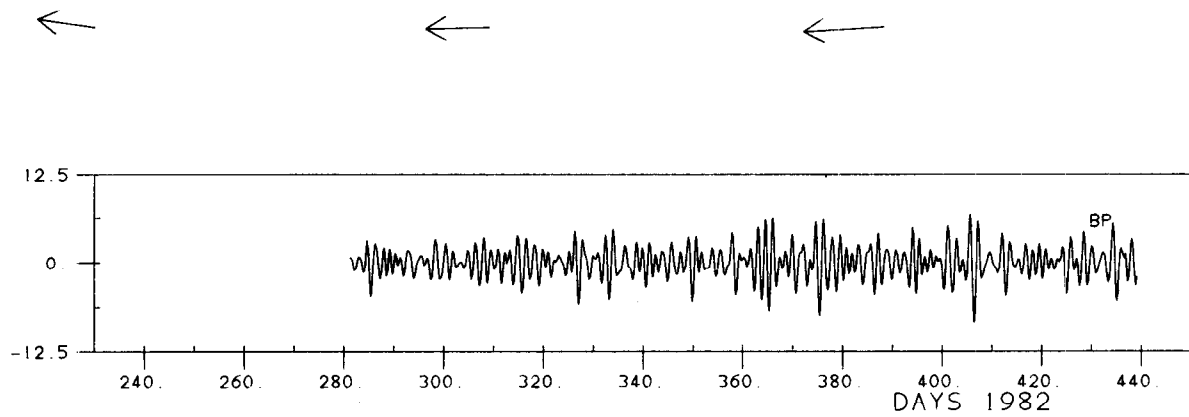
F3

G4

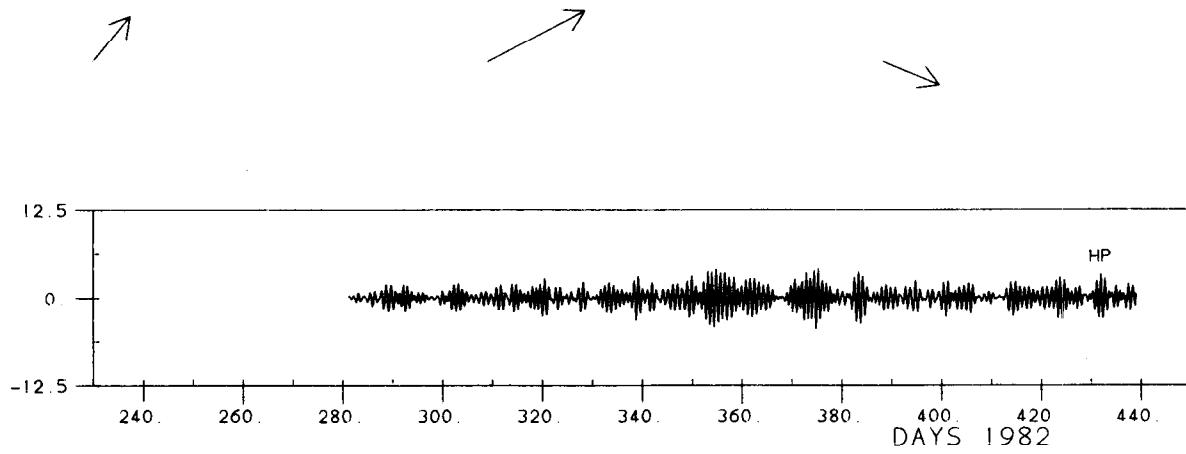
LOWPASS

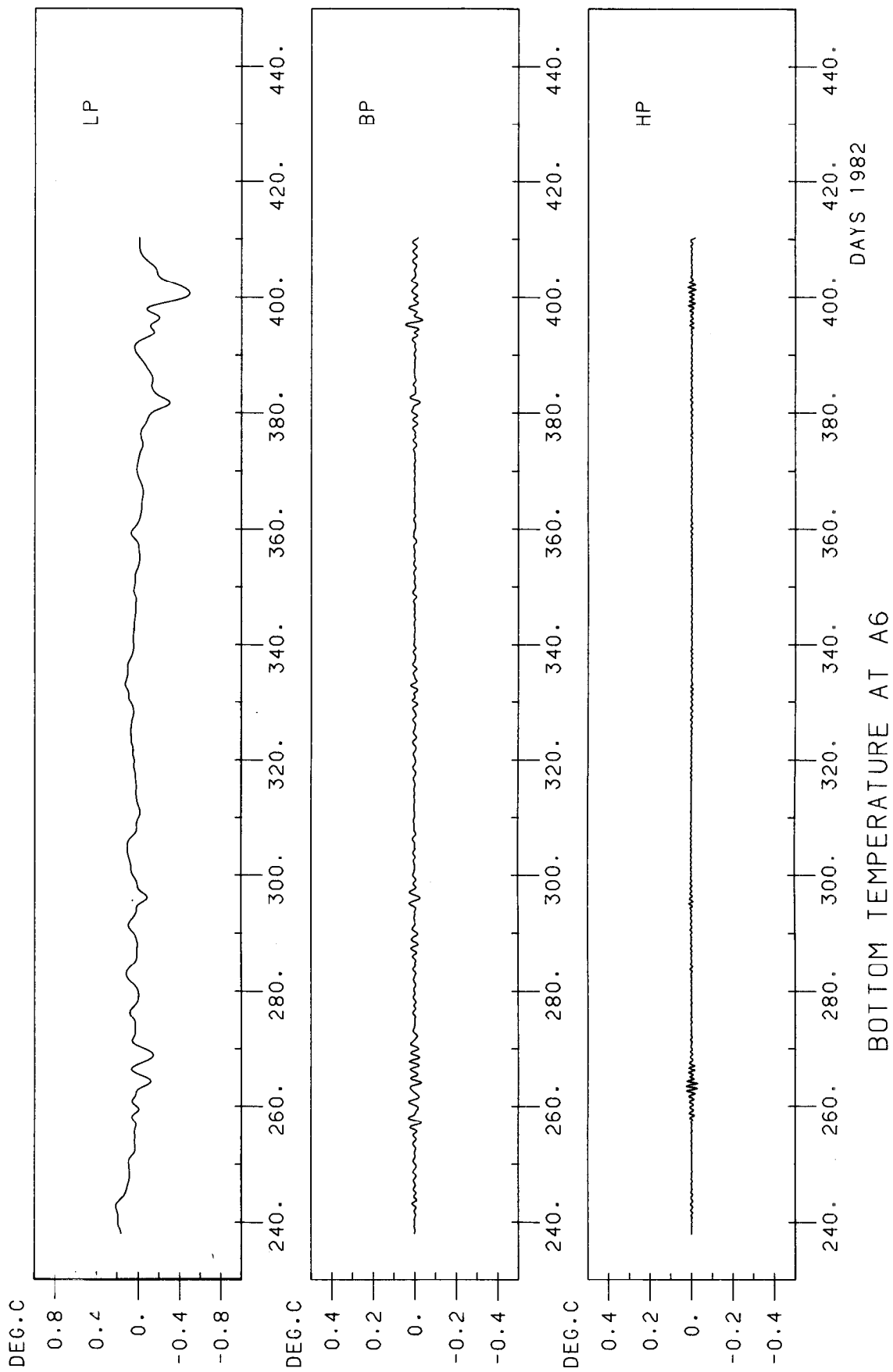


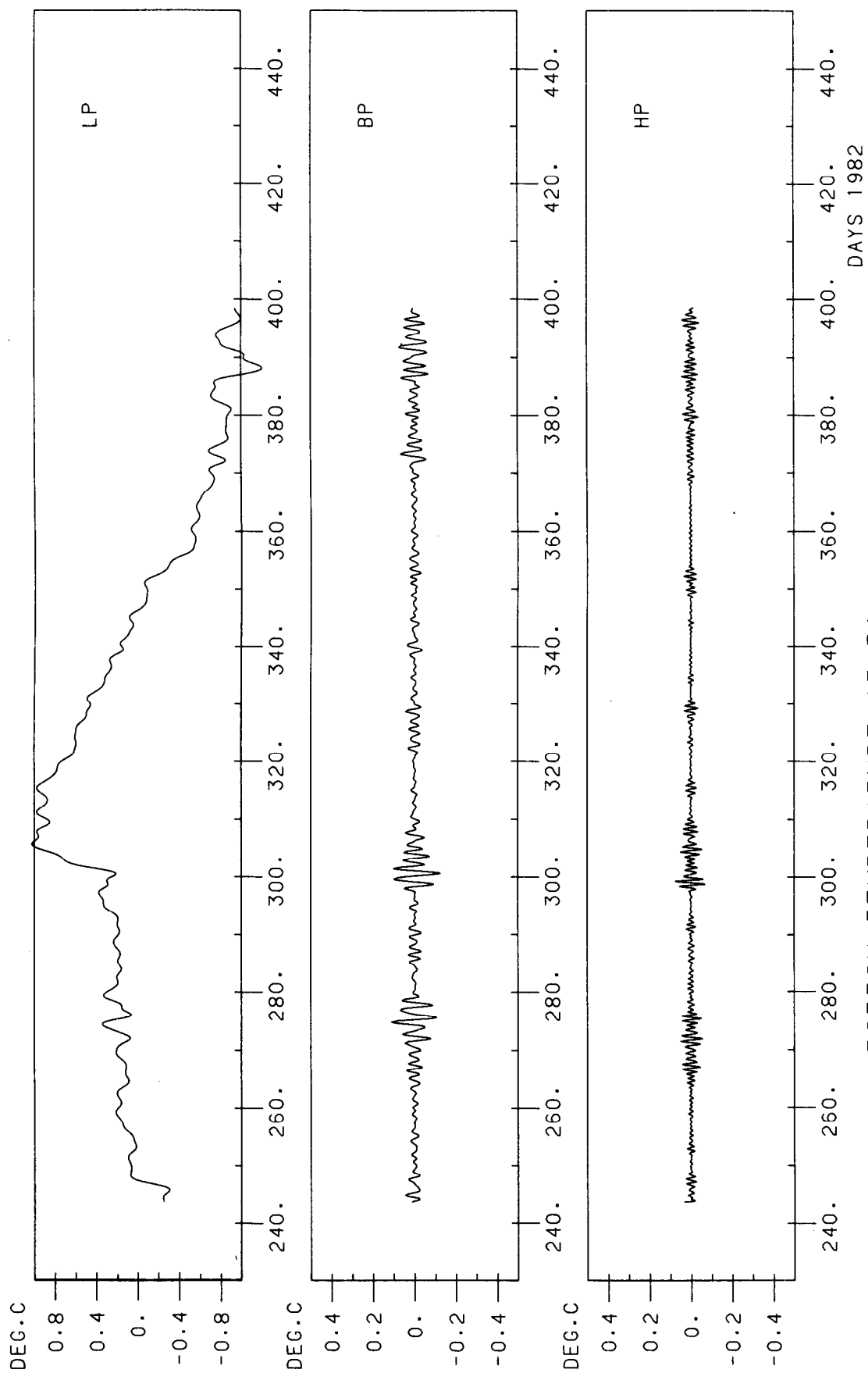
BANDPASS

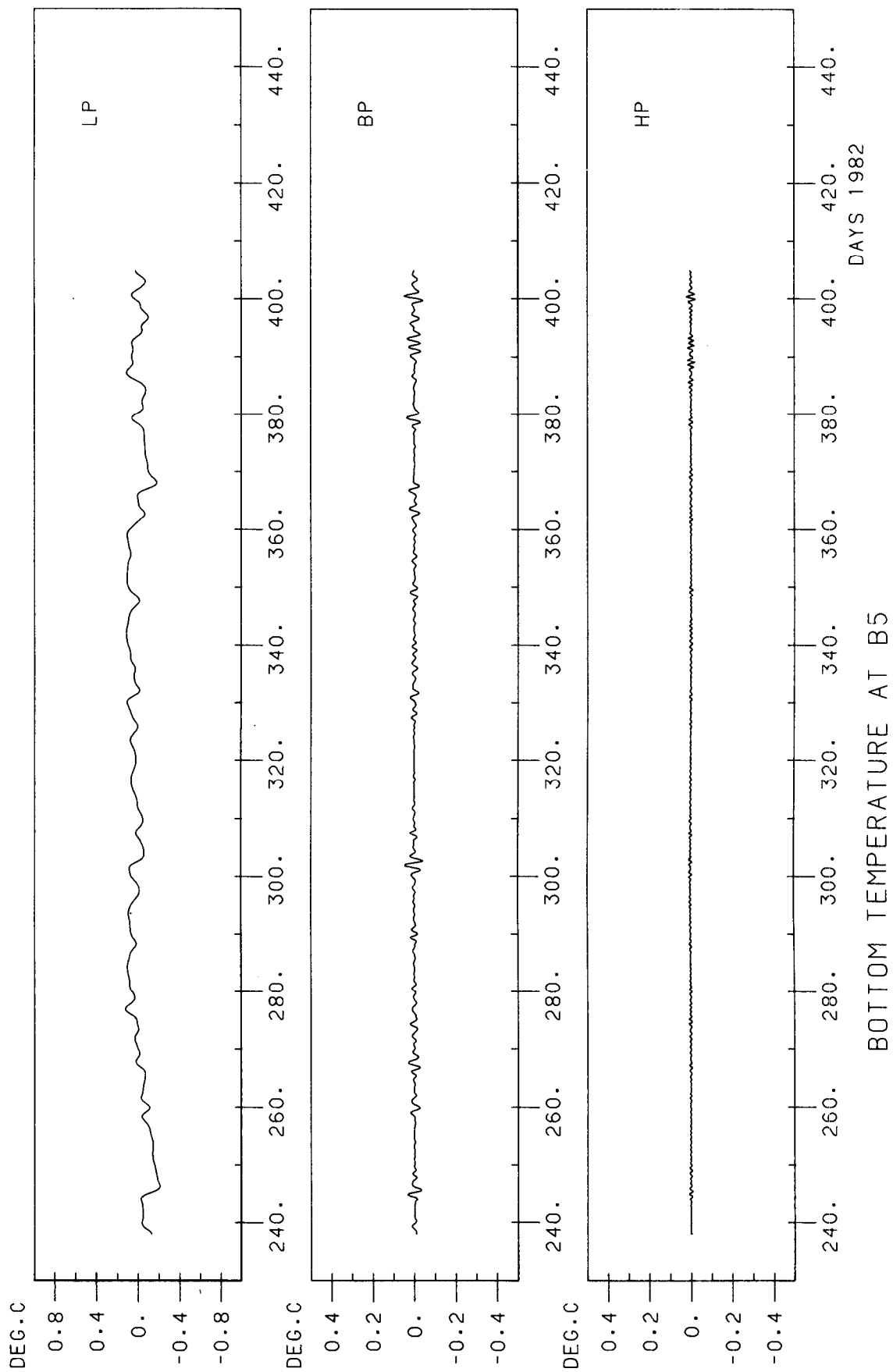


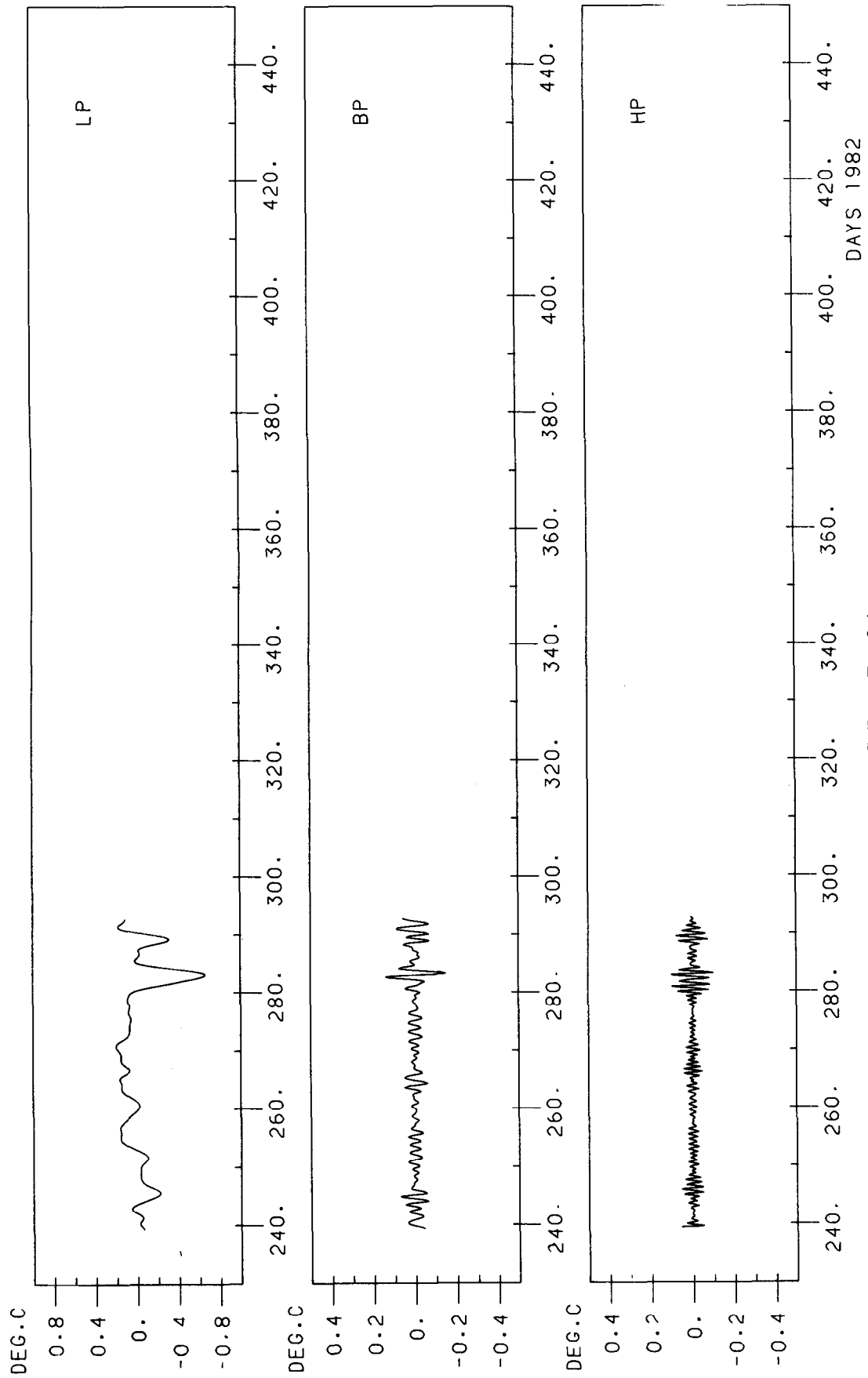
HIGHPASS

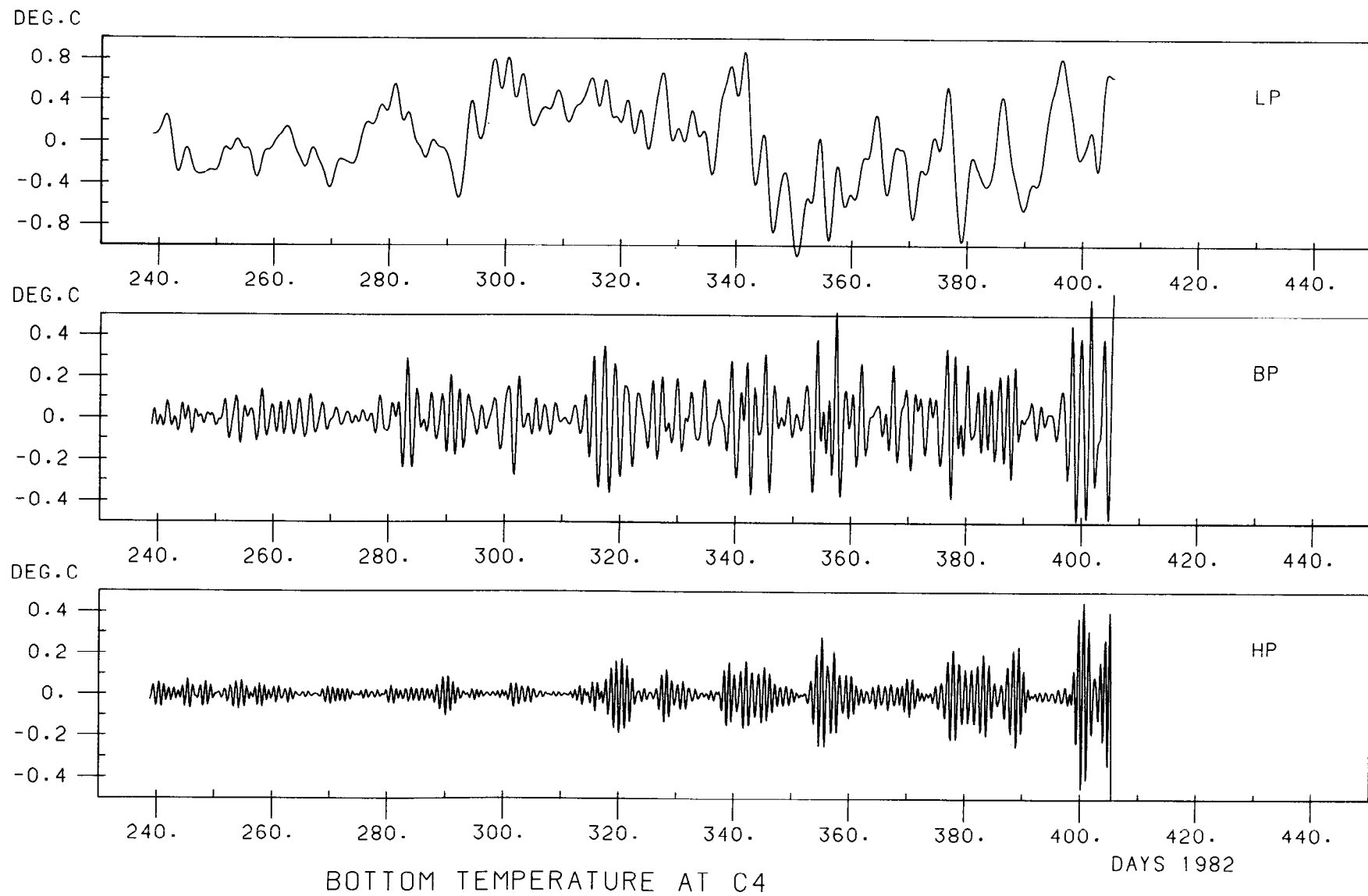


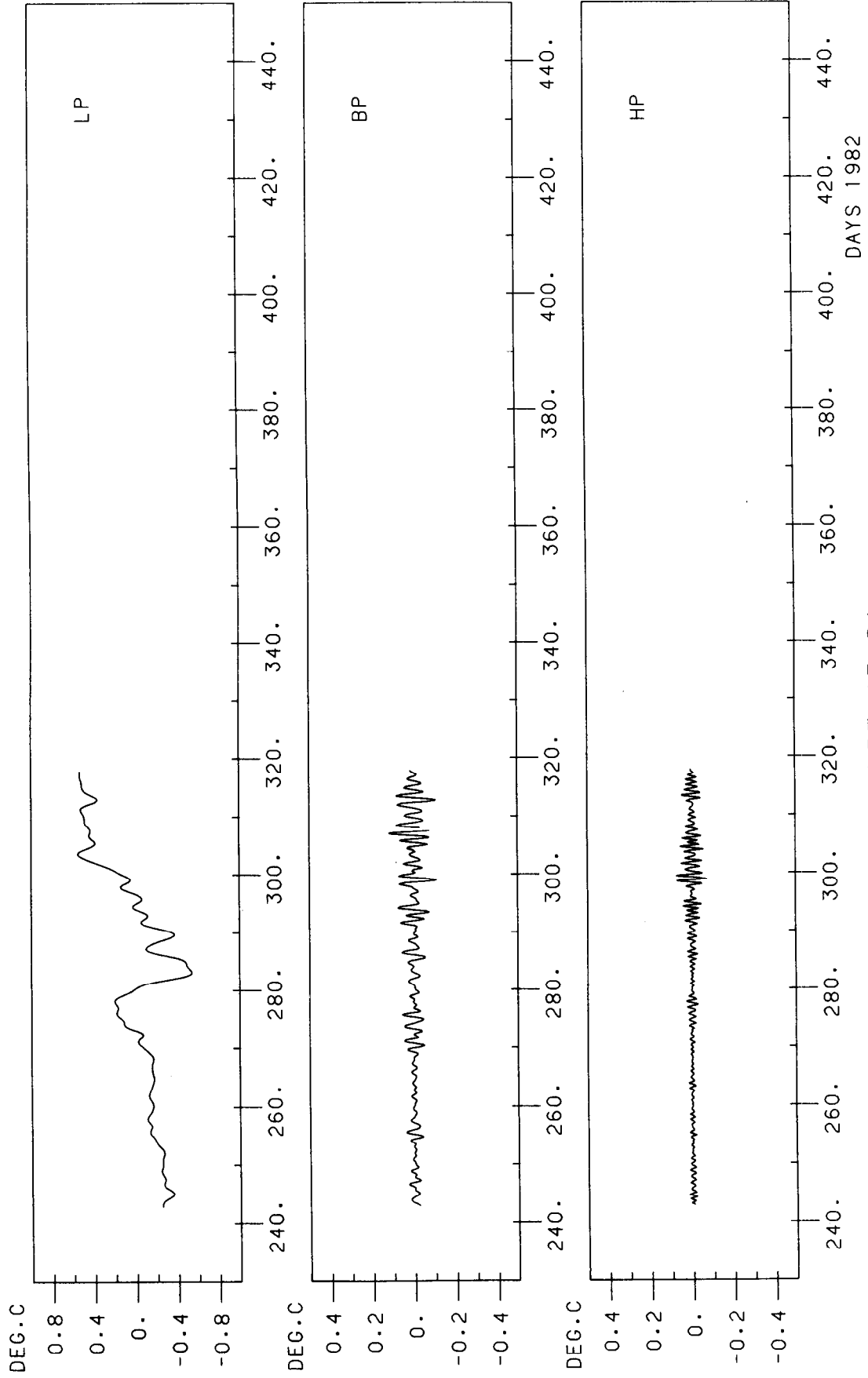


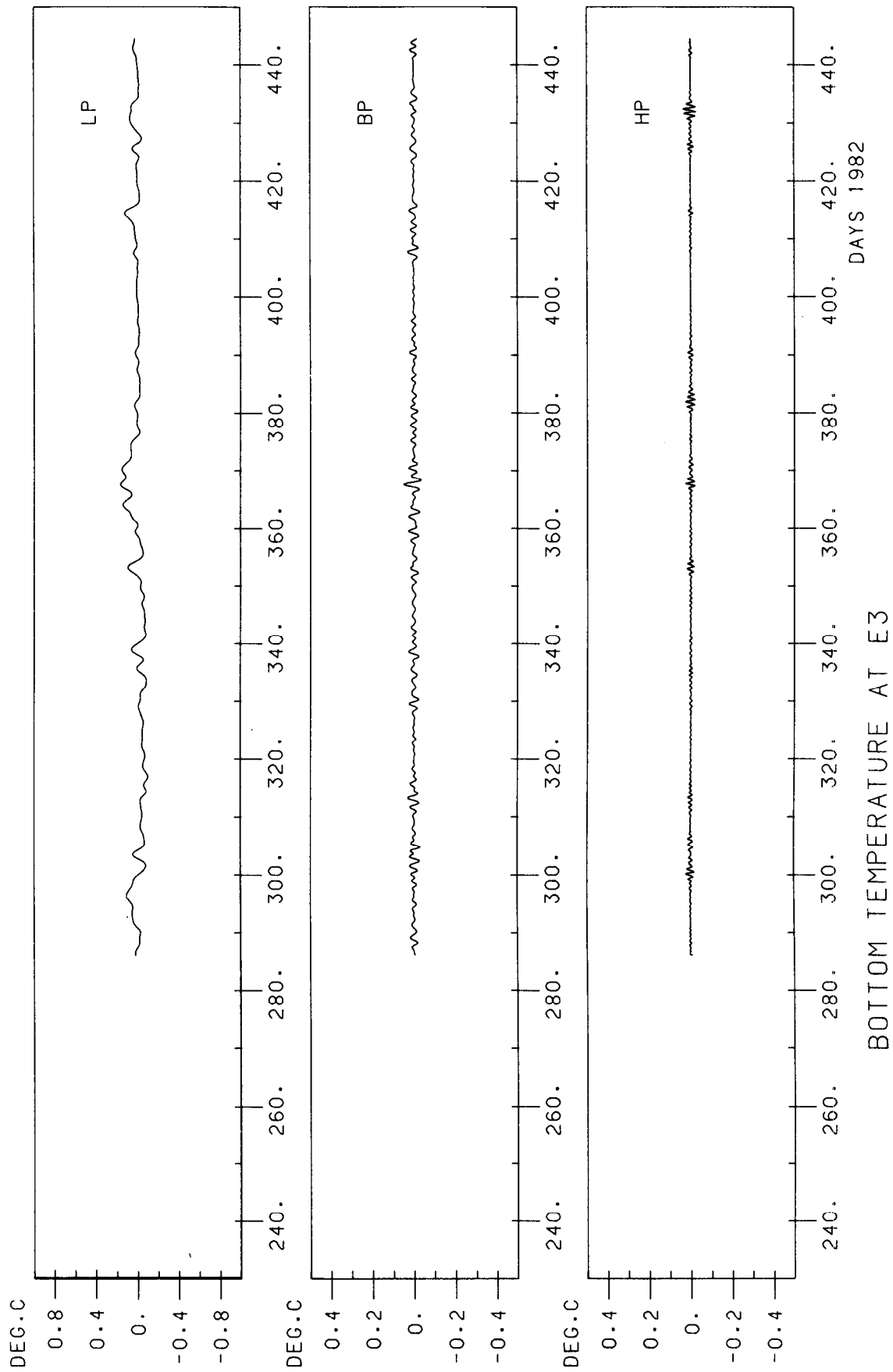


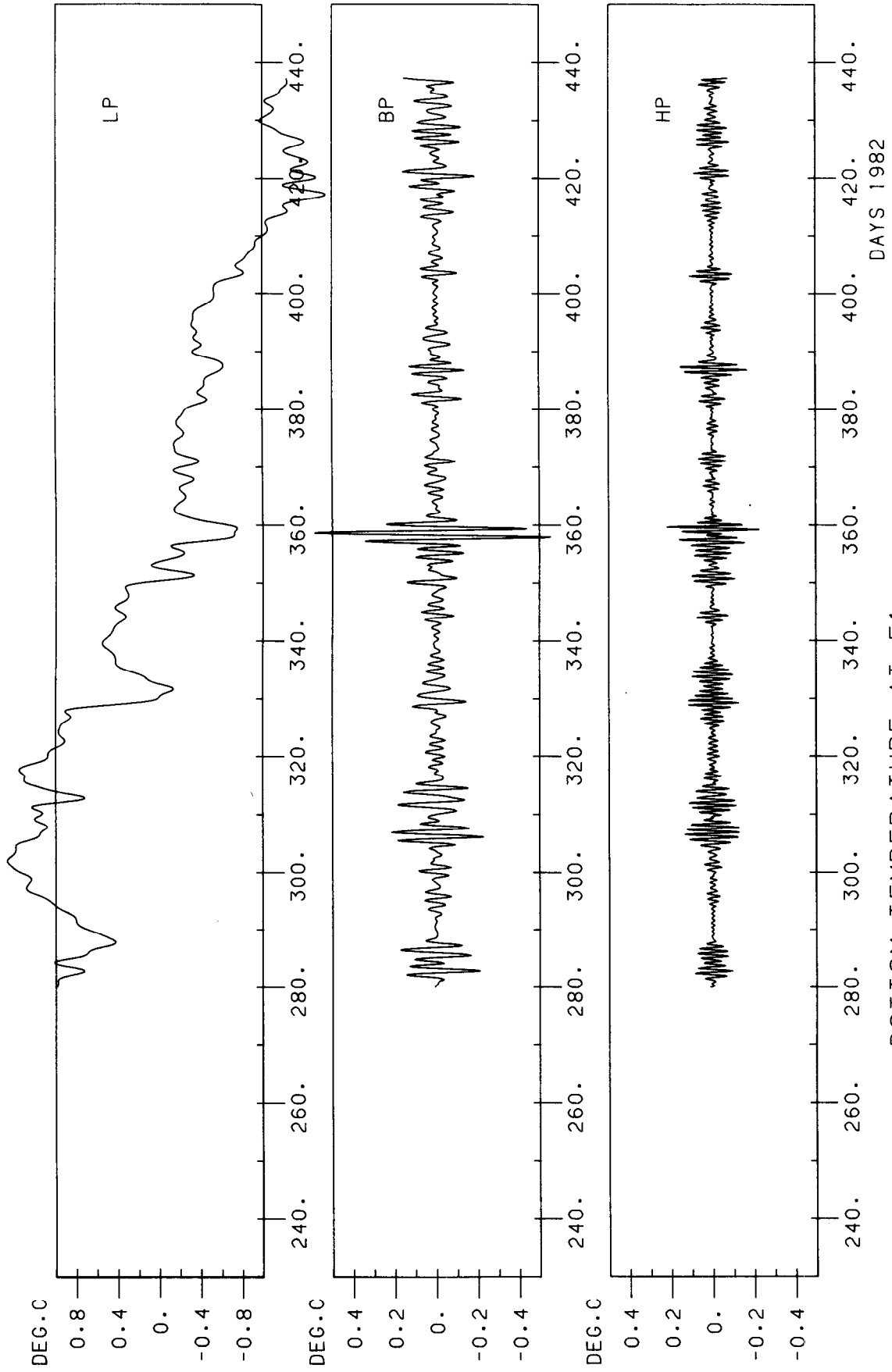


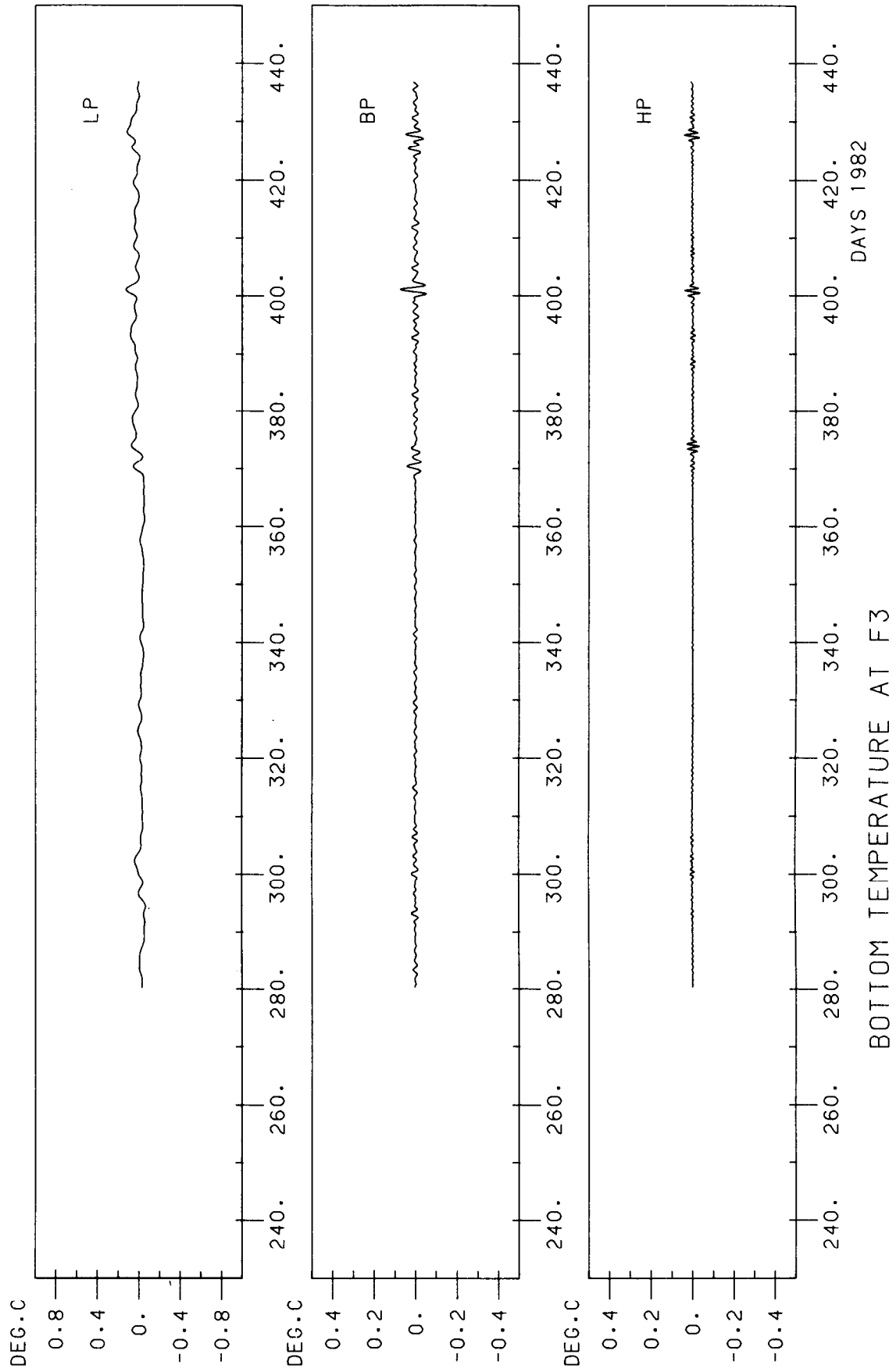


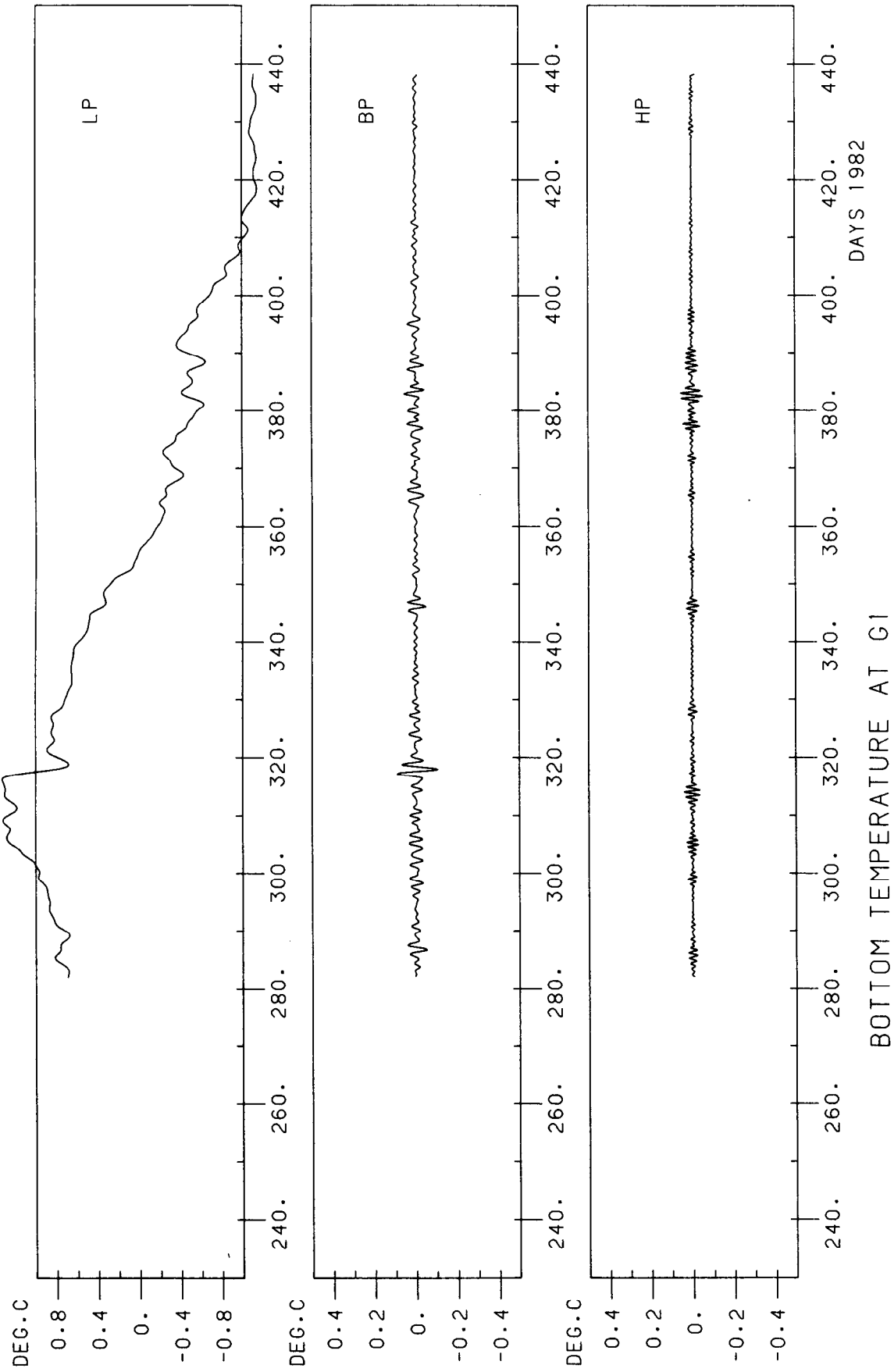


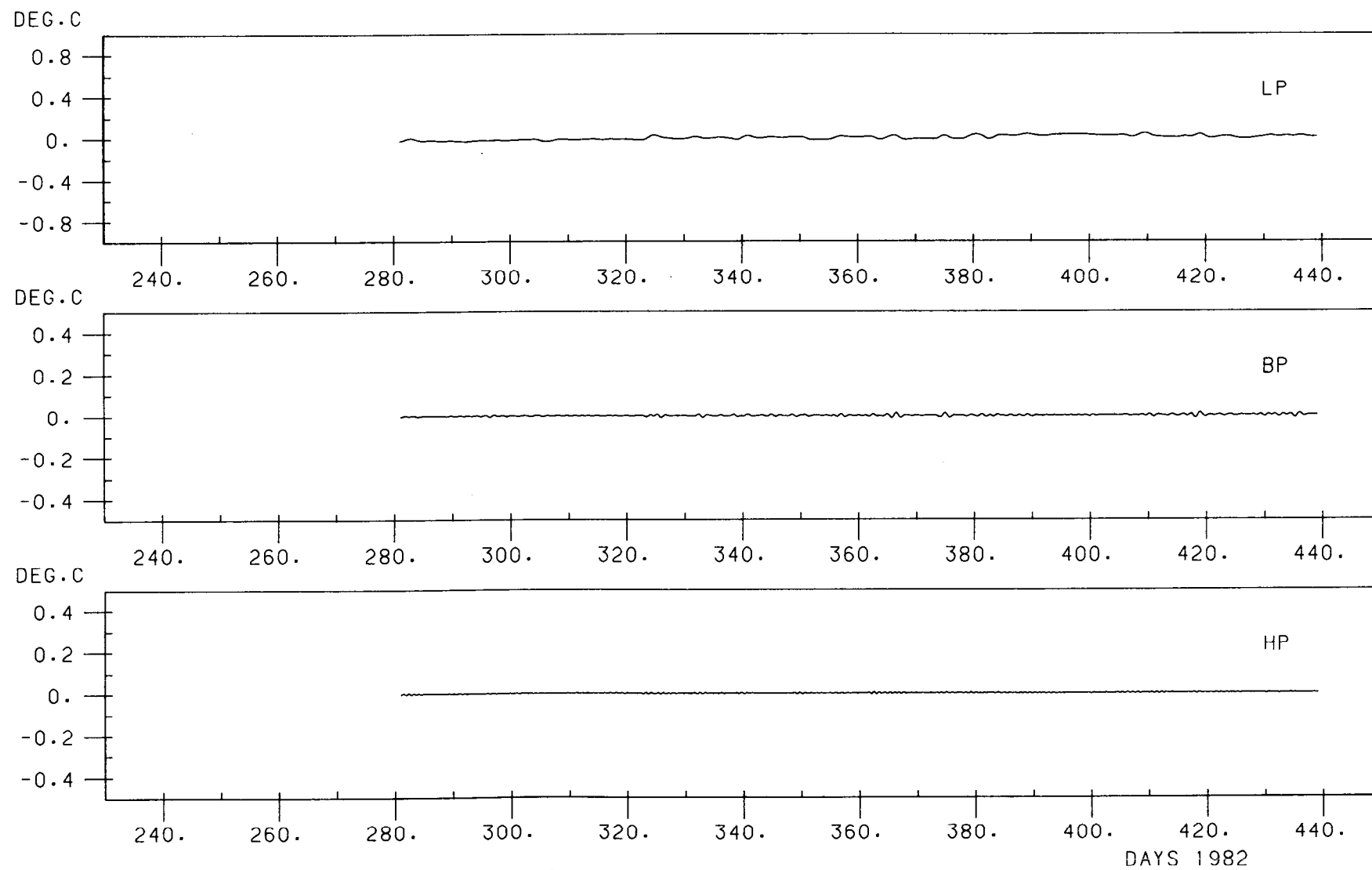












BOTTOM TEMPERATURE AT G4

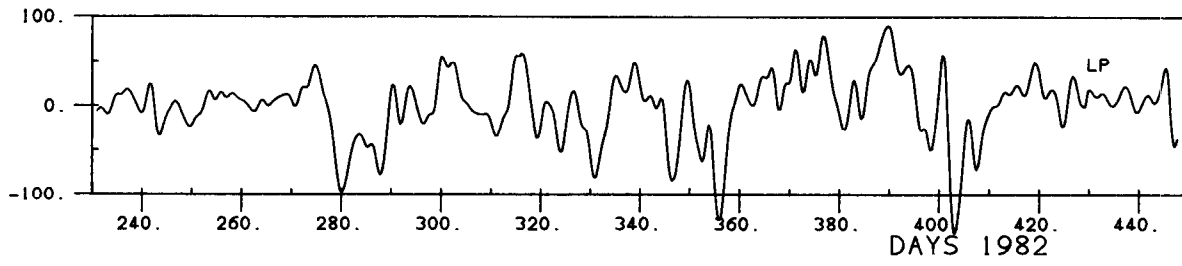
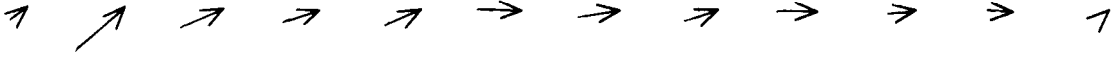
APPENDIX D. COASTAL SEA LEVEL

The plot is for all locations taken together to form one representative series in each frequency band. (Sea level has been reduced to sub-surface pressure as described in I.) Conventions are as for Appendices B and C.

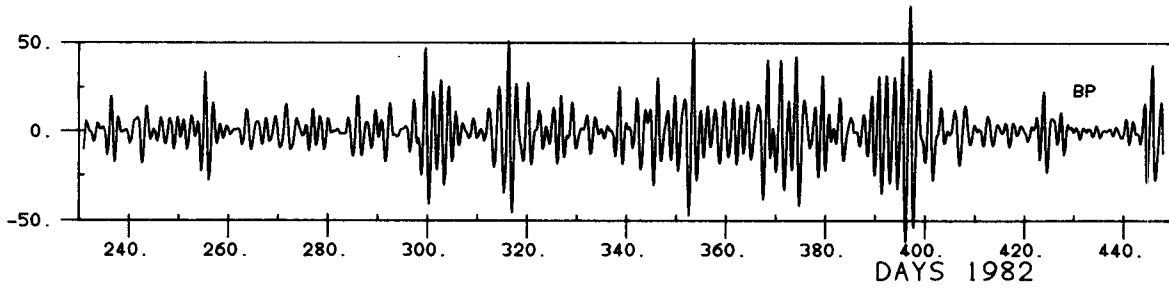
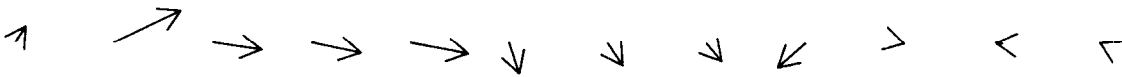
COASTAL PRESSURES

NE AU MA PO MI GR UL ST WI WA LE TO

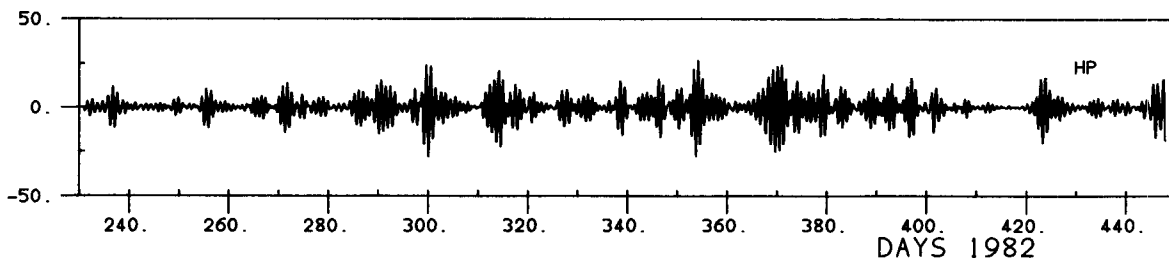
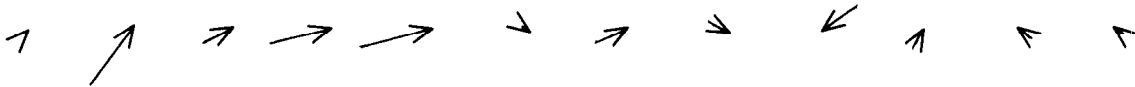
LOWPASS



BANDPASS



HIGHPASS



0 1 MB.

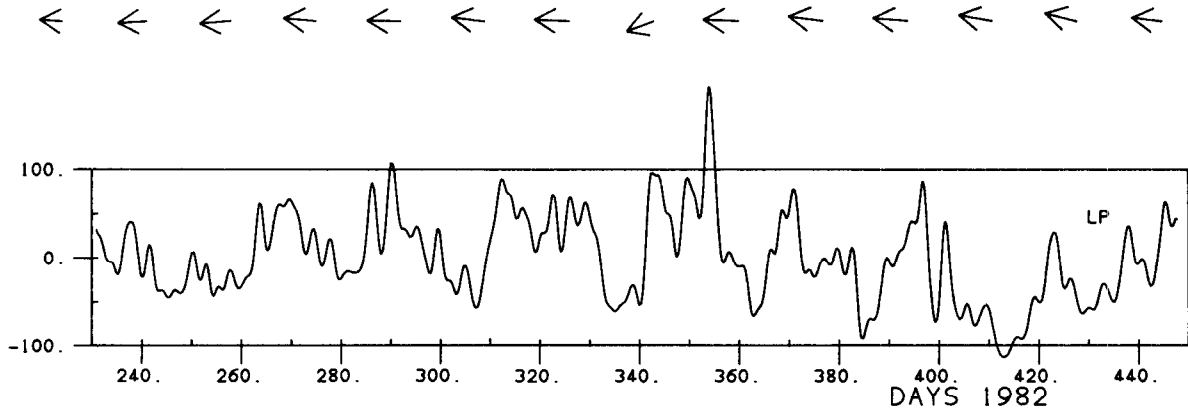
APPENDIX E. ATMOSPHERIC PRESSURE AND WINDS

Separate plots follow for atmospheric pressure, alongshore winds and transverse winds (section 2.4). For each variable, all chosen locations are taken together as labelled on the diagrams. Conventions for the diagrams are as in Appendices B, C and D.

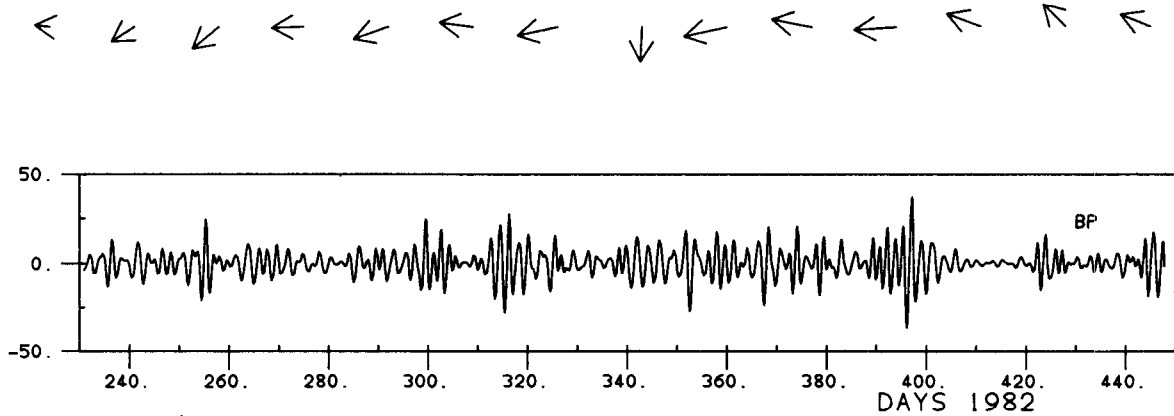
ATMOSPHERIC PRESSURES

GWEN SHAN BELM MULO MALI ABBO TIRE OWSL BENB CAPE STOR WICK LERW TORS

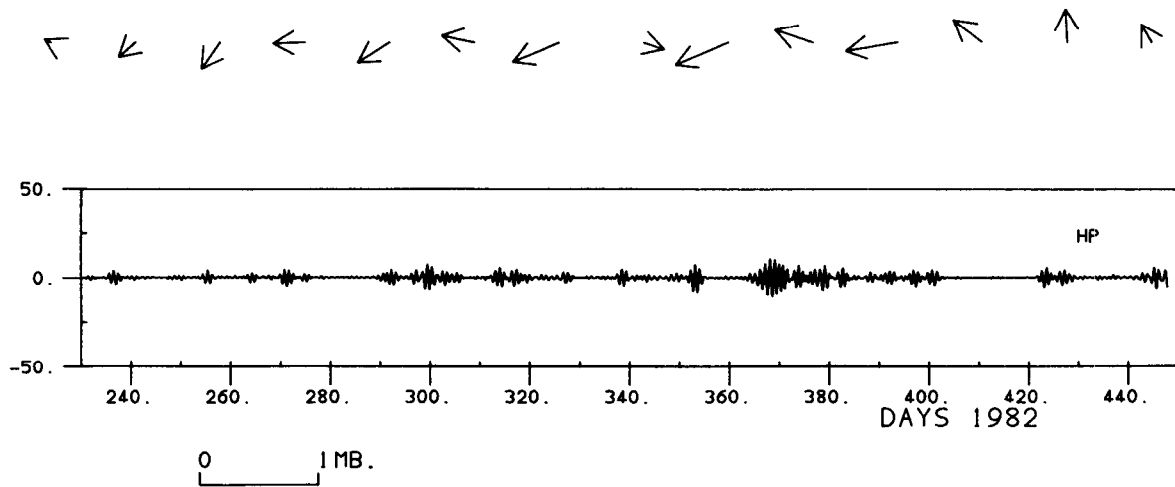
LOWPASS



BANDPASS



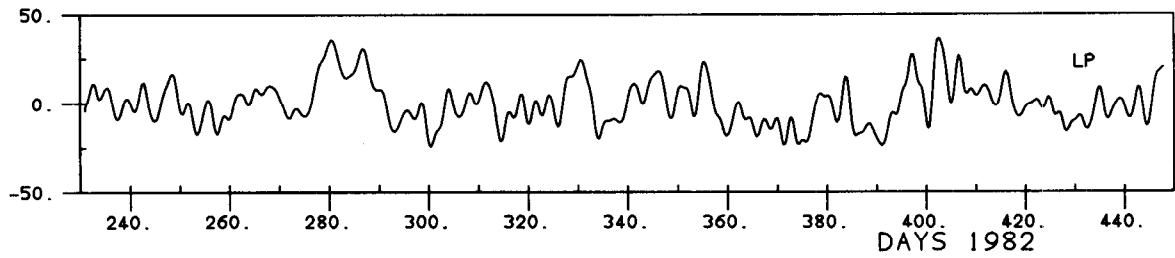
HIGHPASS



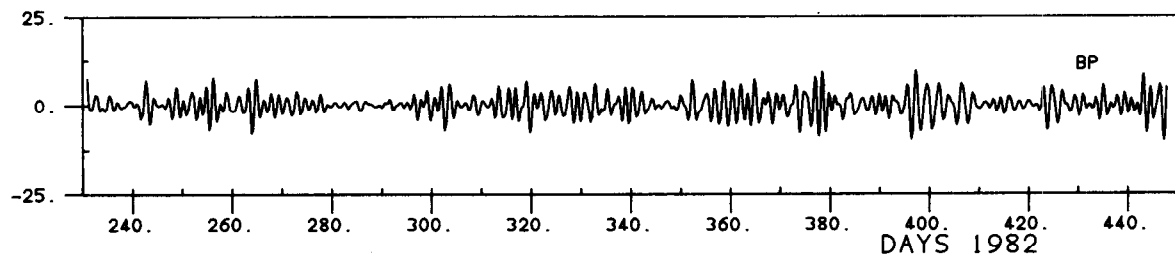
LONG-SHELF WIND

TIRE BENB STOR SULE LERW TORS

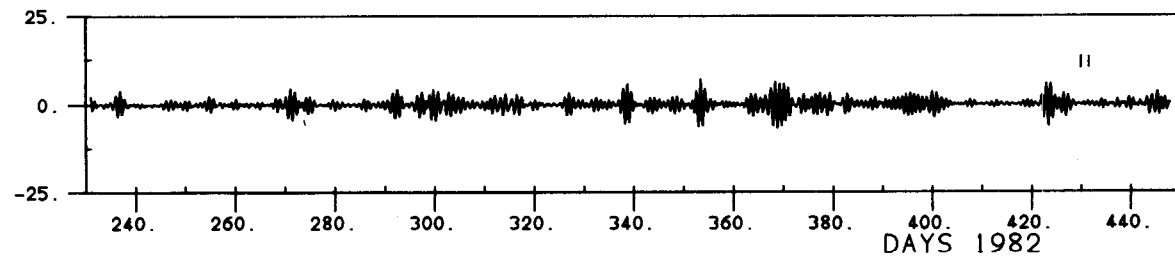
LOWPASS



BANDPASS



HIGHPASS



0 1 M/S

CROSS-SHELF WIND

TIRE

BENB

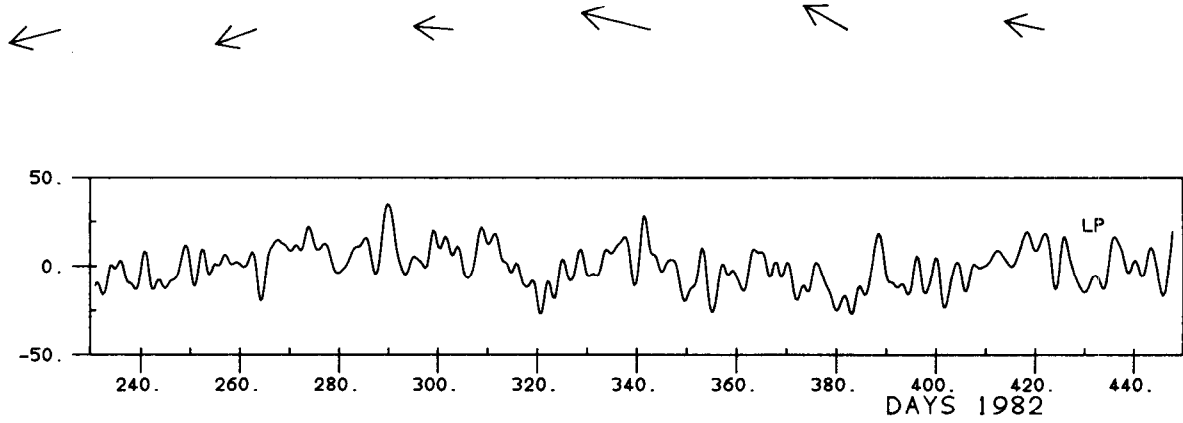
STOR

SULE

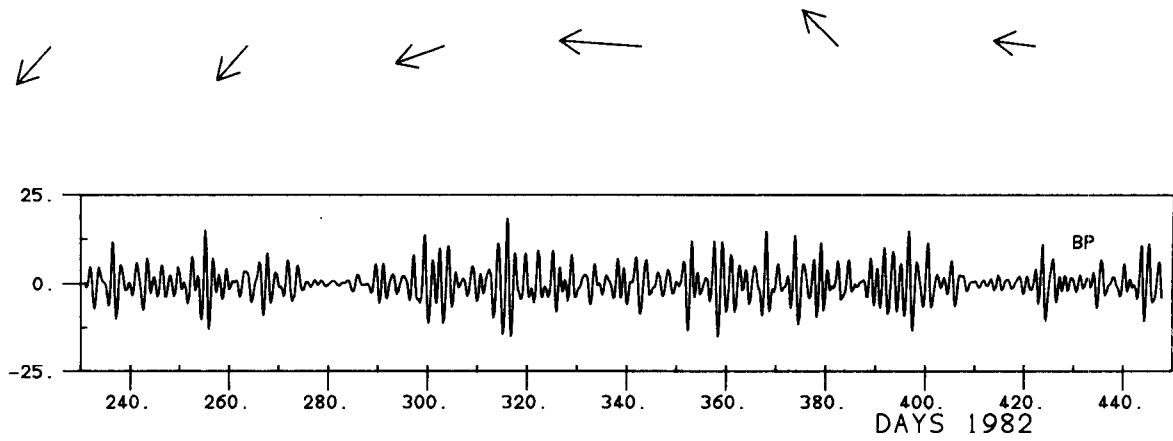
LERW

TORS

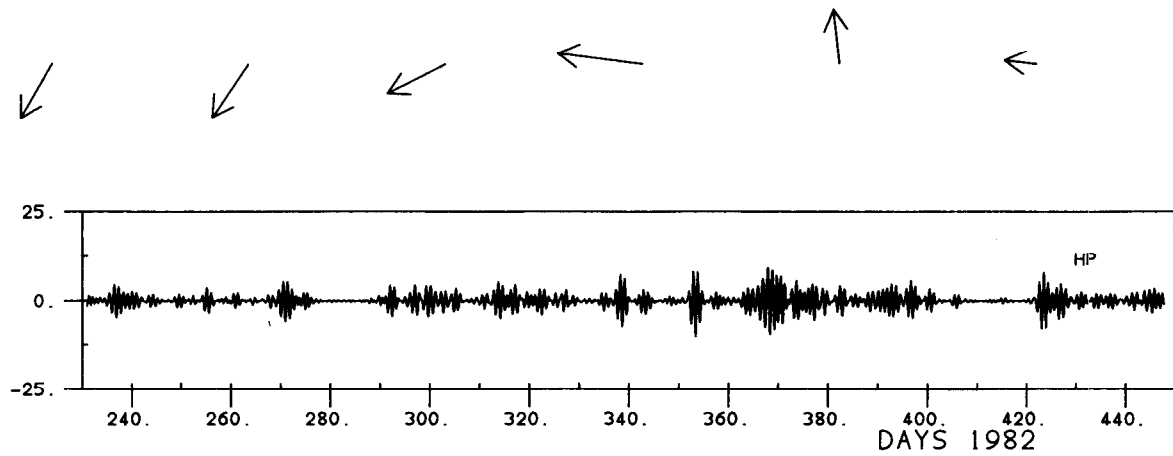
LOWPASS



BANDPASS



HIGHPASS



0 1 M/S